國立臺灣大學工學院環境工程學研究所

碩士論文

Graduate Institute of Environmental Engineering

College of Engineering

National Taiwan University

Master Thesis

利用旋轉填充床進行化學氧化吸收去除氮氧化物之性能評估

Performance Evaluation of Nitrogen Oxides Removal Using Chemical Oxidation and Absorption via a Rotating Packed Bed

洪振耀

Chen-Yao Hong

指導教授：蔣本基 博士

Advisor: Pen-Chi Chiang, Ph.D.

共同指導：潘述元 博士

Co-advisor: Shu-Yuan Pan, Ph.D.

中華民國 110 年 8 月

August, 2021

doi:10.6342/NTU202102462

國立臺灣大學碩士學位論文
口試委員會審定書

利用旋轉填充床進行化學氧化吸收去除氮氧化物之
性能評估

Performance Evaluation of Nitrogen Oxides Removal
Using Chemical Oxidation and Absorption
via a Rotating Packed Bed

本論文係 洪振耀 君(學號 R08541205)在國立臺灣大學環境工程學研究所完成之碩士學位論文，於民國 110 年 7 月 27 日承下列考試委員審查通過及口試及格，特此證明

論文審查委員：

顧洋 博士
國立臺灣科技大學化學工程學系講座教授

陳奕宏 博士
國立臺北科技大學化學工程與生物科技系教授

潘述元 博士
國立臺灣大學生物環境系統工程學系助理教授

林逸彬 博士
國立臺灣大學環境工程學研究所教授

蔣本基 博士
國立臺灣大學環境工程研究所名譽及兼任教授

指導教授：

所　　長：

doi:10.6342/NTU202102462

致謝

從基礎課程的學習，學術研究的鑽研，再到工程實務的應用，各個階段的過程都環環相扣，而研究所的訓練更是扮演著承先啟後的角色。學生也相當幸運地順利完成了研究所的學業，非常感謝這一路上相助的每一位貴人。

感謝在求學生涯中一直陪伴著我的家人，讓我在求學過程中衣食無虞也無後顧之憂，可以將精力集中於課業上，非常感謝家人一路上的支持與照顧。

感謝指導教授蔣本基老師這兩年來的栽培，讓學生參與不同領域的研討會與計畫，增進學生在環工領域的眼界，此外也提供學生於研究上的各種資助，讓研究能順利完成，學生相當感謝；感謝口試委員林逸彬老師、潘述元老師、陳奕宏老師與顧洋老師，撥冗擔任學生的口試委員，並提供學生寶貴的意見，使論文內容更臻完備。

感謝中興環工魏銘彥老師提供設備並指導學生參與大專生研究計畫；感謝曾惠馨老師細心指導學生研究與實驗上的細節；感謝綠色能源與資源實驗室的所有同仁於學生大學時期的各種協助。感謝台大環工所蕭大智老師，席行正老師開授一系列的空組課程，增進學生於流體與膠體等各種污染物相關知識也豐富學生對於材料應用認識。感謝每一位教導過學生的中興環工與台大環工所老師、系上與所上的每一位工作人員，讓學生於大學、研究所的求學過程皆一路順遂。

感謝實驗室助理明儀姐於計畫、會議中等各項協助；感謝渤之學長分享生活中的各種經驗；感謝則綸學長不吝給予實驗與研究上的意見，幫助學弟實驗上的問題；感謝彥勛學長指導讓學弟更快認識實驗的架構與設計；感謝威宇學長、珮瑜學姊、棋蓉學姊在實驗室相關會議上的各類幫助。

感謝實驗室同儕晏瑄共同分擔計畫上的大小事；感謝家語在計畫、會議與實驗上的各種協助，以及在書寫論文的過程中，分享許多生活趣事與人生經歷，讓撰寫論文的過程中更添趣味。

doi:10.6342/NTU202102462

感謝空組同學，一同修習空組課程，於實驗中遇到問題時，也不吝給予意見及設備的借用。感謝中興環工的好同學、來到台大環工所後認識的新朋友、學長姐和學弟妹，與我共同修習課程、吃飯、聊天、打球與分享生活趣事，豐富了我的研究生生活。

最後感謝諸佛菩薩與老祖師尊的慈悲加持護佑，讓我在求學生涯中，無論是生活上或課業上遇到各種疑難雜症時，可以用易，與其無所生，使事情能夠順利圓滿。

洪振耀 謹誌

國立台灣大學環境工程學研究所

2021 年 8 月

doi:10.6342/NTU202102462

中文摘要

自工業革命以來，科技與經濟活動蓬勃發展，大幅的改善與提高的人們的生活品質，然而伴隨著空氣污染物的排放，過去易被忽略的環境與生態問題也逐一浮現，其中，氮氧化物為指標性空氣污染物之一，對於環境與人體的傷害日益受到重視，政府部門所訂定的氮氧化物排放標準逐漸加嚴，也使科學家開始發展更有效率的氮氧化物去除技術。應用超重力旋轉床去除氮氧化物為相當具有潛力的空氣污染控制技術，透過離心力使反應器內產生高質傳的特性，可於一般常溫下操作，也大幅縮減傳統氧化吸收的濕式洗滌法所需要的設備體積。

本研究為利用超重力旋轉填充床進行化學氧化吸收程序去除氮氧化物，過程中包含測試各式氣相與液相藥劑、旋轉床操作條件與高中低濃度污染物負荷於氧化吸收程序中的去除效率。研究結果顯示以一氧化氮為主要成分 ($NO/NO_X \approx 0.9$) ，總濃度為 200 ppm 的氮氧化物，於氣液比 20、超重力因子 86、氣相氧化劑為二氧化氯與液相吸收劑為亞硫酸鈉的操作條件下，氮氧化物的總去除率達 98.99 %；當污染物濃度提高至 750 ppm 時，以相同的操作條件，氮氧化物的總去除率仍可維持在 98 %以上，且尾氣濃度也符合法規排放標準。此外，本研究中也對系統質傳係數進行因次分析，並建立相關的數學模式；另一方面，為了考量此技術於未來實務操作的可能性，對系統進行簡易的能耗評估與成本分析。期盼透過本研究的模組實驗、數學模式與能耗成本分析，提高此技術於實廠中應用的可行性。

關鍵字：氮氧化物控制技術、超重力技術、旋轉填充床、氧化吸收程序、質量傳輸、成本分析

doi:10.6342/NTU202102462

Abstract

Since the industrial revolution, technological and economic activities have developed vigorously, which greatly improves people's quality of life. However, with the emission of air pollutants, environmental and ecological problems that were easily overlooked in the past have gradually emerged. Among them, more and more people are concerned about the harm of nitrogen oxides to the human body and the environment. Besides that, nitrogen oxide emission standards set by government agencies are becoming stricter. Therefore, scientists have started to develop more efficient technologies for removing nitrogen oxides. Using a high-gravity rotating bed to remove nitrogen oxides is a potential technology for air pollution control. The centrifugal force creates high mass transfer properties in the reactor. It can operate at normal temperature and greatly reduces the volume required for traditional wet scrubbing of oxidation absorption.

This study uses the rotating packed bed to perform a chemical oxidation absorption process to remove nitrogen oxides. The method includes testing various gas and liquid phase agents, rotating bed operating conditions, and removing high, medium and low concentration pollutants in the oxidation absorption process. The research shows that when using nitrogen oxides with a total concentration of 200 ppm ($NO/NO_X \approx 0.9$) as the pollutant source, the overall removal efficiency of nitrogen oxides reaches

doi:10.6342/NTU202102462

98.99% under the best operating conditions (gas-liquid ratio of 20, high gravity factor of 86, chlorine dioxide as a gas phase agent and sodium sulfite as a liquid phase agent); if the pollutant concentration has been increased to 750 ppm, the total degree of separation of nitrogen oxides can still be kept above 98% under the same operating conditions, and the exhaust gas concentration also corresponds to the legal emission standards. In addition, the dimensional analysis of the mass transfer in the system, the estimation of the mass transfer coefficient and the associated prediction models were established in this study; In the practical implementation, a simple cost analysis of the system was carried out. By simulating module experiments, establishing mathematical models and evaluating economic efficiency, this technology should be more realistic in the future.

Key words: NO_X control technology, High-gravity technology (HiGee), Rotating packed bed, Oxidation-absorption process, Mass transfer, Cost analysis

doi:10.6342/NTU202102462

List of Content

doi:10.6342/NTU202102462

doi:10.6342/NTU202102462

doi:10.6342/NTU202102462

List of Figure

doi:10.6342/NTU202102462

doi:10.6342/NTU202102462

doi:10.6342/NTU202102462

doi:10.6342/NTU202102462

doi:10.6342/NTU202102462

List of Table

doi:10.6342/NTU202102462

doi:10.6342/NTU202102462

doi:10.6342/NTU202102462

Comment for Oral Defense

顧洋 老師

NO.	Comment	Answer
1	添加液相藥劑時，藥劑與污染物的反應為氧化，還原還是單純透過調整 pH 來酸鹼中和?	謝謝老師的提問，已將相關內容補充於 4-5 頁與 4-6 頁。
2	圖 4-2 (a)為何濃度會先下降後上升?	謝謝老師的提問，主要原因尚未確定，但推測原因可能為實驗架設有關，初始濃度會透過 bypass 的方式測量，開始操作後則將三通球閥轉至經過 RPB 的系統，此處將產生短暫的時間差，導致濃度驟降，其後有將管道調整有稍微改善濃度會先驟降的情況。
3	4-8 頁，為何使用 plug flow reactor 的模型來描述汙染物的變化?	謝謝老師的提問，已將相關內容補充於 4-8 頁。
4	圖 4-4 中 Reaction distance 的定義應說明清楚。	謝謝老師的建議，已經圖的座標名稱修改，並說明。
5	為何於 4.1.2 章節中推估氧化後產生的物種，其重要性為何?	謝謝老師的提問，此處學生希望可透過分析氧化後的產物，來了解吸收劑與污染物之間的反應機制。
6	Plug flow reactor 模式中使用的速率常數是否適用於本研究的系統中?	謝謝老師的提問，由模式的結果可得知與實際情況有相當大的差異，可能原因及文獻提供的速率常數不適用於此系統及未考量到系統中所有正逆反應。因此後續有使用其他模式替代。
7	實驗規模與實廠規模的成本計算相差差近百萬倍，是否合理?	謝謝老師的提問，已重新計算，將有問題的地方修正!

doi:10.6342/NTU202102462

陳奕宏 老師

NO.	Comment	Answer
1	改變 RPB 液體流量與轉數所影響的因子為何?	謝謝老師的提問，此處學生主要以持液量，有效接觸比表面積及液膜厚度作為影響參數的探討。
2	實驗操作的氣液比範圍與實廠操作的氣液比範圍為何?	實廠的氣液比操作範圍區間較大，最高於文獻中有達到 120，最低則有 0.5，實驗中由於設備的限制則將範圍設至為 5~40。
4	G/L 與 β 於 RPB 中同時改變時，G/L 可大致看成持液量，而 β 則為分散程度，大致可由此角度思考質傳條件的差異性。	謝謝老師的建議，可供學生於未來操作 RPB 相關實驗時進行討論。
5	為何圖 4-5 中，添加氫氧化鈉後，就可以馬上測得亞硝酸鹽?	謝謝老師的提問，相關內容以補充在 4-12 頁。
6	對於吸收劑是否對污染物產生氧化還原反應，或者純粹為酸鹼中和，可對吸收劑的 ORP 與 pH 進行測量。	謝謝老師的意見，可供學生於未來進行吸收劑與污染物反應機制探討時的討論方向。
7	4-10 頁中，圖 4-4 為經過多少秒達到 steady state?	謝謝老師的提問，圖 4-4 的模式未計算達到穩態的時間，而搭配圖 4-3 (a)，整體系統呈現操作達 4 分鐘時趨近於穩態，可大致推論吸收程序前的氣相氧化程序，達穩態的時間小於 4 分鐘。
8	論文中，圖表較多以顏色進行區分，可盡量以符號呈現較能於黑白影印中區分。	謝謝老師的建議，已加上條紋與符號，幫助於黑白輸出時的辨識性。

doi:10.6342/NTU202102462

潘述元 老師

NO.	Comment	Answer
1	去除的氣相汙染物與吸收劑中的污染物可進行質量平衡，建議可補充相關數據。	謝謝老師的意見，可供學生或學弟妹於未來操作 RPB 相關實驗時進行討論。
2	結果討論中使用的公式，應補充其假設與適用條件。	謝謝老師的建議，已補充相關敘述在模式的章節中。
3	表 4-5 中的 RPD 為 200%，是否合理?	謝謝老師的提問，已將表 4-5 的內容進行修正。
4	表 4-9 中，污染源以 NO 為主，而 NO 的去除效率達 99%，為何 NOx 的去除效率僅 71.8%?	謝謝老師的提問，由於 NO 的去除主要歸因於 NO 被氧化劑氧化成 NO_2 與其他含氮化合物。經氧化後，污染源的 NO_X 以 NO_2 為主，因此η_{NO_X}主要受η_{NO_2}影響。
6	表 4-15 中可再補充各個無因次參數的 p value。	謝謝老師的建議，已將相關內容補充於表 4-15。
7	圖 4-24 中可將成本與能耗的考量列入計算，較符合”系統化”的標題。	謝謝老師的意見，可供學生或學弟妹於未來操作 RPB 相關實驗時進行討論。
8	表 4-21 中 capacity 的單位可再調整，且成本可再考量使用年限。	謝謝老師的建議，已補充相關內容於章節 4-5。
9	表 4-20 中，可再將成本與操作參數再分類。	謝謝老師的建議，已在相關內容處進行修正。
10	可再補充未使用此項技術所需要負擔的成本(BAU)。	謝謝老師的建議，已在補充相關內容於章節 4-5-2。

doi:10.6342/NTU202102462

林逸彬 老師

NO.	Comment	Answer
1	氧化吸收中，一個為化學反應，另一個則為物理反應，而文中對於 Oxidation-Absorption 的定義為何?	謝謝老師的提問，學生參考文獻中對於氧化吸收法描述，使用 Direct oxidation absorption 作為氧化吸收法的總稱，之後可再細分為 oxidation-absorption 與 absorption-oxidation，詳細內容已補充於 2-8 頁。
2	圖 4-2 (a)中使用的藥劑其濃度為何，使用不同濃度進行操作則結果是否可比較?	謝謝老師的提問，藥劑濃度以吸收劑與污染物之間的化學劑量進行計算，相關補充在表 3-3。
3	圖 4-4 的近似解為何不使用 Matlab 等其他程式求解?	謝謝老師的提問，由於系統的條件使用 Excel 即可求解，較可避免使用 Matlab 時複雜的 coding 程序。
4	圖 4-8 中，各項參數變化時，去除率落差僅 5%，這樣是否還可以比較?	謝謝老師的提問，實驗中每組實驗均進行重複，而相對差異百分比均在 3%以內，故每組實驗之間去除率的差異為 5%時，判定為顯著差異。
5	各項藥劑的反應機制為何，是氧化，還原還是酸鹼中和?	謝謝老師的提問，已將相關內容補充於 4-5 頁與 4-6 頁。
6	圖 4-2 (a)為何濃度會先下降後上升?	謝謝老師的提問，推測原因可能為實驗架設有關，為轉換氣體路徑時所造成儀器偵測污染物的時間差。
7	以氧化力而言，臭氧高於二氧化氯，為何實際操作時去除效率反而是二氧化氯較佳?	謝謝老師的提問，相關內容以補充於 4-15 與 4-16 頁。

doi:10.6342/NTU202102462

蔣本基 老師

NO.	Comment	Answer
1	應將各種藥劑與污染物的反應機制說明清楚，並列出各項藥劑使用的濃度。	謝謝老師的建議，已將相關內容補充於 2-18 頁與 3-14 頁。
2	若使用還原型液相藥劑，於氣相中將污染物氧化後，進入水中被還原，是否會造成污染物再逸散?	謝謝老師的提問，文獻回顧與實驗中均並未發現還原型吸收劑將污染物還原成 NO 與 NO_2 而再逸散的情況。
3	實驗中成本規劃與實際操作的誤差約為 30%以下，而表 4-21 與表 4-23 相差甚遠，是否合理?	謝謝老師的提問，已重新計算，將有問題的地方修正!
4	空氣污染設備進行成本評估時，由實驗規模放大至實廠規模通常有一放大係數，可由此方式進行實廠成本的評估。	謝謝老師的意見，可供學生或學弟妹於未來操作 RPB 相關實驗時進行討論。
5	使用的模式包含假設條件與適用性應在說明清楚。	謝謝老師的建議，已將相關內容補充於模式相關內容中。

doi:10.6342/NTU202102462

Nomenclature

Symbol	Identification	Unit
η	Removal efficiency	%
C	Concentration	mole m^{-3}
$C_{Gi/Li}$	Inflow concentration in gas/liquid	mole m^{-3}
$C_{Go/Lo}$	Outflow concentration in gas/liquid	mole m^{-3}
C_X	Concentration in X	mole m^{-3}
$C_{X+\Delta X}$	Concentration in $X + \Delta X$	mole m^{-3}
Q_g	Influent gas flow	m^3/s
Q_l	Influent liquid flow	m^3/s
N	Rotational speed	rpm
β	High-gravity factor	-
$\bar{r}$	Average radius	m
g	Acceleration of gravity	m/s^2
k_i	The rate constant of reaction number "i"	-
v	Velocity of flow	m/s
k_L	Liquid side mass transfer film coefficient	m/s
D_L	Diffusion coefficient in liquid phase	m^2/s
l	Thickness of liquid mass transfer film	m
S	The frequency of renew on the interface	m^2/m^2s
ε_L	Liquid holdup	m^3/m^3
a_c	High-gravity field strength	m^2/s
a_o	Characteristic high-gravity field strength	m^2/s
u	Mean radial flow rate of liquid in the rotor	m s^{-1}
u_o	Characteristic flow rate per unit area	m s^{-1}
ν	Kinematic viscosity of liquid	m^2 s^{-1}
ν_o	Characteristic kinematic viscosity	m^2 s^{-1}
ω	Rotational speed	rad s^{-1}
r	Mean radius	m
δ	Liquid film thickness	m
Z	Axial length of the packing	m
E_C	Experimental constant	-
L	Average liquid superficial velocity	m s^{-1}
a_t	Specific area of the packing	m^2m^{-3}
a_e	Total specific area of mass transfer	m^2m^{-3}
σ	Surface tension of liquid	N m^{-1}

doi:10.6342/NTU202102462

σ_C	Critical surface tension of packing	N m^{-1}
ρ_L	Density of liquid	kg m^{-3}
t	Liquid residence time	s
N_{NO_X}	Flux of NO_X	mole s^{-1} m^{-2}
a_d	Effective droplet area	m^2m^{-3}
a_f	Effective liquid film area	m^2m^{-3}
k_{Lf}	Liquid side film mass transfer film coefficient	m/s
k_{Ld}	Liquid side droplet mass transfer film coefficient	m/s
k_c	Pseudo-first-order rate constant	s^{-1}
d_h	Hydraulic diameter	m
St	Stripping factor	-
H	Henry's constant	-

doi:10.6342/NTU202102462

Chapter 1 Introduction

1.1 Background

Since the industrial revolution, people have flourished in technological and economic activities. At the same time, many pollutants are released into the atmosphere, which have a major impact on the environment. Among the many air pollutants, nitrogen oxides (NO_X) are the most important pollutants discussed by humans [1]. Nitrogen oxide emissions come from many sources of pollution, including mobile sources (such as cars) and stationary sources (such as boiler incineration and surface treatment processes [2, 3]). The negative effects of nitrogen oxide emissions on the human body include chest pain, eye/throat irritation, disgust and headache as well as environmental influences such as acid rain, ozone depletion in the stratosphere, photochemical smog [4-6]. With this in mind, the regulations on nitrogen oxide emission standards have gradually been tightened, and scientists have also begun to study techniques to control and remove nitrogen oxides in order to meet emission requirements and improve quality of life.

Among the flue gas treatment technologies for nitrogen oxides, the wet scrubbing method (chemical oxidation and absorption) can simultaneously remove a variety of acid gases (nitrogen oxides and sulfur oxides) and be operated at room temperature [7], so it is one of the technologies with considerable development potential.

doi:10.6342/NTU202102462

It is also noteworthy that the wet washing process is carried out with high-gravity technology. High-gravity technology (also known as HiGee) consists in the process which was operated in a rotating packed bed (RPB) and the centrifugal force makes the system in a high-gravity field in order to achieve the effect of process intensification [8]. When using high-gravity technology for wet scrubbing to remove air pollutants, the liquid film generated in the packed bed and the droplets can greatly increase the material transport efficiency of pollutants [9]. Compared to the conventional packed bed, wet washing with RPB reduces the height of the transfer unit (HTU) due to the increase in the mass transfer coefficient, and the design volume of the fixed bed can be greatly reduced [10].

Based on the above, it is imperative to develop more effective nitrogen oxide control technologies so that nitrogen oxide emission levels comply with Taiwan standard and reduce the impact on the environment and ecology. The wet scrubbing process combined with the high-gravity technology for nitrogen oxide control will be a promising technology.

doi:10.6342/NTU202102462

1.2 **Objectives**

In this study, the nitrogen oxide removal experiment was carried out with a pilot experiment. During the experiment, various reagents were tested in the gas phase and liquid phase in order to investigate the removal mechanism of nitrogen oxides in the oxidation and absorption process.

The mass transfer conditions in the rotating packed bed were changed by manipulating the high-gravity factor and the gas-liquid ratio, and the control effects of nitrogen oxides were compared. In addition, different combinations of gas/liquid phase reagent and different concentration ranges were also tested in the experiment in order to improve the efficiency of nitrogen oxide removal and to extend the available pollutant concentration interval via this method. Regression analysis and theoretical derivation are used to create a predictive model for the nitrogen oxide removal.

Finally, through the analysis methods of energy consumption and cost evaluation, comprehensively evaluated the feasibility and development of actual operations in the future market about this method.

doi:10.6342/NTU202102462

In brief, the objectives of this research were shown below:

A. To evaluate the effect of removing nitrogen oxides by a rotating packed bed (RPB) under the different operating conditions

B. To elucidate the contribution of oxidation and absorption for nitrogen oxides removal ratio respectively.

C. To establish theoretical and empirical models for predicting the mass transfer coefficients during the RPB process.

D. To comprehensively analyze the pros and cons of removing nitrogen oxides by the RPB.

doi:10.6342/NTU202102462

Chapter 2 Literature Review

2.1 Nitrogen Oxides

The term (nitrogen oxides) is actually a collection of various compounds made up of nitrogen and oxygen. In order to classify these nitrogen oxides more effectively, the United States Environmental Protection Agency divided the nitrogen oxides into three groups (NO_X, NO_Y and NO_Z) in the research report on nitrogen oxides [11]. The abbreviation NO_Y refers to nitrogen oxides including all forms of oxidized nitrogen (N) compounds (nitrogen oxide, nitrogen dioxide and all other oxidized N-containing compounds that are formed from nitrogen oxide and nitrogen dioxide). The term NO_X specifically refers to the sum of nitrogen oxide and nitrogen dioxide. The word NO_Z refers to various nitrogenous species that are produced by oxidation-reduction reactions. Figure 2- 1 shows the relationship between NO_X, NO_Y and NO_Z and reactions of nitrogen oxides in the ambient air. The area enclosed by the dashed line is NO_X (the sum of nitrogen oxide and nitrogen dioxide). The outer layer refers to NO_Z, which contains nitrogen oxides that are formed from reactions of NO_X. Nitrogen oxides in the outer and inner boxes (NO_X + NO_Z) are collectively referred to as NO_Y [12].

doi:10.6342/NTU202102462

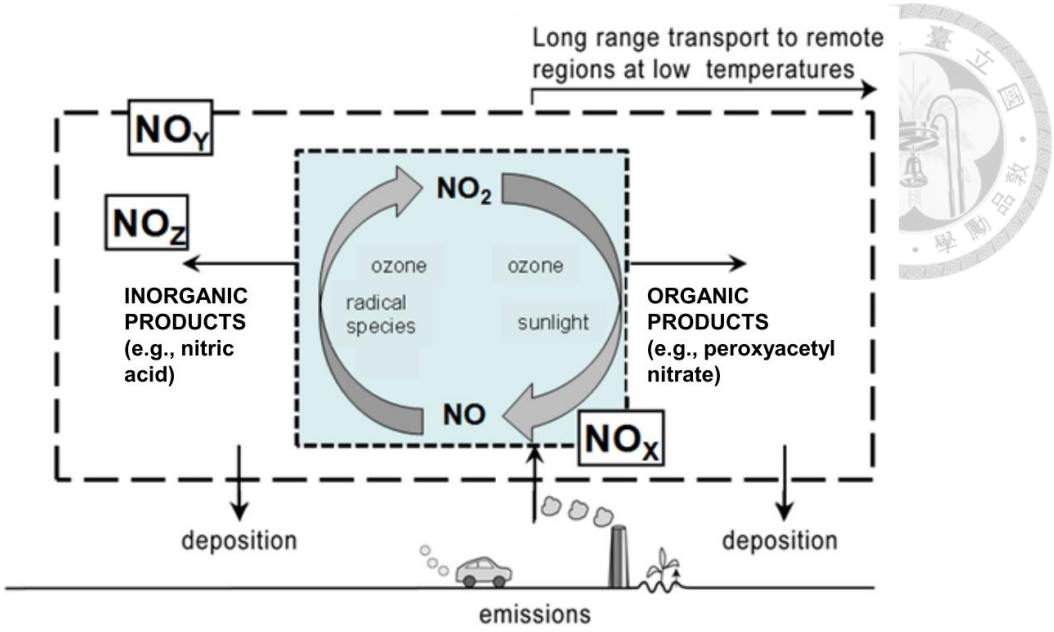

Figure 2- 1 Reactions of oxides of nitrogen species in the ambient air [12]

2.1.1 Formation and Emission Source about Nitrogen Oxides

The source of nitrogen oxides can be roughly divided into combustion process (high temperature process) and chemical industries related to nitric acid treatment (as shown in Figure 2- 2).

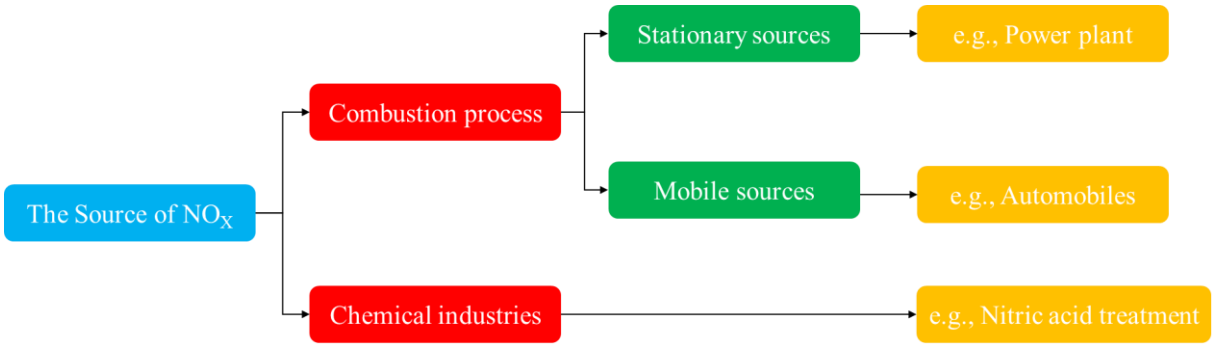

Figure 2- 2 Source classification of nitrogen oxides

doi:10.6342/NTU202102462

Figure 2- 4 and Figure 2- 3 show the contribution of individual industries to Europe and the United States of nitrogen oxide emissions, either in Europe or the United States, it could be found that the transportation system accounts for the largest amount, followed by energy related [13, 14].

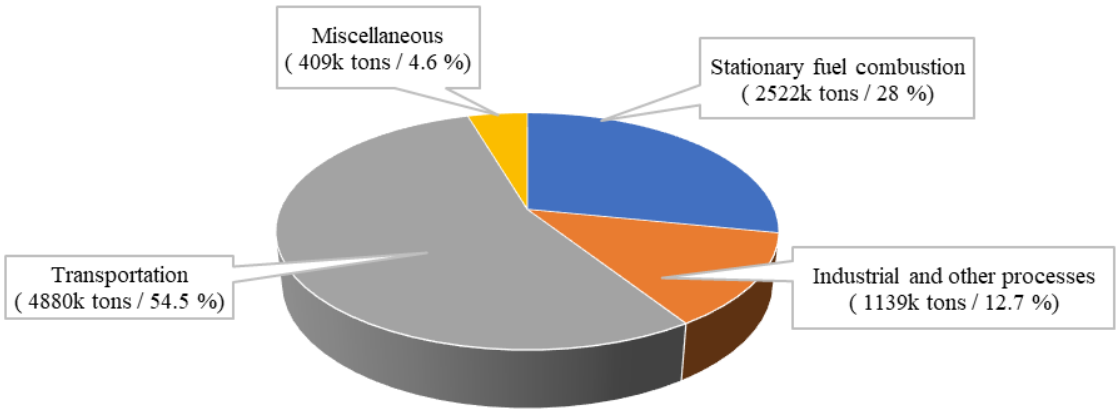

Figure 2- 4 Nitrogen oxides emission contributions in 2019 in the United States

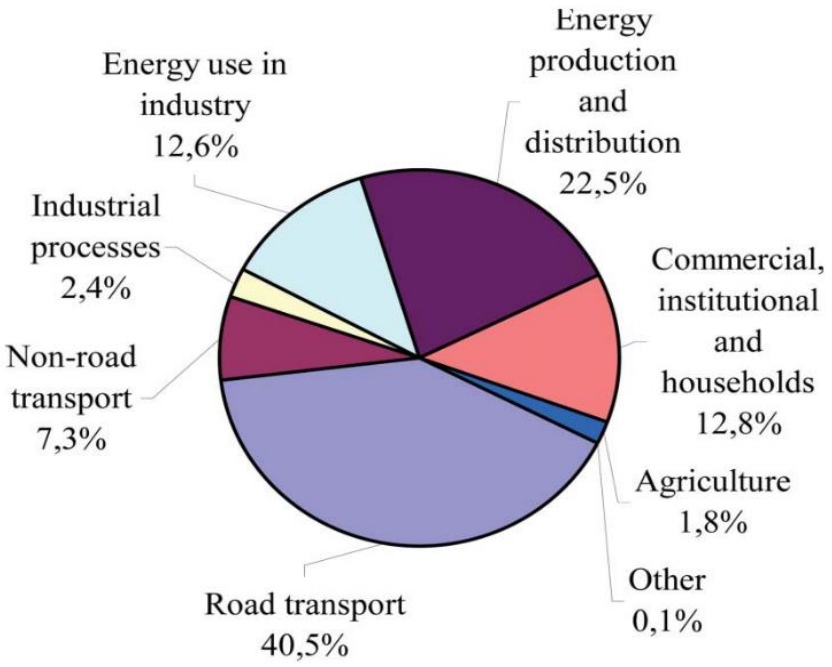

Figure 2- 3 Nitrogen oxide emission sources in 2011 in the EU [14]

doi:10.6342/NTU202102462

It is noteworthy that nitrogen oxide emissions from the transportation and energy industries are all related to the combustion process. NO_X, which is emitted from high-temperature processes, consists of 95% NO and 5% NO_2 [15]. On the other hand, the proportion of nitrogen oxide emissions from vehicles is also influenced by the composition of the fuel. Map Book et al. stated that the ratio of NO_2 / NO_X for various fuels: <0.2 vol.% for petroleum; 5.9 vol.% For diesel; 11.0 vol.% For diesel trucks [16].

The mechanism of the nitrogen oxides produced during combustion has also been extensively investigated (Table 2- 1) [17, 18]. There are three mechanisms for the formation of NO_X (thermal, fuel and prompt NO_X): (a) Thermal NO_X, which is formed at high temperatures in reaction with oxygen atoms. NO_X formation takes place at temperatures above 1500 ° C; (b) fuel NO_X produced by oxidation of N-containing fuel; (c) instant NO_X produced by the reaction of hydrocarbon (HC) free radicals with molecular nitrogen by burning HCs at low temperatures under fuel-rich conditions can be and within a short period of resistance [18-20].

Table 2- 1 The mechanism of nitrogen oxides produced by the combustion process

Type	Reaction	Remark
Fuel NO_X	$NH_2 + 1/2O_2 \rightleftharpoons NO + H_2$ $N\cdot + O_2 \rightleftharpoons NO + O\cdot$	-
Thermal NO_X	$N_2 + O\cdot \rightleftharpoons NO + N\cdot$ $N\cdot + O_2 \rightleftharpoons NO + O\cdot$	>1500 °C
Prompt NO_X	$HC\cdot + N_2 \rightleftharpoons HCN + N\cdot$ $N\cdot + O_2 \rightleftharpoons NO + O\cdot$	-

doi:10.6342/NTU202102462

2.1.2 Characteristics and Hazard of Nitrogen Oxides

There are numerous kinds of nitrogen oxides in the environment: NO, NO_2, NO_3, N_2O, N_2O_3, N_2O_4 and N_2O_5 (Table 2- 2)[15, 21]. Among the many nitrogen oxides, N_2O, NO, and NO_2 have be attracting the more attention due to chemical properties and emission characteristics.

Table 2- 2 Properties of selected nitrogen oxides [15, 21]

Properties / Species	Color	State (25°C, 1atm)	Density (g/dm^3)	Henry Law Constant ($mole \cdot m^{-3} \cdot Pa^{-1}$)	Solubility in water (g/dm^3)
NO	Colorless	Gas	1.34	$1.9\times10^{-5} \sim 2.3\times10^{-5}$	0.032
NO_2	Red-brown	Gas	3.4	$6.9\times10^{-5} \sim 3.4\times10^{-4}$	213.0
NO_3	-	Gas	-	$3.4\times10^{-4} \sim 1.2\times10^{-1}$	-
N_2O	Colorless	Gas	1.8	$1.8\times10^{-4} \sim 2.5\times10^{-4}$	0.111
N_2O_3	Black	Liquid	1447	$5.9\times10^{-3} \sim 2.5\times10^{-1}$	500.0
N_2O_4	Colorless	Liquid	1492	$1.3\times10^{-2} \sim 3.1\times10^{-2}$	213.0
N_2O_5	White	Solid	2050	$2.1\times10^{-2} \sim \infty$	500.0

* Density for NO in 293 K; for N_2O_3 in 275 K; for N_2O_4 in 273 K; for N_2O_5 in 288 K

* Henry Law Constant for 298.15 K

N_2O in the troposphere is a more stable species. Therefore, the lifespan of N_2O is longer than that of the other nitrogen oxides. If N_2O got into the stratosphere, it would break down into NO and NO_2, which depletes the ozone layer and reduces the ozone. In addition, N_2O is also a greenhouse gas which not only has a longer lifespan, but also absorbs infrared radiation with an intensity 270 times higher than carbon dioxide [22, 23], so that the effects of N_2O on the environment cannot be neglected.

doi:10.6342/NTU202102462

NO and NO_2 were considered to be more toxic compounds in nitrogen oxides. NO can cause eye and throat irritation. As most radicals, NO is unstable and oxidized into nitrogen dioxide easily in the environment. Therefore, in many nitrogen oxide studies related to human health hazards, the main objective of investigation is nitrogen dioxide. NO_2 which even at low doses can result in acute lung injury with pneumonitis and fulminant pulmonary edema [24]. Besides, Chaloulakou et al. also indicated that high outdoor NO_2 concentration observed in residential areas contributes to increased respiratory and cardiovascular diseases and mortality [25].

On the other hand, many complex reactions involved in NOx in the atmosphere (Figure 2- 5) [26]. NO_X reacted with various components in the atmosphere to generate nitric acid, which acidifies rainwater, and nitrates also become the main source of particulate matter; NO_X affects the ozone cycle. It may change into a precursor for ozone generation in the troposphere and cause ozone depletion in the stratosphere; NO_X is the precursor of photochemical smog. Hydrocarbon compounds were converted into peroxy radicals via hydroxyl radicals and oxygen, and then peroxy radicals reacted with nitrogen dioxide to form peroxyacetyl nitrate (PAN) which was the main component of photochemical smog [27]. It could be seen that nitrogen oxides have a considerable impact on human health and the natural environment.

doi:10.6342/NTU202102462

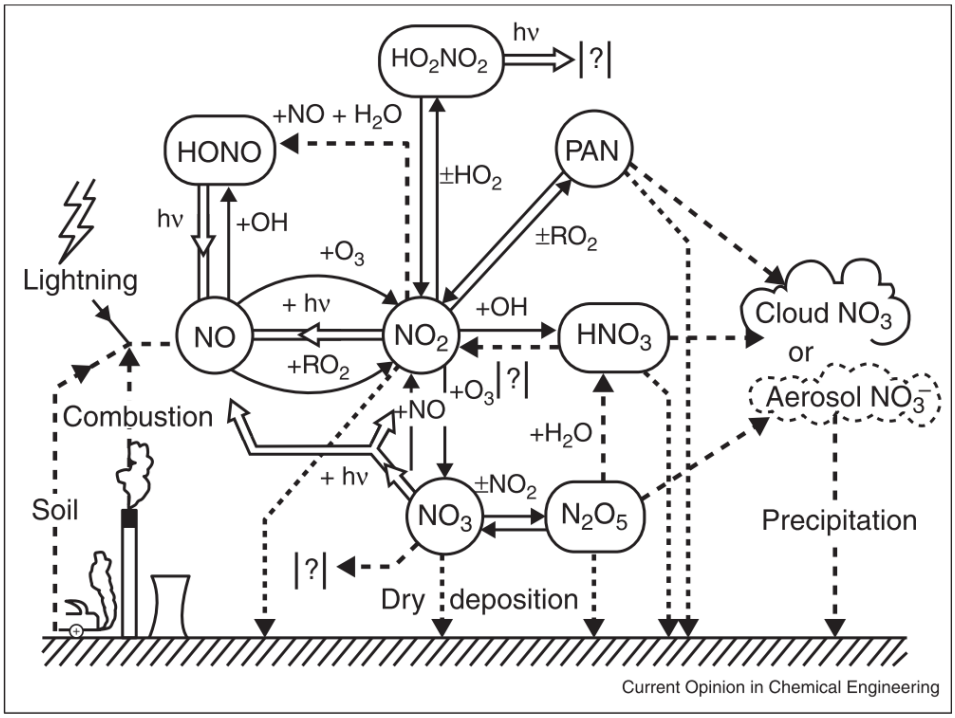

Figure 2- 5 Chemical transformations of atmospheric nitrogen oxides

doi:10.6342/NTU202102462

2.2 **Abatement Technology for Nitrogen Oxides Control**

The control methods of nitrogen oxides could be roughly divided into two categories: process modification and flue gas treatment (Figure 2- 6) [7]. Process modification included fuel purification (reduction of nitrogen content) and adjustments of operational conditions for purpose of decreasing the NO_X formation; flue gas treatment mean that dealing with nitrogen oxides in exhaust gases from process.

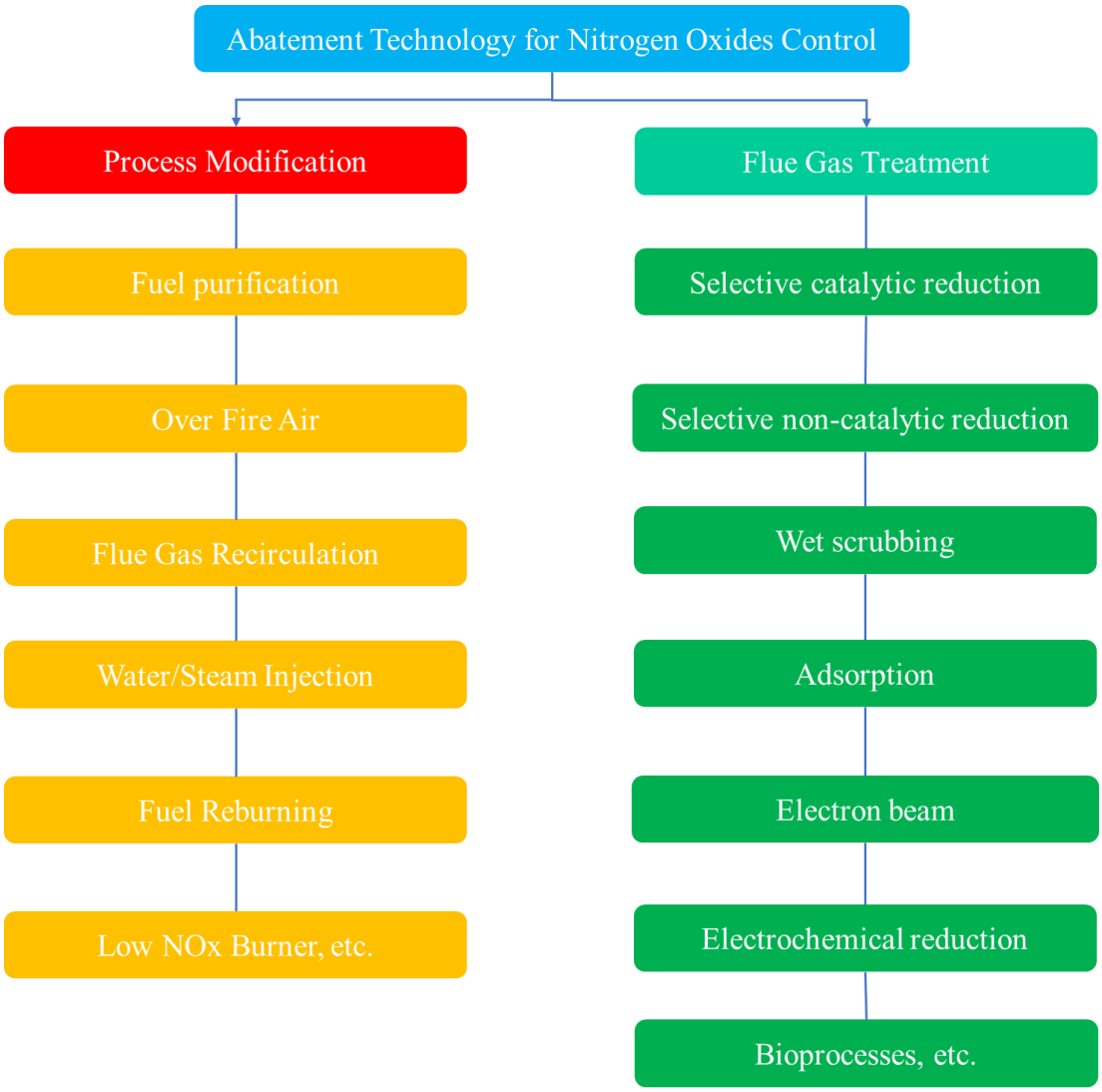

Figure 2- 6 Classification of abatement technology for nitrogen oxides control [7]

doi:10.6342/NTU202102462

2.2.1 Technology about Removing Nitrogen Oxides

The following briefly introduced the principle and comparison of various nitrogen oxide control methods (Table 2- 3 and Table 2- 4) [7, 13, 15, 17, 28]. Next, the application of wet scrubbing method would be explained in detail.

A. Process modification:

(a) Fuel Purification: reduce the formation of nitrogen oxides by diminishing the nitrogen content of the fuel or choosing alternative fuels [29].

(b) Over Fire Air: In the case of sufficient fuel, air was injected in stages to reduce the oxygen concentration and combustion temperature, and reduce the concentration of nitrogen oxides [30].

(c) Flue Gas Recirculation: reduce the oxygen concentration and combustion temperature in the reaction zone by means of flue gas reflux to inhibit the formation of nitrogen oxides.

(d) Water/Steam Injection: inject steam or water to lower the temperature in the combustion zone.

(e) Fuel Reburning: add additional fuel into the combustion chamber to make it appear a second combustion zone, where hydrocarbon radicals would be generated which could react with nitrogen oxides [31].

doi:10.6342/NTU202102462

(f) Low NOx Burner: a burner that injected air and fuel in stages, the effect is similar to “Over Fire Air” and “Fuel Reburning”.

Table 2- 3 The comparison of process modification [7, 13, 15, 17, 28]

Method	Efficiency	Advantages	Disadvantages
Fuel Purification	-	(1) Easy to operate (2) Suitable for existing factories	(1) Higher alternative fuel prices (2) Poor efficiency on thermal NO_X and prompt NO_X
Over Fire Air	10 ~ 44 %	(1) Useful for retrofit of existing power plants (2) Suitable for all fuels	(1) Low NOx reduction
Low NOx Burner	20 ~ 60 %	(1) Suitable for existing factories (2) Low operating cost	(1) High levels of CO (2) High capacity cost
Flue Gas Recirculation	20 ~ 50 %	(1) High NOx reduction potential for low nitrogen fuels	(1) High capital cost (2) High operating cost (3) Affects heat transfer and system pressures (4) High energy consumption (5) Flame instability
Water/Steam Injection	70 ~ 80 %	(1) Moderate capital cost (2) NOx reduction similar to FGR	(1) Efficiency penalty (2) Fan power higher
Fuel Reburning	50 ~ 60 %	(1) Moderate cost (2) Moderate NOx removal	(1) Extends residence time (2) Incomplete combustion

doi:10.6342/NTU202102462

B. Flue gas treatment:

(a) Selective catalytic reduction: the most commonly used technology to clean the flue gases by using ammonia, urea, or hydrocarbon reductants to convert NO and NO_2 to nitrogen [32].

(b) Selective non-catalytic reduction: in spite of using catalyst, the reduction reaction takes place at high temperatures [33].

(c) Electron beam: off-gas was irradiated through the electron beam, generating the radicals which would undergo a series of reactions and finally become $(NH_4)_2SO_4$ and NH_4NO_3 [34].

(d) Electrochemical reduction: in spite of using chemicals reductant for oxidation, used electromotive force to drive the reduction reaction of nitrogen oxides and generated nitrogen or other forms of oxidized ions [35].

(e) Bioprocesses: the denitrification reaction of microorganisms was used to remove nitrogen oxides from the air. The actual method included bio-scrubber, trickle-bed reactor, biofilter, etc.[15]

(f) Wet scrubbing: the nitrogen oxides in the air were first oxidized to higher valence compounds and then absorbed by water.

doi:10.6342/NTU202102462

Table 2- 4 The comparison of flue gas treatment [7, 13, 15, 17, 28]

Method	Condition	Efficiency	Advantages	Disadvantages
Selective catalytic reduction	NO_X: 100 ~ 5000 ppm	89 ~ 100 %	(1) High efficiencies (2) Low operating cost (3) Relatively simple installation	(1) High costs of catalysts ammonia (2) Corrosion of equipment (3) Limited life span of catalyst (4) Large amount of wastes
Selective non-catalytic reduction	NO_X: 125 ~ 1450 ppm	30 ~ 80 %	(1) Low capital and operating cost (2) High PM level are acceptable	(1) Low efficiency (2) Unsuitable for low concentration feed (3) High temperature required
Electron beam	NO_X: 160 ~ 1000 ppm	Up to 80 %	(1) Dry method (2) No wastes (3) Useful by-product	(1) High energy costs
Electrochemical reduction	NO_X: 3000 ppm	Up to 99.6 %	(1) Not consuming any reductant	(1) In early stage of development (2) Still lots of mechanisms unknown
Bioprocesses	NO_X: 20 ~500 ppm	36 ~ 100 %	(1) Low operating cost	(1) Requires cooling system for exhaust gases (2) Problem with excess biomass
Wet scrubbing	NO_X: 50 ~ 5000 ppm	36 ~ 100 %	(1) Conduct in ambient temperature (2) Highly adaptable to flue gas load	(1) High volume of liquid wastes (2) Large multi-stage scrubbers

doi:10.6342/NTU202102462

C. The wet scrubbing

The wet scrubbing method mainly transfer the NO_X from the flue gas to the water phase. However, the solubility of NO is low (1.93×10^{-3} mol·L^{-1}·atm^{-1}, at 25 °C), so the wet scrubbing method added chemical reagent, catalyst or energy to the gas or liquid phase to oxidize NO, and make it easier to be captured by water.

According to the way of oxidizing nitrogen oxides, the wet scrubbing could be classified into three categories (Figure 2- 7):

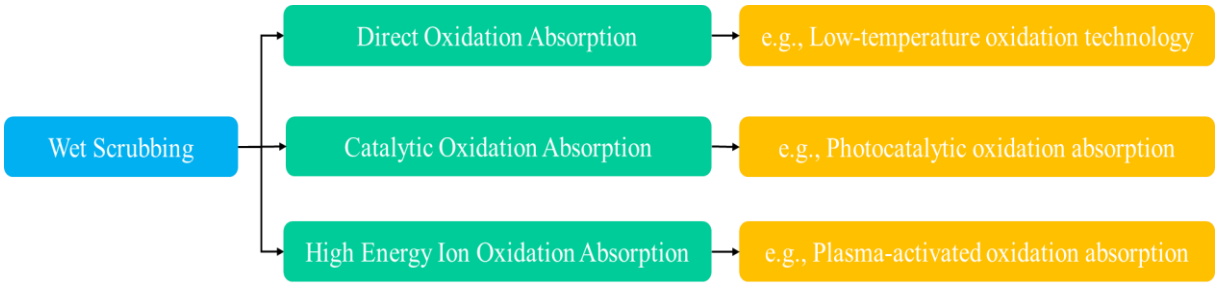

Figure 2- 7 The types of the wet scrubbing

(a) Direct oxidation absorption: this technique included oxidation-absorption pathway and absorption-oxidation pathway [36]. In the oxidation-absorption pathway, NO_X were directly oxidized into high-valent nitrogen oxides by the agent in the gas phase, and then absorbed by water. On the contrary, the absorption-oxidation process pathway was to first absorb nitrogen oxides into water, and NO_X were oxidized subsequently in liquid phase.

doi:10.6342/NTU202102462

(b) Catalytic oxidation absorption: the method was similar to direct oxidation absorption. Furthermore, a catalyst would be added to increase the reaction rate and efficiency of nitrogen oxides and reagents [37]

(c) High energy ion oxidation absorption: the difference between this technology and the previous two was that it did not use chemicals agent to react with nitrogen oxides, but use high-energy corona electron beams, etc. [38, 39]

Among the three types of wet washing methods, the direct oxidation method was the earliest developed and lower cost, so it was a commonly used technique. Next, the following would introduce the commonly used agents in the direct oxidation method.

doi:10.6342/NTU202102462

2.2.2 Oxidation-Absorption with Gas Phase Agents

The oxidation-absorption process in direct oxidation absorption was a way to remove nitrogen oxides through first oxidation and then absorption. Therefore, chemical agents are added in the gas phase to react with nitrogen oxides. Usual gaseous oxidant included:

A. Ozone (O_3)

Many studies have pointed out that ozone was an effective gas phase oxidant with high oxidation efficiency, fast oxidation speed, and nontoxic by-products (Table 2- 5) [40]. Skalska et al. found that NO_2 conversion rate was up to almost 100% with a residence time around 7 seconds [41]. In addition, there were also many techniques developed with ozone, including LoTOx, PhoSNOX, Thermalmox^{TM}, etc. [42, 43]

Table 2- 5 Reaction kinetic of NO_X reactions with ozone [40]

Reaction	Rate Constant ($m^3 \cdot kmole^{-1} \cdot s^{-1}$)	Number
$NO + O_3 \rightleftharpoons NO_2 + O_2$	2.59×10^{9} exp (-3.176/RT)	R- 1
$NO_2 + O_3 \rightleftharpoons NO_3 + O_2$	8.43×10^{7} exp (-4.908/RT)	R- 2
$NO_2 + NO_2 \rightleftharpoons N_2O_4$	6.98×10^{-15} exp (6866/T)	R- 3
$NO + NO_2 \rightleftharpoons N_2O_3$	4.12×10^{-13} exp (4869/T)	R- 4
$N_2O_3 + O_3 \rightleftharpoons N_2O_4 + O_2$	-	R- 5
$N_2O_4 + O_3 \rightleftharpoons N_2O_5 + O_2$	$7.98\times10^{17}\times T^{-3.9}$	R- 6
$N_2O_5 \rightleftharpoons NO_2 + NO_3$	1.21×10^{17} exp (-25.4/T)	R- 7
$NO_2 + NO_3 \rightleftharpoons N_2O_5$	$3.86\times10^{8}\times T^{0.2}$	R- 8
$NO + NO_3 \rightleftharpoons 2NO_2$	1.08×10^{10} exp (0.219/RT)	R- 9
$HNO_2 + O_3 \rightleftharpoons HNO_3 + O_2$	$^{*}3.01\times10^{5}$	R- 10

* Rate constant for $L \cdot mole^{-1} \cdot s^{-1}$ in R- 3, R- 4, R- 6 and R- 10.

doi:10.6342/NTU202102462

B. Chlorine dioxide (ClO_2)

Chlorine dioxide has been proved to be the very promising oxidant for NO_X removal (Table 2- 6) [44, 45]. Hulte´n et al. had carried out the experimental about oxidation of NO by gaseous ClO_2 and absorption was carried out, the total NOx reduction at 0.6 (ClO_2/NO) mole ratio was between 79 % and 94 % [46]. Furthermore, ClO_2 was soluble, so the use of chlorine dioxide could simultaneously oxidize nitrogen oxides in the gas and liquid phases, and both acidic and alkaline presented high oxidation efficiency and removal efficiency [47].

Table 2- 6 Reaction kinetic of NO_X reactions with $ClO_{2(g)}$ in 298 K [44, 45]

Reaction	Rate Constant ($m^3 \cdot kmole^{-1} \cdot s^{-1}$)	Number
$NO + ClO_2 \rightleftharpoons NO_2 + ClO$	6.62×10^{7}	R- 11
$NO + ClO \rightleftharpoons NO_2 + Cl$	3.73×10^{9}	R- 12
$NO_2 + ClO \rightleftharpoons ClNO_3$	$^{*}5.94\times10^{10}$	R- 13
$ClNO_3 \rightleftharpoons NO_2 + ClO$	1.66×10^{15}	R- 14
$ClNO_3 + Cl \rightleftharpoons Cl_2 + NO_3$	3.73×10^{9}	R- 15
$Cl + ClO_2 \rightleftharpoons 2ClO$	1.93×10^{10}	R- 16
$2ClO \rightleftharpoons Cl + ClO_2$	2.11×10^{8}	R- 17
$2Cl \rightleftharpoons Cl_2$	$^{*}5.80\times10^{8}$	R- 18

*Different unit ($cm^6 \cdot mole^{-2} \cdot s^{-1}$) and order (3) for R- 13 and R- 18

C. Vaporized composite oxidant (VCO)

VCO was a gas-phase oxidant mixed with multiple agents. It was worth noting that the main components of the mixed reagents were not gaseous under normal temperature and pressure, so the reagents were vaporized through different procedures.

doi:10.6342/NTU202102462

2.2.3 Absorption-Oxidation (Reduction) with Liquid Phase Agents

The absorption-oxidation (reduction) process in direct oxidation absorption was a way to remove nitrogen oxides through first absorption and then oxidation (reduction). Therefore, chemical agents are added in the liquid phase to react with nitrogen oxides. Usual liquid reagents included:

A. Sodium hydroxide (NaOH)

Sodium hydroxide mainly provided a strong alkaline environment, so that nitric acid and nitrous acid could be neutralized [40].

B. Sodium carbonate (Na_2CO_3)

Solution of sodium carbonate was used to react with nitrogen dioxide from flue gas. Na_2CO_3 would react with NO_2 to produce $NaNO_3$, $NaNO_2$ and CO_2. Usually used in gases with a high ratio of NO_2/NO_X [48].

C. Sodium sulfite (Na_2SO_3)

The scientist found that the main component of the absorption liquid about simultaneous removal of nitrogen oxides and sulfur dioxide was sulfite. Therefore, engineers began to study the reaction between sulfite and nitrogen oxides, and found that sulfite could convert nitrogen oxides into other species [49, 50]. It was noteworthy that Na_2SO_3 was used as a reducing agent instead of an oxidizing agent.

doi:10.6342/NTU202102462

D. Urea ($(NH_2)_2CO$)

Urea was a strong reducing agent with slightly alkaline. Compared to other reagents, urea was non-toxic reactant, and reaction product could be recycled or released into the atmosphere directly [51].

E. Other chemical agents

In addition to the above mentioned, there were still many oxidants that had been continuously studied, and some had also been used commercially (sodium chlorite, hydrogen peroxide, potassium permanganate, etc.)

Table 2- 7 Reaction kinetic of NO_X reactions with liquid agents in 298 K

Species	Reaction	Number
NaOH	$HNO_3 + NaOH \rightleftharpoons NaNO_3 + H_2O$	R- 19
	$HNO_2 + NaOH \rightleftharpoons NaNO_2 + H_2O$	R- 20
Na_2CO_3	$2NO_2 + Na_2CO_3 \rightleftharpoons NaNO_3 + NaNO_2 + CO_2$	R- 21
	$3HNO_3 + NaNO_2 \rightleftharpoons 3NaNO_3 + 2NO_2 + H_2O$	R- 22
Na_2SO_3	$2NO_2 + SO_3^{2-} + H_2O \rightleftharpoons 2NO_2^- + SO_4^{2-} + 2H^+$	R- 23
	$2NO + 2SO_3^{2-} \rightleftharpoons 2SO_4^{2-} + N_2$	R- 24
	$NO_2^- + 2HSO_3^- + H^+ \rightleftharpoons HON(SO_3)_2^{2-} + H_2O$	R- 25
	$NO_2^- + HSO_3^- + H^+ \rightleftharpoons HSO_4^- + 1/2N_2O + H_2O$	R- 26
	$HNO_2 + HSO_3^- \rightleftharpoons HSO_4^- + 1/2N_2O + 1/2H_2O$	R- 27
	$N_2O + SO_3^{2-} \rightleftharpoons SO_4^{2-} + N_2$	R- 28
$(NH_2)_2CO$	$2HNO_2 + (NH_2)_2CO \rightleftharpoons 2N_2 + CO_2 + 3H_2O$	R- 29
	$6HNO_3 + 5(NH_2)_2CO \rightleftharpoons 8N_2 + 5CO_2 + 13H_2O$	R- 30
	$6NO_2 + 4(NH_2)_2CO \rightleftharpoons 7N_2 + 4CO_2 + 8H_2O$	R- 31
	$6NO + 2(NH_2)_2CO \rightleftharpoons 5N_2 + 2CO_2 + 4H_2O$	R- 32
	$(NH_2)_2CO + 2H_2O \rightleftharpoons 2NH_4^+ + CO_3^{2-}$	R- 33

doi:10.6342/NTU202102462

2.3 **Rotating Packed Bed: Principle and Practice**

Rotating packed bed (RPB) was process intensification technologies. RPB has been widely researched and applied in recent years, due to its high mass transfer efficiency [52]. The first RPB was proposed by Ramshaw and co-authors in 1983. Since the development of RPB, many different types of rotating packed beds have been developed, such as different gas-liquid contact types (counter-current, cross-current and counter-current), varied packings (nickel foam and wire mesh), etc. The various RPB have been applied in many fields (distillation, absorptions, adsorption, stripping, extraction, heat transfer, and so on)[10]. RPB can generate a high-gravity environment in the internal packed bed through rotation, and the high-gravity environment can increase the mass transfer efficiency between different phases. Therefore, the following would introduce the mass transfer theory and characteristics between gas and liquid and the practical operation in RPB.

2.3.1 Principle: Characteristics and Mass Transfer

A. Characteristics of gas flow

Regarding the characteristics of the gas in RPB, scientists often discuss the influence of gas flow and velocity on the operation of the rotating packed bed. Gas flow and velocity often affect important parameters such as pressure drop and mass transfer efficiency during operation, so they are widely mentioned in the related research.

doi:10.6342/NTU202102462

Guo, et al. indicated that the increasing gas flow rate could enhance the mass transfer coefficient in cross-flow rotating packed bed [53]. In addition, Liu et al. discussed the adsorption characteristics of activated carbon in rotating packed bed, and they found that it had better adsorption efficiency with high flowrate [54].

Furthermore, pressure drop is also an important operating parameter. The pressure drop of a rotating packed bed is mainly caused by three reasons (centrifugal force, shear stress and structure) [55]. At present, many scholars have used dimensional analysis and regression to predict the pressure drop of a rotating packed bed [56-58]. In recent years, they have also used computational fluid dynamics to observe the gas movement in a rotating packed bed [59]. Therefore, people can use the qualified model according to the actual situation during operation to help us predict the pressure drop [60].

B. Characteristics of liquid flow

The characteristics of liquid in a rotating packed bed include liquid flow pattern, liquid hold-up, liquid film thickness, residence time, etc. Through changes in operating conditions, the characteristics of liquid in RPB may be affected, and the results of process may be change.

In the rotating packed bed, the liquid enters the packed bed from the distributor, and starts to accelerate and disperse due to centrifugal force. Research indicates that liquids may exhibit three flow pattern under different gravitational fields (centrifugal

doi:10.6342/NTU202102462

force): pore flow, film flow and droplet flow (Figure 2- 8)[61]. Researchers also performed the visual study of flow pattern and found that the liquid in the packing existed as films attached to the packing wire and filling the voids of the packing with low high-gravity factor (<60 g), but as films on the packing wire, the droplets and small amounts of filaments in the voids of the packing when the gravity level was high (>100 g)[62, 63].

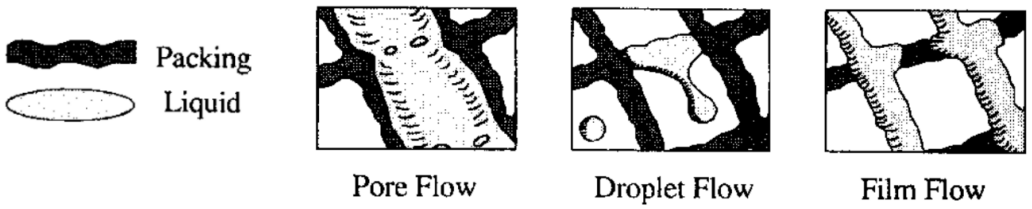

Figure 2- 8 Three types of liquid flow within a rotating packed bed [61]

In terms of liquid flow, Burn et al. discussed the liquid hold-up and residence time in the RPB with high-porosity packing by measuring conductivity. This study found that the liquid hold-up decreased as the rotational speed increased, but rise as the superficial velocity and viscosity of the liquid increase, and before reaching the overflow point, the liquid hold-up was almost unaffected by the gas flow rate [64]; in the light of liquid film thickness, Munjal et al. proposed that the thickness of the liquid film is inversely proportional to the 2/3 power of the rotational speed and the smaller the thickness of the liquid film, the smaller the mass transfer resistance [65, 66].

doi:10.6342/NTU202102462

On the other hand, residence time and effective mass transfer area are also important characteristics of liquids. The residence time needs to reach a certain time to achieve the ideal process enhancement effect, and the common residence time is about 0.2 to 0.8 seconds [67]; the effective mass transfer area is the interface for actual mass transfer. Some scholars have proposed that the effective mass transfer area in a rotating packed bed can be predicted by the regression equation from traditional packed bed [68]. In recent years, a prediction model has been developed by dimensional analysis and regression during the actual experiments with rotating packed beds [69, 70].

In order to predict each important liquid parameter, many theoretical and experimental prediction models have been established through the integration of computational fluid dynamics and experimental data [71-73].

Table 2- 8 Calculation formula of liquid parameters

Parameter	Expression	References	Number
ε_L	$\varepsilon_L = 0.039(\frac{a_c}{g_o})^{-0.5}(\frac{u}{u_o})^{0.6}(\frac{\nu}{\nu_o})^{0.22}$	[64]	Eq- 1
u	$u = \frac{\omega \cdot Q_L^{0.4} r^{0.1} \nu^{-0.22}}{2 \cdot \pi \cdot Z \cdot E_C}$	[64]	Eq- 2
δ	$\delta = 4.20 \times 10^8 \frac{\nu L}{a_t \omega^2 R}$	[53]	Eq- 3
$\frac{a_e}{a_t}$	$\frac{a_e}{a_t} = 1 - \exp[-1.45(\frac{\sigma_c}{\sigma})^{0.75} Re_L^{0.1} We_L^{0.2} Fr_L^{-0.05}]$	[68]	Eq- 4
$\frac{a_e}{a_t}$	$\frac{a_e}{a_t} = 66510 \cdot Re_L^{-1.41} We_L^{1.21} Fr_L^{-0.12} \varphi^{0.12}$	[74]	Eq- 5
d_p	$d_p = 0.7284(\frac{\sigma}{\omega^2 R \rho})^{1/2}$	[75]	Eq- 6

doi:10.6342/NTU202102462

C. Gas-liquid contact theory of absorption and mass transfer

In the process of strengthening the gas-liquid reaction, the mass transfer theories for describing gas-liquid contact in absorption include two-film theory [76], penetration theory [77], surface renewal theory [78], and film-penetration model [79].

The various theories used to explain gas-liquid mass transfer are similar in the gas phase, substance entered the gas-phase boundary film before entering the liquid phase, approaching the interface of the two phases gradually, and then reached a gas-liquid equilibrium state on the interface without interfacial resistance. However, the mass transfer in the liquid phase had a different description.

(a) Two-film theory: the two-film theory assumed that there is a liquid membrane on the liquid side of the interface, where the substance does not accumulate, and the substance transport is in a steady state, so the liquid side mass transfer film coefficient can be expressed as $k_L = \frac{D_L}{l}$

(b) Penetration theory: the penetration theory improves the assumption of the two-film theory for the steady-state mass transfer in the liquid phase. It described the mass transfer of the substance in an unsteady state, and deduced that mass transfer coefficient on the interface can be expressed as $k_L = \sqrt{\frac{4D_L}{\pi \cdot l}}$

(c) Surface renewal theory: the surface renewal theory also describes the mass transfer phenomenon in an unsteady state. In addition, this theory assumes that

doi:10.6342/NTU202102462

the liquid phase is composed of fluid elements that flow all the time, the flowing elements will always "renew" the composition of the interface, and mass transfer coefficient is expressed as $k_L = \sqrt{D_L \cdot S}$

(d) Film-penetration model: combined with the advantages of the previous theory, the film-penetration model points out that even in the case of turbulent flow, there is still a stagnant liquid film at the boundary of the liquid phase, and the material is transported in an unsteady state in the film.

At present, various gas-liquid contact theories have been applied to the mass transfer coefficient prediction of packed beds [65, 68, 80, 81](Table 2- 9). Moreover, many semi-theoretical models have been established through dimensional analysis and regression of experimental data. For the past few years, some scholars have used artificial neural networks to predict the mass transfer coefficient [82, 83].

Table 2- 9 The mass transfer coefficient prediction in packed beds through different gas-liquid contact theories

Theory	Expression	Reference	Number
Two film	$k_L(\frac{\rho_L}{\mu_L g})^{\frac{1}{3}} = 0.0051\left(\frac{L}{a\mu_L}\right)^{\frac{2}{3}}\left(\frac{\mu_L}{\rho_L D_L}\right)^{-\frac{1}{2}}(a_t d_p)^{0.4}$	[68]	Eq- 7
Penetration	$\frac{k_L d}{D} = \frac{2\cdot 3^{1/3}}{\pi} Sc_L{}^{1/2} Re_L{}^{1/3}(\frac{a_t}{a_e})^{1/3}(Gr_L)^{1/6}$	[80]	Eq- 8
Surface renewal	$k_L = \frac{S+1}{t}\sqrt{\frac{D_L}{S}}[(S\cdot t+0.5)\sqrt{erf(S\cdot t)} + e^{-St}\sqrt{\frac{S\cdot t}{\pi}}]$	[81]	Eq- 9

doi:10.6342/NTU202102462

In addition to the gas/liquid phase (or side) mass transfer (film) coefficient (k_G and k_L), in order to facilitate calculations, scientists also proposed the concept of overall gas/liquid phase mass transfer coefficient (K_G and K_L) and overall volumetric gas/liquid mass transfer coefficient, also known as capacity coefficient (k_Ga, k_La, K_Ga and K_La). Furthermore, the absorption process is often accompanied by solute reaction, so the absorption rate will be accelerated and the mass transfer coefficient will increase. At this time, the enhance factor (E) can be used to describe the degree of improvement on the mass transfer coefficient. In the enhance factor, it is often expressed as a function of the Hatta number (M), which is the ratio between the absorption rate and the diffusion rate. Table 2- 10 shows the relationship between each parameter.

Table 2- 10 The expression of parameter about mass transfer

Parameter	Expression	Reference	Number
k_G, k_L, K_G and K_L	$\frac{1}{K_G} = \frac{1}{k_G} + \frac{H}{k_L}$ $\frac{1}{K_L} = \frac{1}{Hk_G} + \frac{1}{k_L}$	[84]	Eq- 10 Eq- 11
E and k_L	$N_A = E \cdot k_L \cdot (C_{Ai} - C_{AL})$	[85]	Eq- 12
E	$E = \frac{\sqrt{M}[\sqrt{M}(\alpha - 1) + \tanh\sqrt{M}]}{\sqrt{M}(\alpha - 1)\tanh\sqrt{M} + 1}$	[86]	Eq- 13
M	$M = \frac{\sqrt{k_c \cdot C_B \cdot D_{AL}}}{k_L} = l \cdot \sqrt{\frac{k_c \cdot C_B}{D_{AL}}}$	[85]	Eq- 14

doi:10.6342/NTU202102462

2.3.2 Practice: Application of RPB

There are many areas where rotating packed beds are used for process enhancement, including removal of air pollutants [87-89], synthesis of nanomaterials, polymerization, emulsification, etc.[10] And here, we would focus on reviewing the related research on nitrogen oxide removal by rotating packed bed.

The method of removing nitrogen oxides in a rotating packed bed is usually classified as a direct oxidation absorption method. Compared with the conventional wet scrubbing, RPB can reduce the space and improve the removal efficiency. Table 2- 11 shows the research of using RPB to remove nitrogen oxides

Table 2- 11 Performance evaluation of NO_X removal by using different oxidants in rotating packed bed [90]

Gas composition	Reagent composition	Efficiency (%)	Remark	References
NO_x (as NO_2): 240 g/m^3	O_3: 6 g/h	90	O_3 oxidation	[91]
NO/NO_2: 0.8~1.5 (mol/mol)	Na_2CO_3: 15%	93	Alkaline absorption	[92]
NO_x: 1200 mg/m^3	O_3/NO_x: 0.6 NaOH (H_2O_2): 0.025 mol/L	NaOH: 80 H_2O_2: 85	Alkaline absorption	[93]
NO_x: 18,000-20,000 mg/m^3	Urea: 20 wt%	96	Wet urea absorption (2-class series)	[94]
NO: 1000 ppm	NaOH, $FeSO_4$•$7H_2O$, Na_2SO_3, Na_2EDTA•$2H_2O$	87	Aqueous Fe^{II}(EDTA) Solution (pH: 7)	[95]

doi:10.6342/NTU202102462

2.4 **Cost Benefit Analysis**

Cost benefit analysis takes project decision one step further, attempting to compare costs with the dollar value of benefits from the program. The cost benefit analysis could be applied at any time (before, after, or during a project implementation), and they can greatly assist decision makers to enhance the efficiency of program

The concepts and basic equations presented about cost benefit analysis were seemingly straightforward. However, obtaining exactly right estimates of costs and benefits could be extremely challenging. Every analysis required a host of assumptions, sometimes complex calculations, and the careful assessment. The process of cost-benefit analysis can be roughly represented by the following steps (Table 2- 12, adapted from Boardman, Greenberg, Vining, and Weimer, 2006) [96].

Table 2- 12 The steps of cost-benefit analysis

Step	Description
1	Set the framework for the analysis
2	Decide whose costs and benefits should be recognized
3	Identify and categorize costs and benefits
4	Project costs and benefits over the life of the program, if applicable.
5	Monetize (place a dollar value on) costs.
6	Quantify benefits in terms of units of monetize benefits.
7	Discount costs and benefits to obtain present values.
8	Compute a net present value for CBA.
9	Perform sensitivity analysis.
10	Make a recommendation where appropriate.

doi:10.6342/NTU202102462

Chapter 3 Materials and Methods

3.1 Research Framework

The research framework of this research is shown in Figure 3- 1. Taking the objectives as the main axis to extension and collection of literature, followed by theoretical calculations and experimental data discussion. Finally taking cost analysis and energy consumption as a comprehensive discussion in this study.

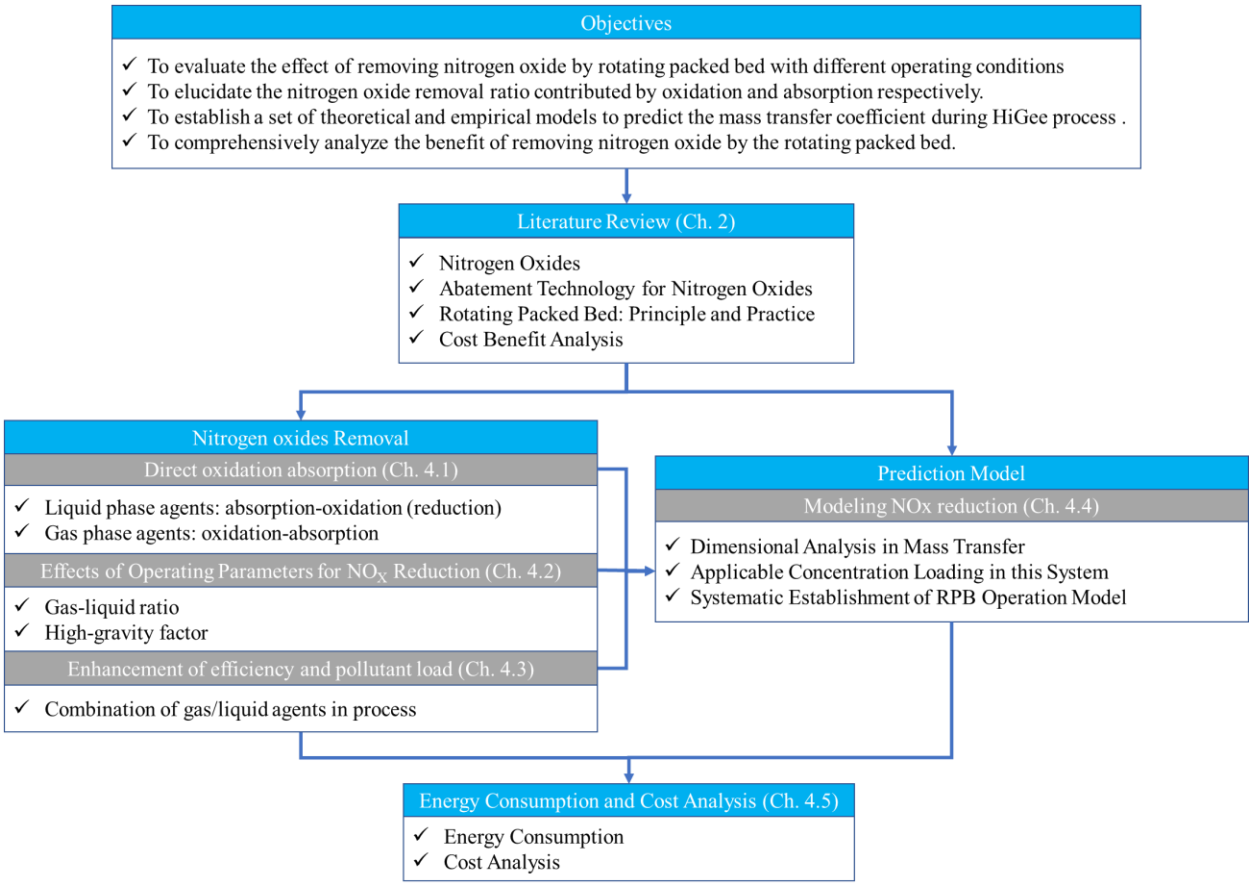

Figure 3- 1 Research framework in this study

doi:10.6342/NTU202102462

3.2 **Materials**

The materials used in this research could be divided into: (1) reagent, the chemical agent used in the experiment; (2) instrument and equipment, the device used in the research; (3) Apparatus, the reactor used in the study.

3.2.1 Reagents

A. Gas cylinder (nitrogen, oxygen and mixture of nitrogen oxides)

Both the nitrogen cylinder and the nitrogen oxide cylinder are provided by Qingfung company in Taiwan. Nitrogen cylinders were used to dilute the concentration of pollutants and serve as the carrier gas for pollutants; oxygen cylinders were used to generate ozone; the nitrogen oxides cylinder was composed of 1125 ppm of nitrogen monoxide and 125 ppm of nitrogen dioxide (the rest was filled with nitrogen), which was used as a pollution source for the experiment

B. Gas phase oxidants (ozone and chlorine dioxide)

Both chlorine dioxide (manufactured by chlorine dioxide generator) and ozone (made by ozone generator) were used as gas-phase oxidants that reacted with nitrogen oxides.

doi:10.6342/NTU202102462

C. Liquid phase agents (NaOH, Na_2CO_3, $NaSO_3$ and urea)

Sodium hydroxide, sodium carbonate, sodium sulfite and urea were all used as liquid-phase agents that reacted with nitrogen oxides. In addition, all the reagents mentioned above were purchased by Uni-ward Company in Taiwan.

D. Standard solution (sodium nitrate and sodium nitrite)

Sodium nitrate and sodium nitrite are used to configure the calibration line, when detecting the concentration of nitrate and nitrite in wastewater. Sodium nitrate and sodium nitrite were purchased by Uni-ward Company in Taiwan.

E. Silicone

Silicone provided by Uni-ward Company in Taiwan was used to remove moisture in gas pipelines.

doi:10.6342/NTU202102462

3.2.2 Instruments and Equipment

A. Mass Flow Controller

Mass flow controller (purchased from Protec Instrument Corporation, in United States, Figure 3- 2 (a)) was used to control the flow of nitrogen (carrier gas).

B. Flow meter

Flow meter (Figure 3- 2 (b)) purchased from All-Field Enterprise Corporation was used as a valve to adjust the flow rate (O_3, ClO_2 and NO_X), and it was calibrated through a precise dry-air flowmeter.

C. Ozone generator

Ozone generator (Figure 3- 2 (c)) was purchased from Triogen company and was equipped before the RPB to provide ozone used for oxidation of NO_X. The ozone generator used oxygen as a raw material, input energy to decompose the oxygen into oxygen atoms, and then oxygen atoms formed ozone through reaction with other oxygen molecules

D. Chlorine dioxide generator

Chlorine dioxide generator (Figure 3- 2 (d)) purchased from Higee Co., Ltd. in Taiwan. Chlorine dioxide gas was produced by the reaction about two agents (called catalyst and oxidant provided by Higee Co., Ltd.) in the RPB reactor.

doi:10.6342/NTU202102462

In addition, the chlorine dioxide concentration could be controlled by the flow rate of the blower inside the device.

E. Precise dry-air flowmeter

The type of precise dry-air flowmeter (Figure 3- 2 (e)) was BIOS Defender 510M, and it was purchased from Jusum Instruments Corporation, Ltd. E. Precise dry-air flowmeter was used to exactly measure volumetric air flow for the flow meter (A- 1).

F. pH meter, conductivity meter and thermometer

Both pH meter (type: TS-100, Figure 3- 2 (f)) and conductivity meter (type: SC-110) were purchased from Suntex Instruments Co., Ltd.; thermometer purchased from Hoyu company in Taiwan. These instruments were used to measure the pH, total solid dissolved, conductivity and temperature in the absorbent and waste liquid.

G. Electronic balance

Electronic balance (Figure 3- 2 (g), purchased from Precisa company) was used to weight the quantity of the agents with powder or granular.

H. Peristaltic Pump

Peristaltic pump purchased from Cole-Parmer Instrument Company in United States was used to drive the absorbent input the RPB. (Figure 3- 2 (h))

doi:10.6342/NTU202102462

I. Pipeline and accessories

Gas pipeline includes hard tubing (composed of Teflon, with an inner diameter of 3.89 mm) and hoses (composed of peroxide-cured silicone, with inner diameter of 0.25 mm and 0.31 mm) which were all purchased from All-Field Corporation company; liquid pipeline (composed of peroxide-cured silicone, with inner diameter of 0.31 mm) were also purchased from All-Field Corporation company.

Other accessories included T/Y-connector, beaker with handle, three-way ball valve and so on. These accessories were used to connect pipelines and control fluid flow. (Figure 3- 2 (i))

J. PG-350 Portable gas analyzer

The PG-350 Portable gas analyzer (PG-350, provided by HORIBA company) was a gas analyzer that can simultaneously measure up to five separate gas components. The PG-350 Portable gas analyzer was used as an analysis of nitrogen oxide concentration in this study. (Detection range: 0~2500 ppm; NO_2/NO conversion: ~72%; analysis method was referred to 3.3.2)

K. Ion chromatography

The ion chromatography (IC, provided by Metrohm AG) was used as an analysis of nitrite and nitrate in the waste liquid. (Analysis method was referred to 3.3.2)

doi:10.6342/NTU202102462

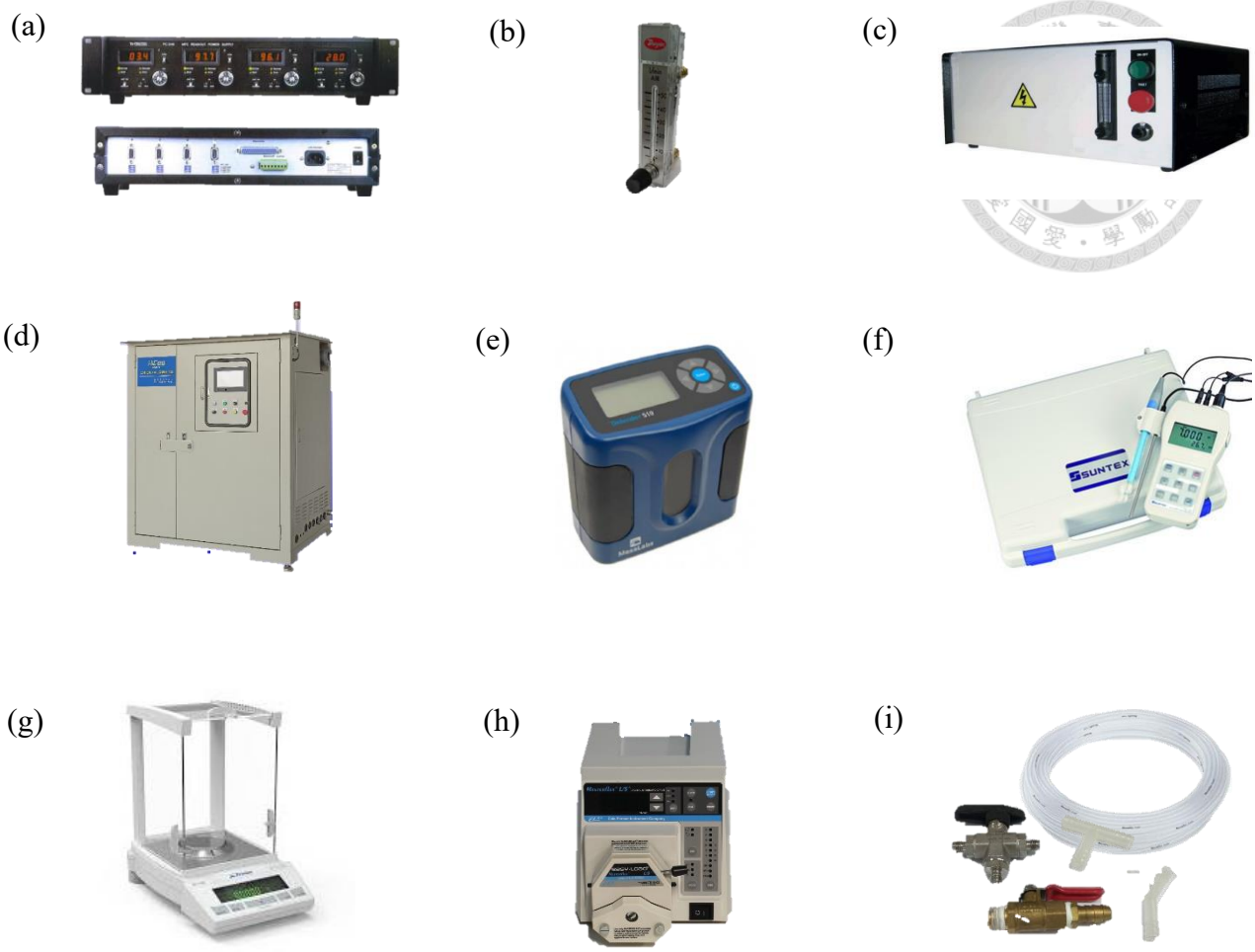

Figure 3- 2 Instrument and Equipment (a) mass Flow Controller, (b) flow meter, (c) ozone generator, (d) chlorine dioxide generator, (e) precise dry-air flowmeter, (f) pH meter, (g) electronic balance, (h) peristaltic pump, (i) pipeline and accessories

doi:10.6342/NTU202102462

3.2.3 Apparatus: Rotating Packed Bed

The rotating packed bed was the main reactor in this experiment. In this study, the type of gas-liquid contact was counter-current. In addition, the packed bed was set in a horizontal form to reduce the vertical size, make the structure more symmetrical and easier to operate. Table 3-1 showed the specification of the RPB used in this study.

Table 3- 1 The specification of the RPB used in this research

Specifications		Operation range or type	Unit
Size	Length × width × height	30 × 30 × 75	cm
Gas-liquid contact	-	counter-current	-
Packed bed	Rotational speed	0-1800	rpm
	Inner radius (r_i)	0.025	m
	Outer radius (r_o)	0.165	m
	Height (Z)	0.045	m
Packing	Weight	0.4	kg
	Porosity (ε)	0.94	-
	Density	7990	g cm^{-3}
	Specific area (a_t)	29.25	cm^2 cm^{-3}
	Material	SS-316 Stainless steel	-
Power supply	-	500	W

Furthermore, combining the aforementioned instruments and equipment, the illustrated experiment setup was shown in Figure 3- 4, and the actual experiment setup was shown in Figure 3- 3.

doi:10.6342/NTU202102462

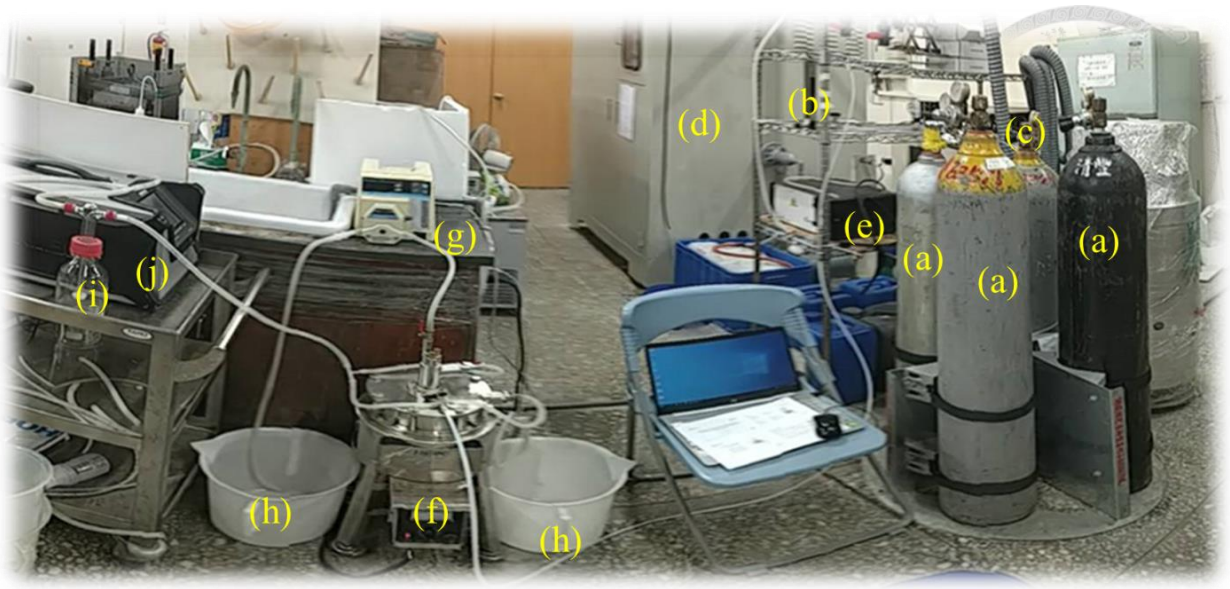

Figure 3- 3 The actual experiment setup in this study (a) gas cylinder, (b) flow meter, (c) mass flow meter, (d) chlorine dioxide generator (e) ozone generator, (f) rotating packed bed, (g) peristaltic pump, (h) absorbent beaker, (i) dewatering device, (j) PG-350

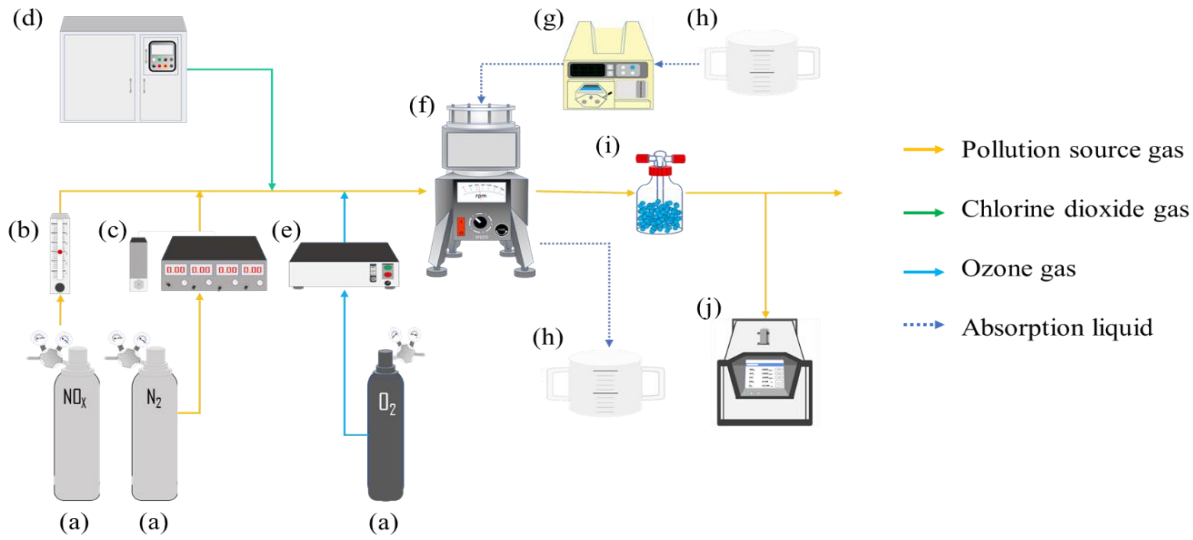

Figure 3- 4 Illustrated experiment setup in this study (a) gas cylinder, (b) flow meter, (c) mass flow meter, (d) chlorine dioxide generator (e) ozone generator, (f) rotating packed bed, (g) peristaltic pump, (h) absorbent beaker, (i) dewatering device, (j) PG-350

doi:10.6342/NTU202102462

3.3 **Methods**

This chapter would elucidate the experimental design, analysis methods and cost benefit evaluation manners of this study

3.3.1 Experimental Design

The experimental design was divided into three parts for introduction: (1) experimental process, (2) parameter design and (3) quality assurance/quality control.

A. Experimental process

There were three parts in the experimental process. The process of the experiment was followed by direct oxidation absorption, mass transfer conditions and enhancement of nitrogen oxides removal efficiency.

(a) Direct oxidation absorption

As mentioned in 2.2.1, direct oxidation absorption was divided into oxidation-absorption and absorption-oxidation. The experimental goal here was to explore the difference between the oxidation-absorption pathway and the absorption-oxidation pathway used in a rotating packed bed. During the process, under the same rotating packed bed operating conditions, different forms of agents (oxidant or reducing agent/gas or liquid phase) were added. Finally, the best reagent was determined by the removal efficiency of nitrogen oxides (η).

doi:10.6342/NTU202102462

(b) Effects of operating parameters for NOx reduction

As described in 2.3.1, the mass transfer coefficient was affected by many factors in the rotating packed bed. Among these factors, the gas-liquid ratio (G/L) and the high-gravity factor (β) were easier to modify. In the part of experiment, the agent with the best effect would be added (determined by the direct oxidation absorption experiment), and then discussed the mass transfer conditions in the rotating packed bed by changing the gas-liquid ratio and high-gravity factor.

(c) Enhancement of NOx reduction and applicable concentration

In the experiment of removal efficiency enhancement, gas and liquid phase agents were added at the same time to improve the removal efficiency of nitrogen oxides under the optimal mass transfer conditions (determined by the experiment of mass transfer conditions). On the other hand, it would also test that the applicable concentration of this nitrogen oxide removal method. This method would be operated at different concentrations and investigate whether the high nitrogen oxide removal efficiency could be maintained.

doi:10.6342/NTU202102462

B. Parameter design

The experimental parameters of this study are shown in Figure 3- 5. The reagent was determined by the direct oxidation absorption experiment first, and then the gas-liquid ratio and the high-gravity factor were determined in sequence. Finally, the enhancement of removal efficiency and applicable concentration experiments were carried out separately. In addition, the calculation method of the parameters was shown in Table 3- 2.

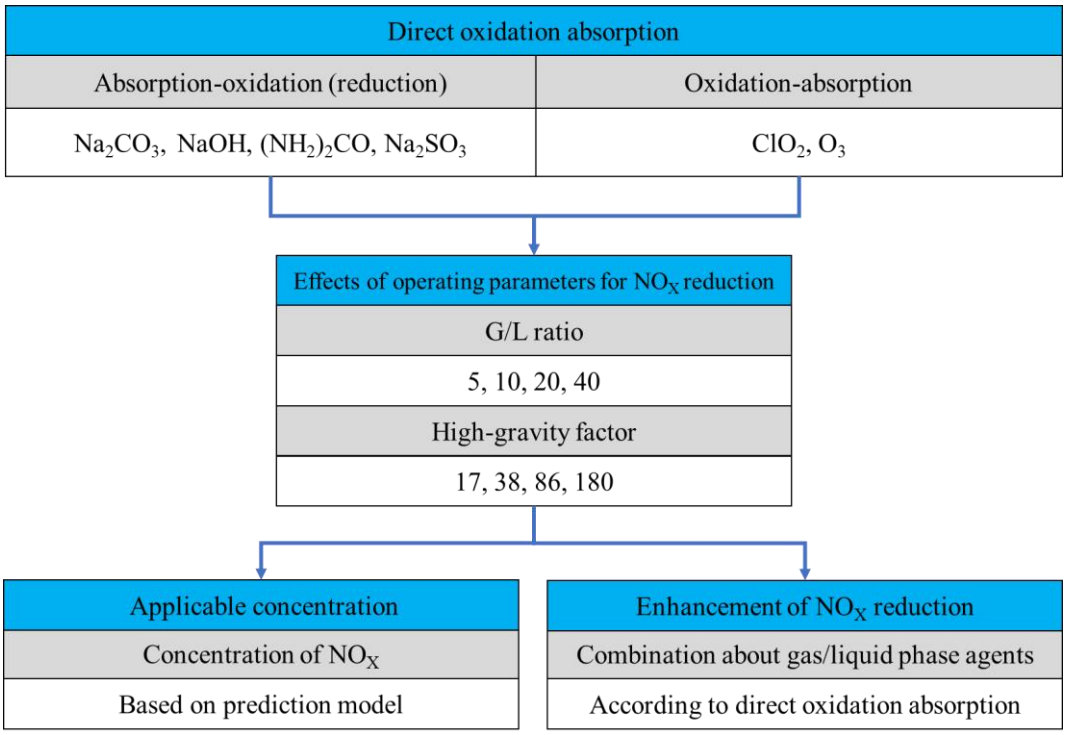

Figure 3- 5 Experiment operating parameters in this study

doi:10.6342/NTU202102462

Table 3- 2 The calculation method of the parameters in this study

Parameter	Equation	Number
Removal efficiency of NO_X	$\eta(\%) = \frac{C_o - C_f}{C_0}$	Eq- 15
Gas-liquid ratio	$\frac{G}{L} = {Q_g}/{Q_l}$	Eq- 16
High-gravity factor	$\beta = \frac{\left(\frac{2\pi N}{60}\right)^2 \cdot \bar{r}}{g}$	Eq- 17

A simulated flue gas with a flow rate of 5 L/min was made up of nitrogen cylinders and nitrogen oxide cylinder, and was used as a source of pollution. Then the gas phase oxidant (chlorine dioxide and ozone) was injected from the branch of the pipeline to oxidize the nitrogen oxide NO_X. The oxidized nitrogen oxides were absorbed in the rotating packed bed and entered the liquid phase from the gas phase. Various absorbents (sodium hydroxide, urea, sodium carbonate and sodium sulfite) and different rotating packed bed operating conditions (gas-liquid ratio and high-gravity factor) were used in the process. The outflow exhaust gas passes through the dewatering device (composed of silicone) and then entered the flue gas detector (PG-350).

On the other hand, regarding the amount of chemicals used, gas phase oxidant was adjusted according to the stoichiometry (Table 2- 5 and Table 2- 6) with the main pollutant (NO) and the scale of the equipment. The chlorine dioxide mole ratio (ClO_2/NO) was 0.5, the safety factor is 1.5~2; the ozone mole ratio (O_3/NO) was 5, the safety factor was 1.0~1.5 (Table 3- 3).

doi:10.6342/NTU202102462

Similarly, the liquid phase absorbent is also adjusted by the stoichiometry. Nevertheless, considering that the pollutants need to undergo gas-liquid mass transfer to react with the liquid-phase absorbent and the convenience of calculation, the safety factor of the liquid-phase absorbent was increased (Safety factor =300). -

Table 3- 3 The dosage of chemical agents in this study

Liquid phase agents: absorption-oxidation (reduction)				
	NaOH	Na_2CO_3	Na_2SO_3	$(NH_2)_2CO$
[a] Mole ratio (NO)	1	1	1	0.33
[a] Mole ratio (NO_2)	1	1	2	0.67
[b] Concentration (M)	4.91×10^{-2}	4.91×10^{-2}	5.39×10^{-2}	1.80×10^{-2}
Safe factor	300			
Gas phase agents: oxidation-absorption				
	ClO_2		O_3	
[a] Mole ratio (NO)	0.5		5	
[a] Mole ratio (NO_2)	0		4	
[b] Concentration (ppm)	120~175		1000~1200	
Safe factor	1.5~1.75		1~1.2	

[a] According to Table 2- 5, Table 2- 6 and Table 2- 7. Mole ratio was calculated by $\frac{\text{Mole}_{\text{oxidant}}}{\text{Mole}_{\text{pollutant}}}$

[b] Under the condition which C_{NOx} was 200 ppm, Q_g was 5 L/min, and G/L ratio was 20

doi:10.6342/NTU202102462

C. Quality control

In order to ensure that the experimental data had the properties of precision, accuracy, representativeness, completeness and comparability (PARCC), the quality control works adopted during the experiment were as follows:

(a) The removal efficiency of nitrogen oxides

Experiments with the same operating parameters would be repeated, and the relative difference percentage (RPD) between the removal efficiency of experiments would be calculated. Valid experimental data was that the relative difference percentage was less than 10 %.

(b) The analysis of pollutant concentration

Related quality control items of the instrument (PG-350): repeatability, above the 100-ppm range was ±1.0 % of the full-scale in NO_X; linearity, ±2.0 % of the full-scale; drift, ±1.0% per day of the full-scale; response time, 45 seconds or less. Analysis method meet the requirements of standard methods (NIEA A411.75C). The liquid phase water quality analysis items complied with the standard method (NIEA W415.54B, NIEA W203.51B and NIEA W424.52A).

doi:10.6342/NTU202102462

3.3.2 Analytical Techniques

The analysis items that would be carried out in this study include: nitrogen oxides, temperature, pH, conductivity, nitrate and nitrite, the phase state of each species and analysis instruments were shown in Table 3- 4

Table 3- 4 Analysis items and instruments

Phase	Species	Instrument
Gas	NO	PG-350 portable gas analyzer
	NO_X	PG-350 portable gas analyzer
	Temperature	Thermometer
Liquid	Temperature	Thermometer
	pH	pH meter
	Conductivity	Conductivity
	TDS	Conductivity
	NO_3^-	Ion chromatography
	NO_2^-	Ion chromatography

Among them, the quantitative analysis items related to pollutants (NO_X) are NO, NO_X, NO_3^- and NO_2^-, and the instruments for quantifying pollutants were PG-350 Portable gas analyzer and Ion chromatography

(a) (b)

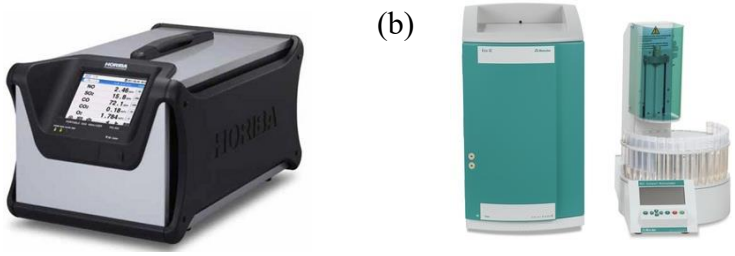

Figure 3- 6 The instrument for quantifying pollutants (a) Portable gas analyzer and (b) ion chromatography

doi:10.6342/NTU202102462

A. PG-350 Portable gas analyzer

PG-350 was a portable multifunctional flue gas analyzer that could simultaneously measure up to five separate gas components including nitric oxide/nitrogen oxides (NO/NO_X), sulfur disulfide, oxygen, carbon monoxide and carbon dioxide (A- 2).

PG-350 operated according to: DIN EN 15267-3, DIN EN 14181 and approved as Standard Reference Method (SRM) for: CO (DIN EN 15058), O_2 (DIN EN 14789), NO_X (DIN EN 14792). The respective analysis principle of pollutant analysis principle: NO_X detector used a cross-flow modulation chemiluminescence detection; the SO_2 and CO detector operated with a cross-flow modulation non-dispersive infrared (NDIR) absorption method; the CO_2 unit used the standard non-dispersive infrared (NDIR) absorption method; and the O_2 unit uses the paramagnetic method for exclusively in EU area. The analysis method of nitrogen oxides also conformed to the standard method (NIEA A411.75C) promulgated by the Environmental Protection Administration Executive Yuan, R.O.C. (Taiwan).

doi:10.6342/NTU202102462

B. Ion chromatography

Ion chromatography was used to analyze nitrogen-compounds produced after nitrogen oxides were absorbed, mainly nitrate and nitrite. The IC used in this study was the Eco IC launched by Metrohum company.

The analysis principle of ion chromatography was to make the movement speed of each anion different through the difference in the affinity between the different anions in the mobile phase and the stationary phase. Finally, different anions entered the conductivity meter to measure the conductivity to achieve qualitative and quantitative purposes. The analysis method of nitrogen oxides also conformed to the standard method (NIEA W415.54B) promulgated by the Environmental Protection Administration Executive Yuan, R.O.C. (Taiwan).

doi:10.6342/NTU202102462

3.3.3 Cost Analysis

The cost analysis method used in this study was as described in 2.4. In order to facilitate data calculation and data collection, this study simplified the cost-benefit analysis steps into Table 3- 5 which merely include the part about cost analysis.

Table 3- 5 The step of cost analysis in this study

Step	Description
1	Set the framework for the analysis
2	Decide whose costs should be recognized
3	Identify and categorize costs
4	Project costs over the life of the program, if applicable.
5	Monetize (place a dollar value on) costs.
6	Compute a net present value for CA.
7	Make a recommendation where appropriate.

The steps "Discount costs and benefits to obtain present values" and "Perform sensitivity analysis" would be negligible through rationalized assumptions. In addition, the monetization and definition about cost and benefit were mainly based on the experimental parameters of this research.

doi:10.6342/NTU202102462

Chapter 4 Results and Discussion

4.1 Direct Oxidation Absorption

In the absorption process, in addition to reacting with the chemical agents, nitrogen oxides also reacted with water molecules, oxygen and other nitrogen oxides (Figure 4- 1). Table 4- 1 shows the reaction of nitrogen oxides in the absorption process. It could be found that when the main pollutants emitted from the pollution source were nitrogen monoxide and nitrogen dioxide, the flue gas would contain nitrogen monoxide, nitrogen dioxide, dinitrogen trioxide, dinitrogen tetroxide, nitric acid and nitrous acid.

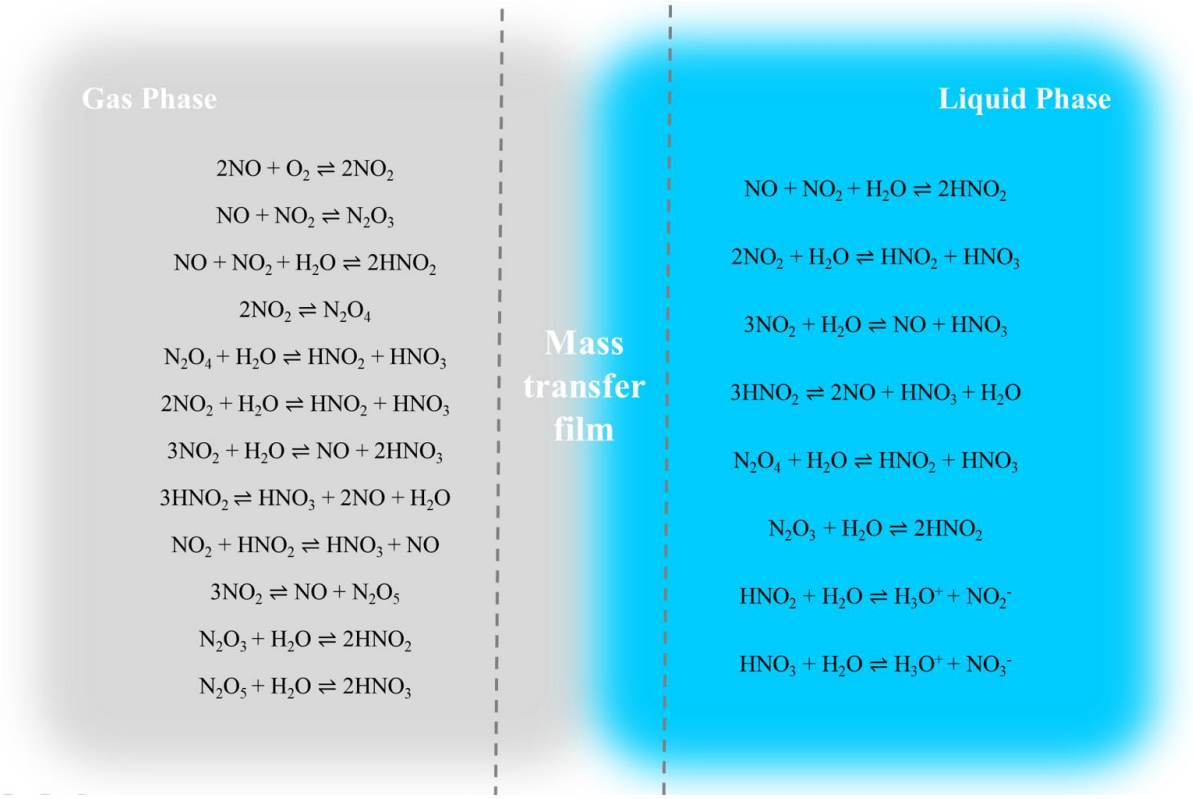

Figure 4- 1 The reaction of nitrogen oxides in the absorption process without the agents

doi:10.6342/NTU202102462

Table 4- 1The reaction of nitrogen oxides in the absorption process without the agents

Phase	Reaction	Number
Gas	$2NO + O_2 \rightleftharpoons 2NO_2$	R- 34
	$NO + NO_2 \rightleftharpoons N_2O_3$	R- 35
	$NO + NO_2 + H_2O \rightleftharpoons 2HNO_2$	R- 36
	$2NO_2 \rightleftharpoons N_2O_4$	R- 37
	$N_2O_4 + H_2O \rightleftharpoons HNO_2 + HNO_3$	R- 38
	$2NO_2 + H_2O \rightleftharpoons HNO_2 + HNO_3$	R- 39
	$3NO_2 + H_2O \rightleftharpoons NO + 2HNO_3$	R- 40
	$3HNO_2 \rightleftharpoons HNO_3 + 2NO + H_2O$	R- 41
	$NO_2 + HNO_2 \rightleftharpoons HNO_3 + NO$	R- 42
	$3NO_2 \rightleftharpoons NO + N_2O_5$	R- 43
	$N_2O_3 + H_2O \rightleftharpoons 2HNO_2$	R- 44
	$N_2O_5 + H_2O \rightleftharpoons 2HNO_3$	R- 45
Liquid	$NO + NO_2 + H_2O \rightleftharpoons 2HNO_2$	R- 46
	$2NO_2 + H_2O \rightleftharpoons HNO_2 + HNO_3$	R- 47
	$3NO_2 + H_2O \rightleftharpoons NO + HNO_3$	R- 48
	$3HNO_2 \rightleftharpoons 2NO + HNO_3 + H_2O$	R- 49
	$N_2O_4 + H_2O \rightleftharpoons HNO_2 + HNO_3$	R- 50
	$N_2O_3 + H_2O \rightleftharpoons 2HNO_2$	R- 51
	$HNO_2 + H_2O \rightleftharpoons H_3O^+ + NO_2^-$	R- 52
	$HNO_3 + H_2O \rightleftharpoons H_3O^+ + NO_3^-$	R- 53

4.1.1 Liquid Phase Agents: Absorption-Oxidation (Reduction)

Beside the reaction between nitrogen oxides and environmental media (Table 4-1), this trial also added different agents to help nitrogen oxides be absorbed. Table 4- 2 shows the operating conditions of the experiment about “Absorption-Oxidation (Reduction) Trials”; Figure 4- 2 presents the results in the experiment about “Absorption-Oxidation (Reduction) Trials”.

doi:10.6342/NTU202102462

Table 4- 2 The operating conditions of Absorption-Oxidation (Reduction) Trials.

Manipulated variable	Controlled variable			
Liquid phase agents	Gas phase agents	Gas-liquid ratio	High-gravity factor	Concentration of NO_X
Tap water	-	20	86 (900 rpm)	200 ppm
Sodium carbonate				
Sodium hydroxide				
Sodium sulfite				
Urea				

From Figure 4-2 (a), it could be observed that different liquid-phase agents reached a stable removal efficiency when the operation time was up to 10 minutes. In addition, it was found in Figure 4-2 (b) that the removal efficiency of NO, NO_2, NO_X was consistent approximately ($Na_2SO_3 \approx NaOH > Na_2CO_3 > (NH_2)_2CO > H_2O$ (tap water)).

The addition of liquid reagents could reduce the concentration of species in the liquid phase and increase the concentration gradient to improve the driving force of mass transfer. Therefore, the removal efficiency of adding the reagent was higher than the removal efficiency using only tap water as the absorbent. In addition, it could be found that these absorbents had a common trend for nitrogen oxide removal. No matter which kind of absorbent, the removal efficiency of NO_2 was better than that of NO. This phenomenon was attributed to the Henry's constant of nitric oxide. Since the Henry's constant of nitric oxide was smaller than that of nitrogen dioxide, it was difficult for nitric oxide to enter the liquid phase, let alone be reacted by the absorbent in the liquid phase. Therefore, the overall NOx removal efficiency was low.

doi:10.6342/NTU202102462

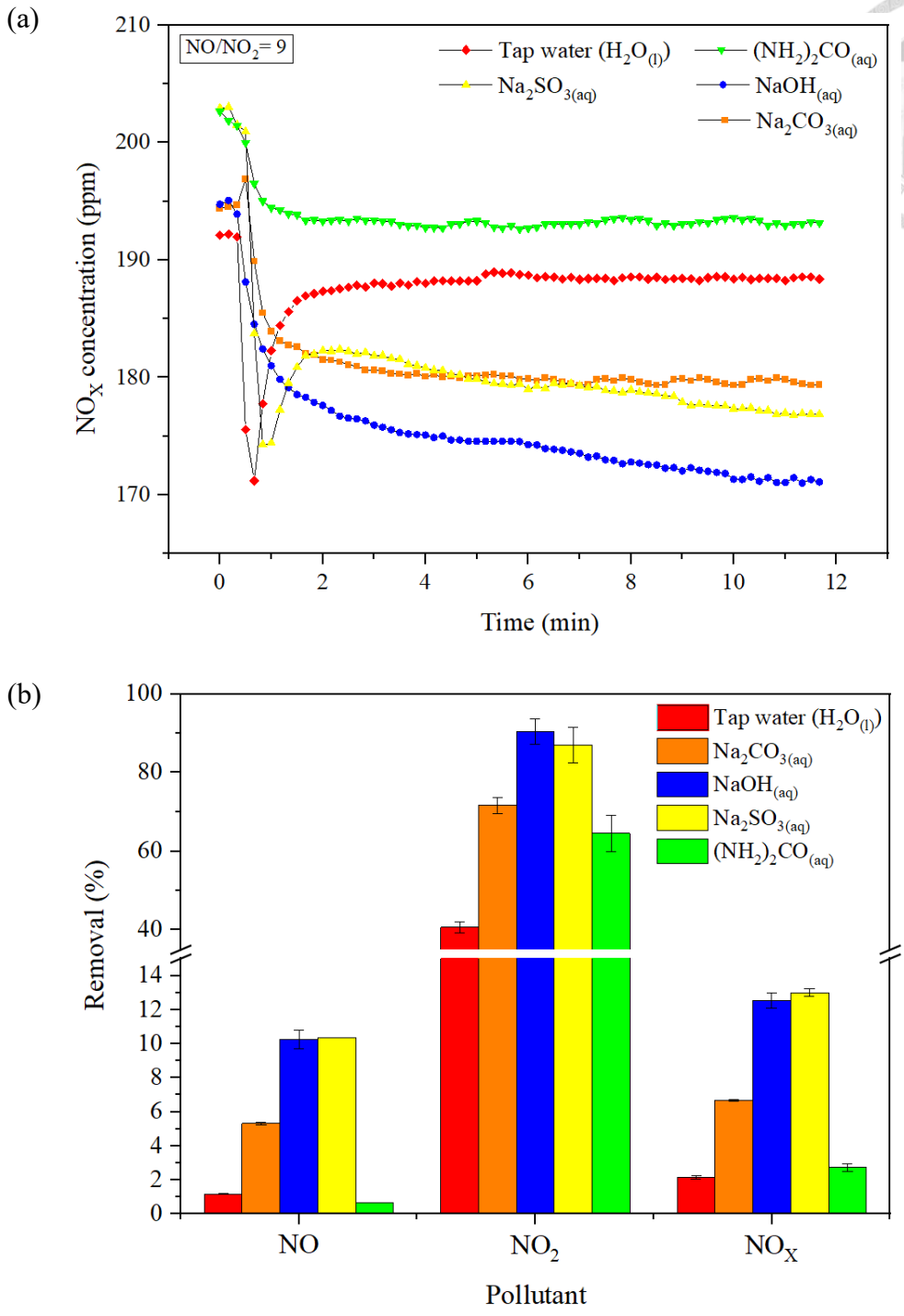

Figure 4- 2 The results in Absorption-Oxidation (Reduction) Trials (a) the relationship between operating time and concentration of nitrogen oxides (b) the removal efficiency of various nitrogen oxides

doi:10.6342/NTU202102462

There was a higher removal efficiency when sodium hydroxide and sodium sulfite were used as liquid phase agents. It was inferred that the reaction between sodium hydroxide and nitrogen oxides was acid-base neutralization (R- 19 and R- 20), which converted nitric acid and nitrous acid into an ion form.

It was worth noting that nitrous acid molecule was an unstable molecule which would decompose itself to produce nitric oxide (R- 49). By converting nitrous acid into nitrite, the chance of regenerating nitrogen oxides could be reduced; In terms of sodium sulfite, it could be found that there were many ways to react with nitrogen oxides, and the reaction rate was also fast (Table 2- 7).

Compared with sodium hydroxide and sodium sulfite, the removal efficiency of sodium carbonate and urea was less significant. The reason was deduced that sodium carbonate mainly reacted with nitrogen dioxide, and the pollution source was mostly composed of nitrogen monoxide, so the effect was poor; although urea had many ways to react with nitrogen oxides, the removal effect was poor due to the poor reaction rate and easy decomposition by itself.

On the other hand, because NO_X is acidic when dissolved in water, the pH of the absorbent was also a parameter worth analyzing (Table 4- 3).

doi:10.6342/NTU202102462

Table 4- 3 The changes on pH value under different operating conditions

Condition	Liquid phase agents				
	Tap water	Na_2CO_3	NaOH	Na_2SO_3	$(NH_2)_2CO$
[a] Initial pH	7.90	7.90	7.52	7.52	7.52
pH after agent addition	7.90	10.69	12.55	9.37	7.97
[b] Finial pH	8.14	10.7	12.26	9.4	8.12

[a] pH value of tap water before adding liquid phase agents

[b] pH value of absorbent after NO_X removal process

Sodium hydroxide increases the pH of the absorbent the most, so the removal effect was better. However, sodium carbonate could increase the pH value to 10.69, but the removal efficiency was lower than that of sodium sulfite (pH= 9.37). This result was due to the low water solubility of NO_X and the pH of the absorbent. The main effect of increasing the pH value was to accelerate the dissociation of nitric acid and nitrous acid, and to increase the reaction rate of the reaction between nitrogen oxides and water. Although sodium carbonate increases the pH, the increase in pH was not as high as sodium hydroxide so the removal efficiency was poor.

In short, the influence of liquid-phase absorbents on the removal of NO_X could be discussed by the pH of the absorbent and the reaction between the agent and the pollutants. Increasing the pH was beneficial to the absorption of nitrogen oxidation, but it was necessary to provide enough hydroxide ions to be effective. The things that the fast reaction rate and more reaction pathways with the pollutants were also conducive to the absorption of pollutants.

doi:10.6342/NTU202102462

4.1.2 Gas Phase Agents: Oxidation-Absorption

After understanding the effect of adding liquid phase agents, the trials of adding gas phase agents would be carried out. Table 4- 4 shows the operating conditions of the experiment about “Oxidation-Absorption Trials”; Figure 4-2 presents the results in “Oxidation-Absorption Trials”.

Table 4- 4 The operating conditions of Oxidation-Absorption Trials

Manipulated variable	Controlled variable			
Gas phase agents	Liquid phase agents	Gas-liquid ratio	High-gravity factor	Concentration of NO_X
-	Tap water	20	86 (900 rpm)	200 ppm
Chlorine dioxide				
Ozone				

It could be perceived that the Oxidation-Absorption Trials with the addition of gas phase reagents achieved a stable removal efficiency faster (Figure 4- 2 (a) and Figure 4- 3 (a)). When the operation time was 3~4 minutes, the exhaust concentration of nitrogen oxides had reached a steady state. Not only did the trial with gas phase agents reach a steady state faster, but it also had much better removal efficiency than liquid phase agents. The reason why nitrogen oxides efficiency could be improved by adding gas phase agents was attributed to the oxidation of NO_X and form high-valence nitrogen oxides. High-valence nitrogen oxides usually had better water solubility and were easier to be removed by washing method [97].

doi:10.6342/NTU202102462

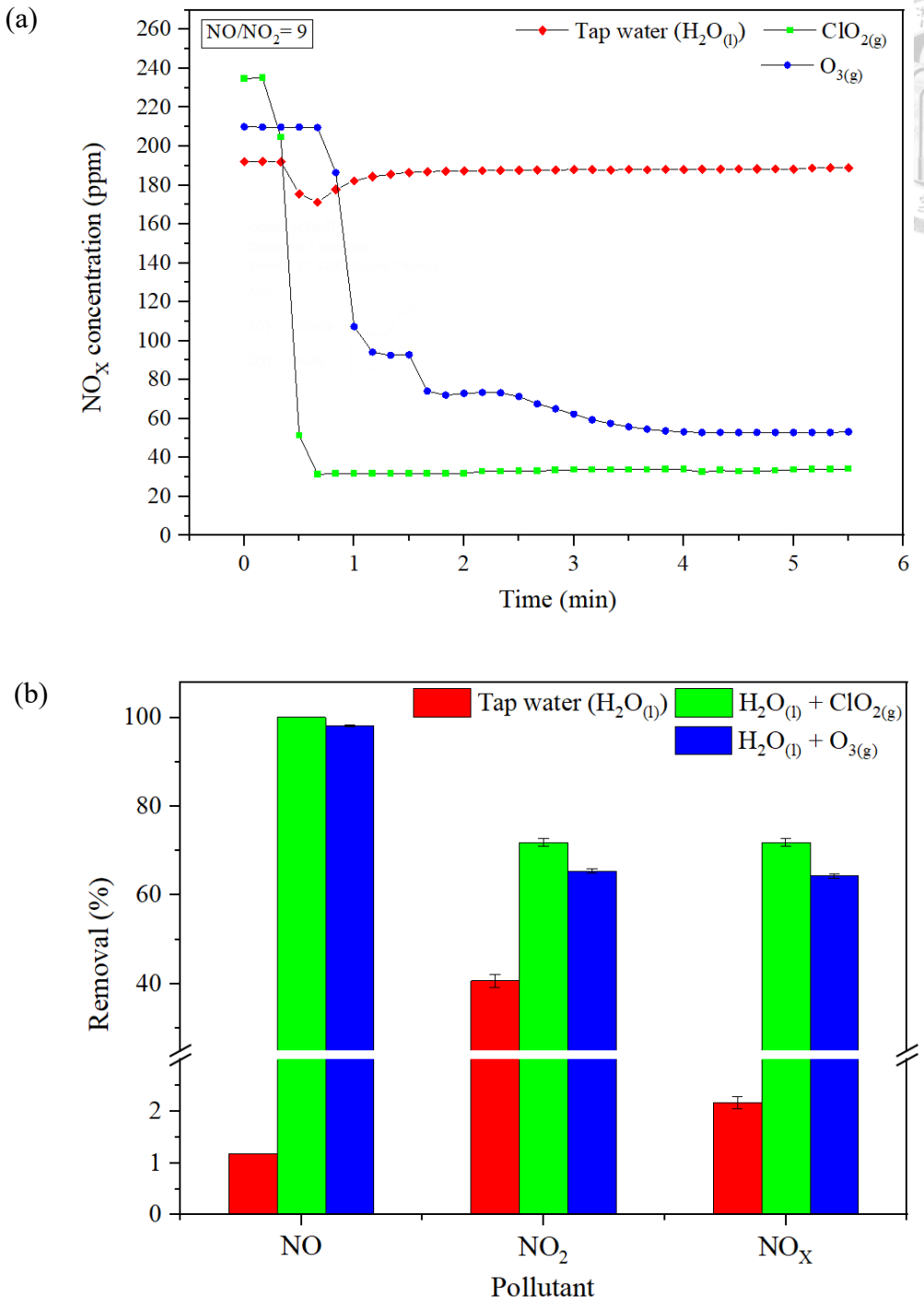

Figure 4- 3 The results in Oxidation-Absorption Trials (a) the relationship between operating time and concentration of nitrogen oxides (b) the removal efficiency of various nitrogen oxides

doi:10.6342/NTU202102462

For the purpose of realizing how the reaction about gas phase reagents and nitrogen oxides in the pipeline produced nitrogen oxides which were easier to remove, Some assumptions about the reaction between gas phase agents and nitrogen oxides was be made: (a) ignore the mass transfer of molecular diffusion in the pipeline; (b) the flow in the pipe was turbulent; (c) The reaction reached a steady state; (d) the reaction took place in an ideal plug flow reactor model. With these assumptions, it could be written down the mass balance equation of the material in the pipeline (Eq- 18).

$$\Delta(CV) = Q_g C_X \Delta t - Q_g C_{X+\Delta X} \Delta t \pm \Delta t \cdot V \sum_{i=1}^{n} k_i C_A^a C_B^b \cdots \quad \text{Eq- 18}$$

$$\rightarrow \quad \frac{\Delta C}{\Delta t} = \frac{Q_g}{V}(C_X - C_{X+\Delta X}) \pm F(C) \quad \text{Eq- 19}$$

$$* \quad F(C) = \sum_{i=1}^{n} k_i C_A^a C_B^b \cdots$$

$$\rightarrow \quad \frac{\partial C}{\partial t} = -v\frac{\partial C}{\partial X} \pm F(C) \quad \text{Eq- 20}$$

$$\rightarrow \quad \frac{dC}{dX} = \frac{\pm F(C)}{v} \quad \text{Eq- 21}$$

It could be obtain that the relationship between the concentration of nitric oxide and the reaction distance (Eq- 22) by taking the reaction equations and rate constants (Table 2- 6) into Eq- 20. In the same way, the relationship between the concentration of NO_2, HNO_2, HNO_3, ClO_2, ClO, Cl_2, Cl and $ClNO_3$ as a function of the reaction distance could be also obtained.

$$\frac{d[NO]}{dX} = \frac{1}{v}(-k_{21}[NO][ClO_2] - k_{22}[NO][ClO] + k_{-35}[N_2O_3]) \quad \text{Eq- 22}$$

doi:10.6342/NTU202102462

Since it was more complicated to solve nine simultaneous differential equations, the differential equations were rewritten as approximate equations (Eq- 24), and similarity solutions are obtained (Eq- 25). Likewise, the similarity solutions could be obtained in NO_2, HNO_2, HNO_3, ClO_2, ClO, Cl_2, Cl and $ClNO_3$.

$$\frac{d[NO]}{dX} = \frac{1}{v}F(C) \qquad \text{Eq- 23}$$

$$* \quad F(C) = -k_{21}[NO][ClO_2] - k_{22}[NO][ClO] + k_{-35}[N_2O_3]$$

$$\rightarrow \quad \Delta[NO] = \frac{\Delta X}{v}F(C) \qquad \text{Eq- 24}$$

$$\rightarrow \quad [NO]_{X+\Delta X} = [NO]_X + \frac{\Delta X}{v}F(C) \qquad \text{Eq- 25}$$

$$* \quad F(C) = -k_{21}[NO]_X[ClO_2]_X - k_{22}[NO]_X[ClO]_X + k_{-35}[N_2O_3]_X$$

The similarity solution about the relationship between the concentration and the location in the pipeline is shown in Figure 4- 4 and the trend of the concentration performance were similar to the research about reaction kinetics of chlorine dioxide and nitrogen oxides [98]. However, there was a considerable difference between the simulated result and the actual pollutant measured value after oxidation (Table 4- 5). It was speculated that the reason was that all the reactions that occurred were not covered in the model. Moreover, due to the limitation of the instrument and partial some rate constants could not be found in this system, and the inverse reaction rate constants of some reaction equations were not easy to obtain from the literature.

doi:10.6342/NTU202102462

Table 4- 5 Actual pollutant concentration before and after oxidation reaction

	Condition	NO (ppm)	NO_2 (ppm)
$ClO_{2(g)}$	Initial	186.07	28.47
	After oxidation	ND	85.13
$O_{3(g)}$	Initial	188.52	23.68
	After oxidation	1.4	147

Nevertheless, other methods need to be figured out to approximate the species concentration. By observing the rate constant, it could be found that the gas phase reaction speed was quite fast, and the gas pipeline set up in this experiment was long, so it could be assumed that the gas phase reaction was close to equilibrium.

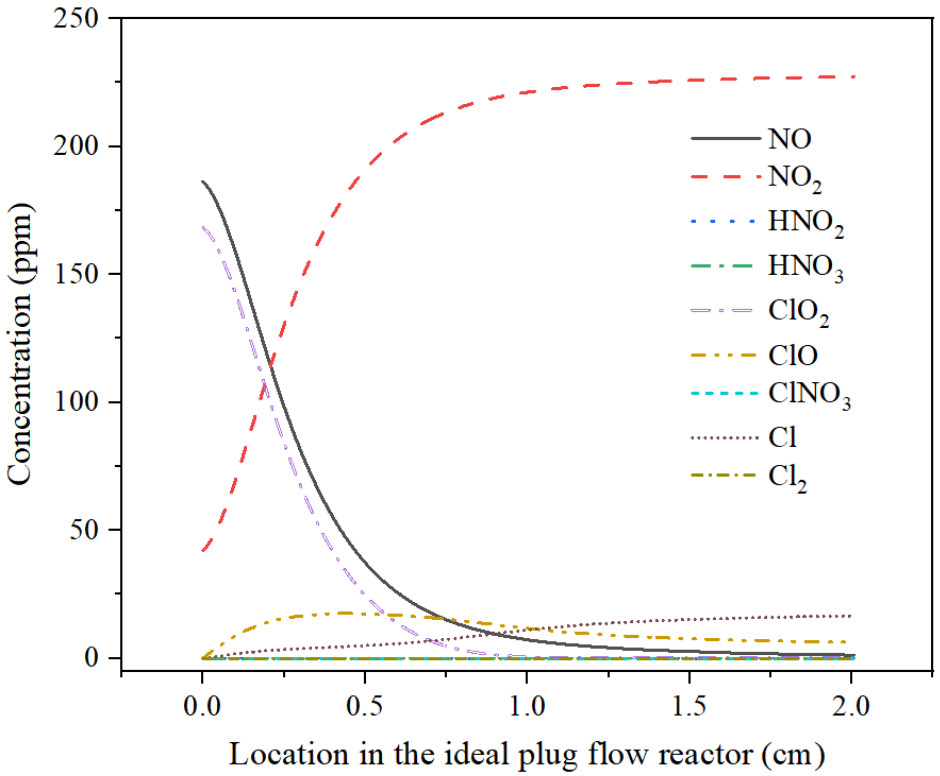

Figure 4- 4 Similarity solution for the reaction kinetics of chlorine dioxide and NO_X

doi:10.6342/NTU202102462

This conjecture allowed us to use equilibrium constants to calculate the concentration of species in the pipeline [99]. The species with known concentration in the pipeline were nitrogen dioxide and water vapor, but these conditions were not sufficient to use the equilibrium constant to obtain the equilibrium concentration of other nitrogen oxides (A- 3 [99]). In view of this, the mass balance relation (Eq- 26) and a concentration of nitric oxide was first assumed to estimate the concentration of other species.

$$[NO_X]_T^* = [NO] + [NO_2] + [NO_3] + [HNO_2] + [HNO_3] + 2[N_2O_3] + 2[N_2O_4] + 2[N_2O_5] \quad \text{Eq- 26}$$

Furthermore, in order to understand the feasibility of the equilibrium model to predict gas phase reaction products and increase the convenience of experimental operations, the concentration of nitrate and nitrite in the absorbent would be used to observe the accuracy of the equilibrium prediction model. Considering the reaction complexity between nitrogen oxides and the absorbent and the difficulty of quantifying liquid products, sodium hydroxide would be added to the absorbent to avoid the escape of nitrite (R- 49). Then, the nitrate and nitrite concentration (operating in $ClO_{2(g)}$+$H_2O_{(l)}$ and $ClO_{2(g)}$+$NaOH_{(aq)}$) were measured and predicted by the equilibrium prediction model and reaction equation (R- 47, R- 53, Eq- 27 and Eq- 28).

doi:10.6342/NTU202102462

$$[NO_{2(aq)}^{-}] = \frac{\Delta[NO_{2(g)}]}{2} \quad \text{Eq- 27}$$

$$[NO_{3(aq)}^{-}] = \Delta[HNO_{3(g)}] + \frac{\Delta[NO_{2(g)}]}{2} \quad \text{Eq- 28}$$

Figure 4- 5 shows the measured and calculated concentrations of nitrate and nitrite in the absorbent. In terms of nitrate, the measured and predicted values were quite close; the difference in the nitrite was far when the absorbent was tap water. The main reason should be the escape of nitrous acid. Therefore, it could be found that the difference between the actual measured value and the predicted value was reduced after addition of sodium hydroxide. Based on the above, it could be roughly understood that the feasibility of using equilibrium mode to roughly estimate gas phase reaction products.

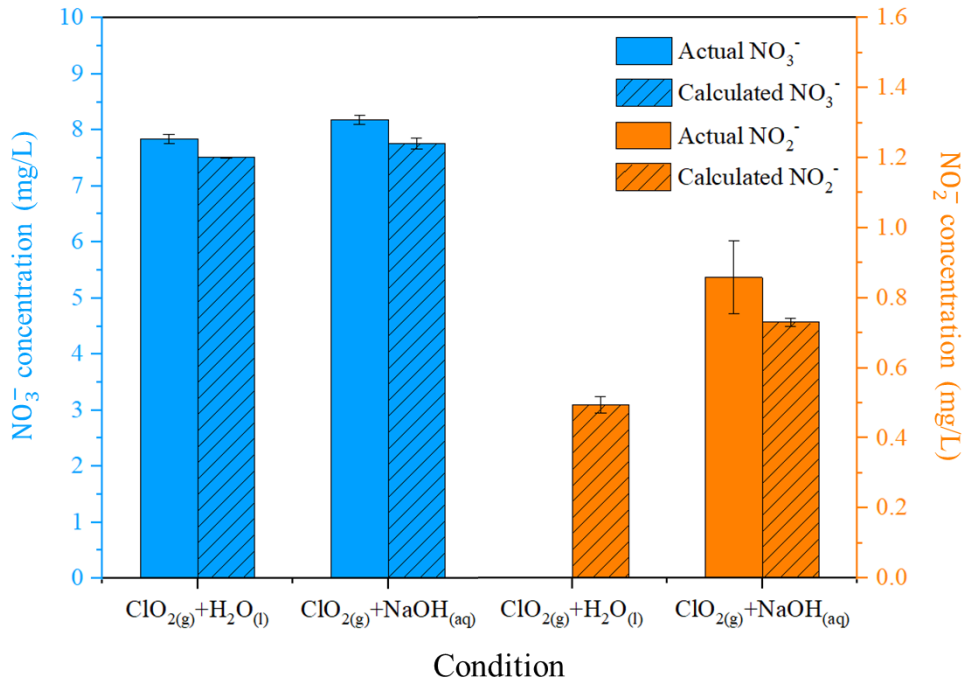

Figure 4- 5 The measured and calculated concentrations of nitrate and nitrite in the absorbent

doi:10.6342/NTU202102462

Table 4- 6 The measured and calculated concentrations of nitrate and nitrite in the absorbent

Condition: $ClO_{2(g)} + H_2O_{(l)}$			
Species	Concentration (ppm)		*RPD (%)
	Actual	Calculated	
NO_2^-	ND	0.470	-
	ND	0.518	
NO_3^-	7.758	7.519	4.28
	7.926	7.507	
Condition: $ClO_{2(g)} + NaOH_{(aq)}$			
Species	Concentration (ppm)		*RPD (%)
	Actual	Calculated	
NO_2^-	0.754	0.719	16.1
	0.962	0.741	
NO_3^-	8.101	7.668	5.22
	8.262	7.861	

$$* \text{RPD} = \left| \frac{C_{\text{avg. of actual}} - C_{\text{avg. of calculated}}}{\frac{(C_{\text{avg. of actual}} + C_{\text{avg. of calculated}})}{2}} \right| \times 100\ \%$$

The trial and error method with equilibrium constant and mass balance was used to estimate the concentration of other species. When the concentration of NO was 0.00239 ppm, the overall nitrogen recovery ratio reached 99.93 %, and this concentration was lower than the detection limit of the instrument, which was consistent with the actual situation.

doi:10.6342/NTU202102462

Table 4- 7 shows the concentration values when the reaction of nitrogen oxides and chlorine dioxide reached equilibrium. Similarly, it could be calculated that the equilibrium concentration after the reaction of ozone and nitrogen oxides through the relationship between equilibrium constant and mass balance (Table 4- 8). Calculations showed that the main products after the reaction of nitrogen oxides and ozone are nitrogen dioxide and nitrous oxide, which are the same as the results summarized by Sun, B., et al [40].

Table 4- 7 The estimated equilibrium concentration and pollutant composition of each species, when chlorine dioxide was used as an oxidant

Concentration (ppm)	NO	NO_2	N_2O_3	N_2O_4	N_2O_5	HNO_2	HNO_3
Initial	186.07	28.47	-	-	-	-	-
Equilibrium	[a] 0.00239	[b] 85.1	1.57×10^{-7}	0.0471	1.09×10^{-6}	0.0649	129
[c] Composition (%)	0.00144	42.11	12.7×10^{-6}	0.0466	9.91×10^{-7}	0.0355	57.8

[a] This value was the result of trial and error.

[b] This value was measured by the instrument.

[c] Pollutant composition $= \left(C_{Pollutant(N-contain)}/C_{NO_x}\right) \times 100\ \%$

Table 4- 8 The estimated equilibrium concentration and pollutant composition of each species, when ozone was used as an oxidant

Concentration (ppm)	NO	NO_2	NO_3	N_2O_3	N_2O_4	N_2O_5
Initial	188.52	23.68	-	-	-	-
Equilibrium	[b] 1.42	[b] 147	2.53×10^{-7}	1.06×10^{-4}	0.108	[a] 26.3
[c] Composition (%)	0.66	69.3	1.25×10^{-7}	1.06×10^{-4}	0.107	29.8

[a] This value was the result of trial and error.

[b] This value was measured by the instrument.

[c] Pollutant composition $= \left(C_{Pollutant(N-contain)}/C_{NO_x}\right) \times 100\ \%$

doi:10.6342/NTU202102462

Research on the reaction of ozone and nitrogen oxides pointed out that when the molar ratio (O_3/NO) was greater than 1.5, nitric oxide was almost completely converted into other nitrogen oxides [100]. In addition, when the molar ratio was greater than 2, the conversion rate of dinitrogen pentoxide was about 30~40 % [97, 101]. The conclusions of the above literatures were also similar to the results of this calculation.

Besides, observing the change in the concentration of hydrogen ions in the absorbent, it could be found that chlorine dioxide had a larger change than ozone (Table 4- 9). This result was ascribed to the production of nitric acid in the reaction of chlorine dioxide, which had high water solubility and could completely dissociate in water.

Table 4- 9 Hydrogen ion concentration of absorbent in different gas phase oxidants

	Chlorine dioxide	Ozone
Initial pH	7.70	7.83
Final pH	7.46	7.77
[a]p($\Delta[H^+]$)	7.83	8.66

[a] $p(\Delta[H^+]) = -\log(\Delta[H^+])$

Integrating the reaction products of nitrogen oxides and the two gas phase agents (Figure 4- 6), it could be concluded that the final composition which contain pollutants with high Henry's constant (Table 2- 2). What was more, the products generated by the reaction of nitrogen oxides and chlorine dioxide had higher water solubility than the products generated by the reaction with ozone, so the removal efficiency of chlorine dioxide was slightly higher than ozone.

doi:10.6342/NTU202102462

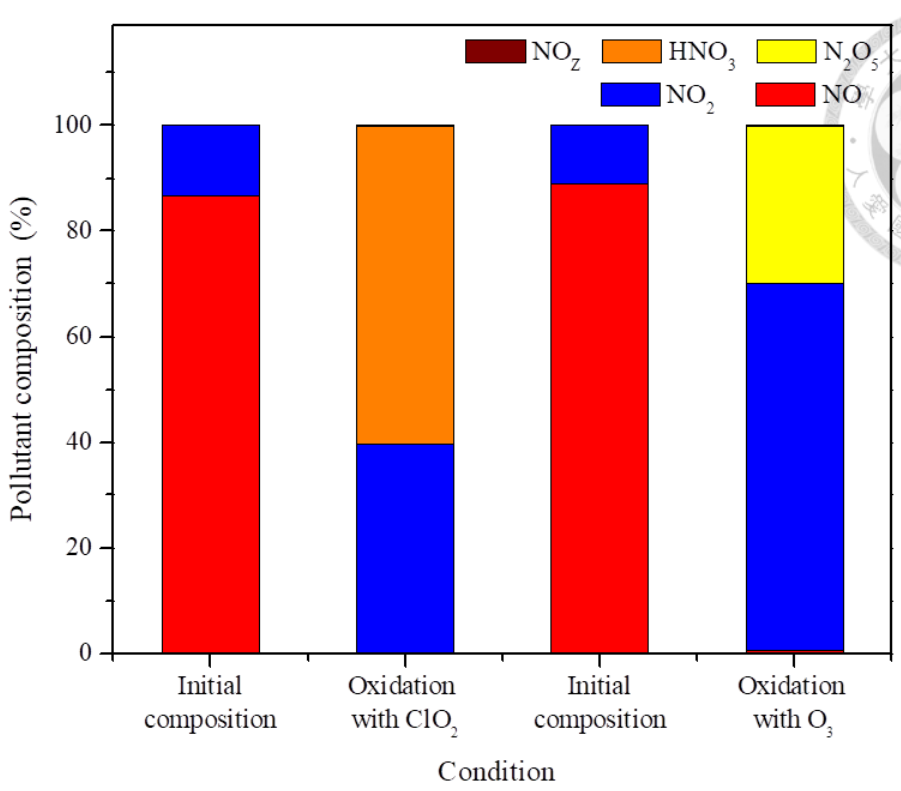

Figure 4- 6 Distribution of NO_X component treated by $ClO_{2(g)}$ and $O_{3(g)}$

On the other hand, it could be found that the dosages of ozone and chlorine dioxide were different. The molar ratio of chlorine dioxide ($\frac{ClO_2}{NO_X}$) was 0.5; the molar ratio of ozone ($\frac{O_3}{NO_X}$) was 5 in this study. In other words, chlorine dioxide could be used in a smaller amount and achieve better removal efficiency. This phenomenon was attributed to the reaction mechanism of oxidants and pollutants (Table 2- 5 and Table 2- 6). Due to the strong oxidizing power of O_3, O_3 could continue to react with the oxidized product of NO, that is, one NO molecule could consume multiple O_3 molecules; however, the reaction product (ClO) of ClO_2 and NO which could continue to react with NO, that is, one ClO_2 molecules could consume multiple NO molecules.

doi:10.6342/NTU202102462

Furthermore, it could be separated that the two stages in the oxidation absorption process and calculate the contribution of removal efficiency in sequence (Table 4- 10 and Figure 4- 7).

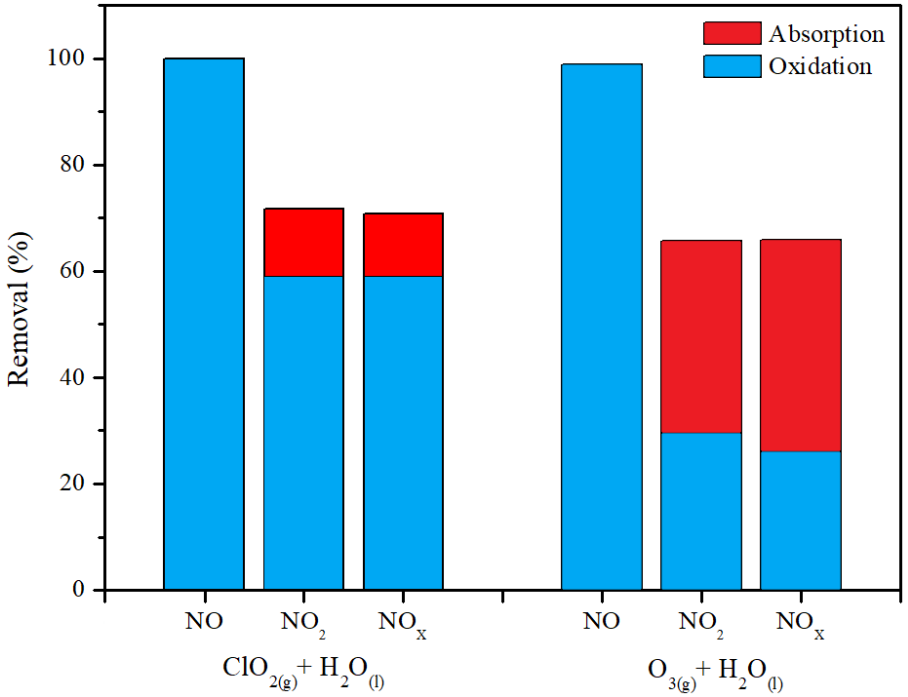

Figure 4- 7 The distribution of NO_X removal in the oxidation and absorption process

Table 4- 10 Removal efficiency of nitrogen oxides in different stages

Condition/Removal (%)		NO	NO_2	NO_X
$ClO_{2(g)} + H_2O_{(l)}$	Oxidation	99.9	58.7	58.7
	Absorption	< 0.1	12.9	11.9
	Total	99.9	71.8	71.8
$O_{3(g)} + H_2O_{(l)}$	Oxidation	99.3	29.4	26.1
	Absorption	< 0.1	36.3	39.7
	Total	99.3	65.3	62.8

It was perceived that the oxidation stage had been able to provide a certain range, but it still could not meet the regulatory standard (<30 ppm), and it needed to be combined with absorption to achieve the ideal removal efficiency.

doi:10.6342/NTU202102462

Through direct oxidation absorption experiments, the treatment effects of different gas phase and liquid phase agents on nitrogen oxides during absorption were analyzed. In the absorption oxidation (reduction) trial, it was inferred that the liquid phase agents with multiple reaction pathways and high reaction rate constant had better removal efficiency, but it still fails to meet the regulatory standards; In the oxidation absorption trial, it was deduced that adding the gas phase agent could help nitrogen oxides be absorbed. Among them, the one that could produce highly water-soluble products generated by reaction had better removal efficiency.

On the basis of the data in direct oxidation absorption experiments, Chlorine dioxide (gas) was chosen as the agent used in subsequent experiments. Under the condition of adding chlorine dioxide gas, the trials of different gas-liquid ratio and high-gravity factor were carried out to find the optimal operating conditions.

doi:10.6342/NTU202102462

4.2 **Effects of Operating Parameters on NO_X Removal**

This chapter discussed the mass transfer changes of pollutants in a rotating packed bed by adjusting the gas-liquid ratio and the centrifugal force field (high-gravity factor).

4.2.1 Gas-Liquid Ratio

Table 4- 11 shows the parameters used in the gas-liquid ratio test. The relationship between pollutants and operating time in the experimental results is shown in Figure 4- 8 (a); the removal efficiency of each species is shown in Figure 4- 8 (b).

Table 4- 11 The operating conditions of Gas-Liquid Ratio Trials

Manipulated variable	Controlled variable			
Gas-liquid ratio	Gas phase agents	Liquid phase agents	High-gravity factor	Concentration of NO_X
5	Chlorine dioxide	Tap water	86 (900 rpm)	200 ppm
10				
20				
40				

It could be observed that when the operation time reached 5 minutes, the concentration of pollutants hardly changed and had reached a steady state. In addition, from Figure 4-8(b), it could be found that the removal efficiency of each species was completely removed regardless of the gas-liquid ratio. However, the removal efficiency of NO_2 and NO_X would first decrease and then increase with the increase of the gas-liquid ratio.

doi:10.6342/NTU202102462

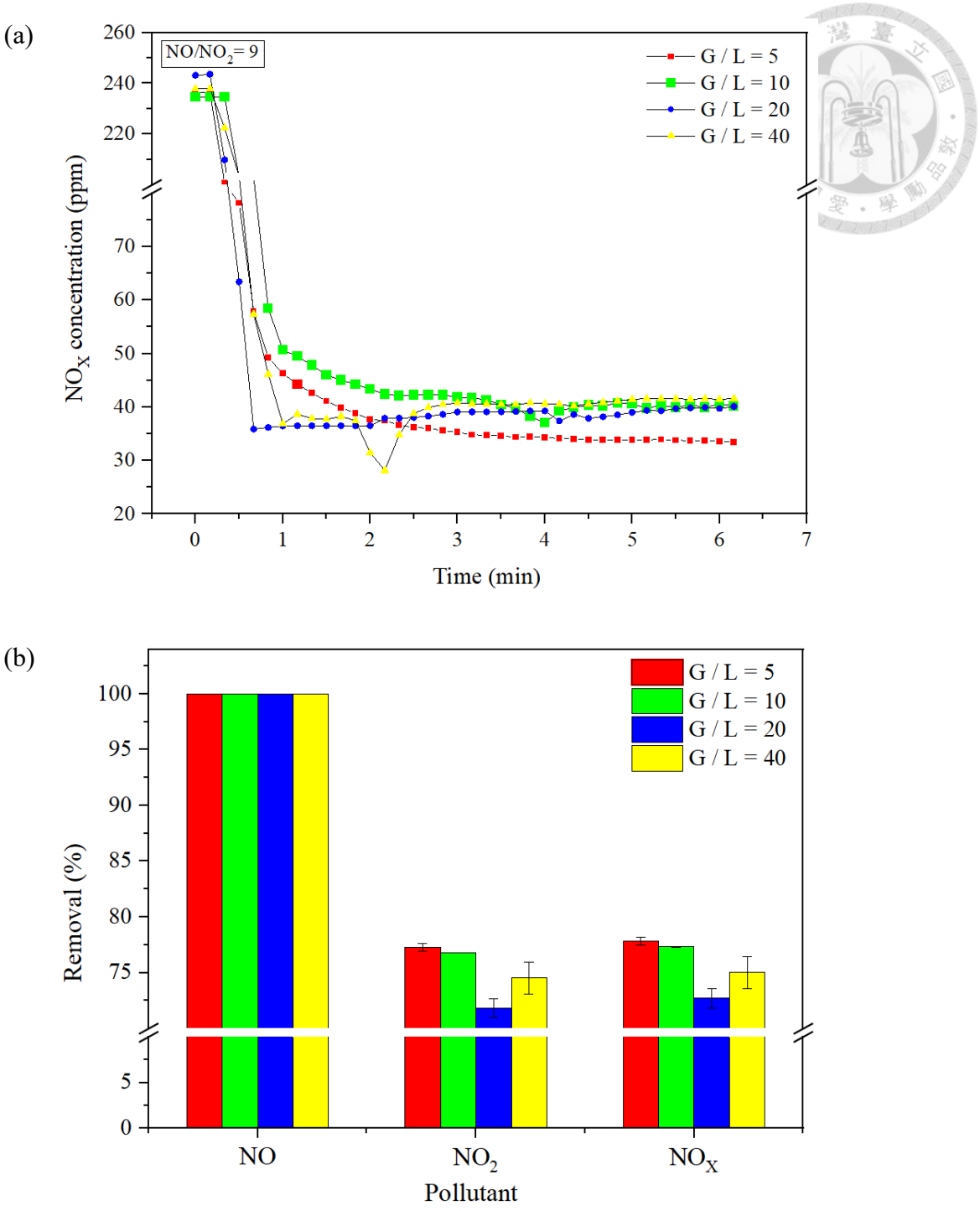

Figure 4- 8 The results in Gas-Liquid Ratio Trials (a) the relationship between operating time and concentration of nitrogen oxides (b) the removal efficiency of various nitrogen oxides

doi:10.6342/NTU202102462

In terms of nitric oxide, since the gas phase reaction had completely converted nitric oxide into other nitrogen oxides (Chapter 4.1.2), the removal efficiency was close to 100%. The removal efficiency of nitrogen dioxide was greatly affected by the gas-liquid ratio.

At present, many scholars have pointed out that the increase in liquid volume is beneficial to the improvement of mass transfer efficiency [53, 65]. This mean that there would be better removal efficiency at low gas-liquid ratio. What was more, it could be understand that the influence of the gas-liquid ratio on the absorption effect from the relationship between the operating line and the equilibrium line (Figure 4- 9).

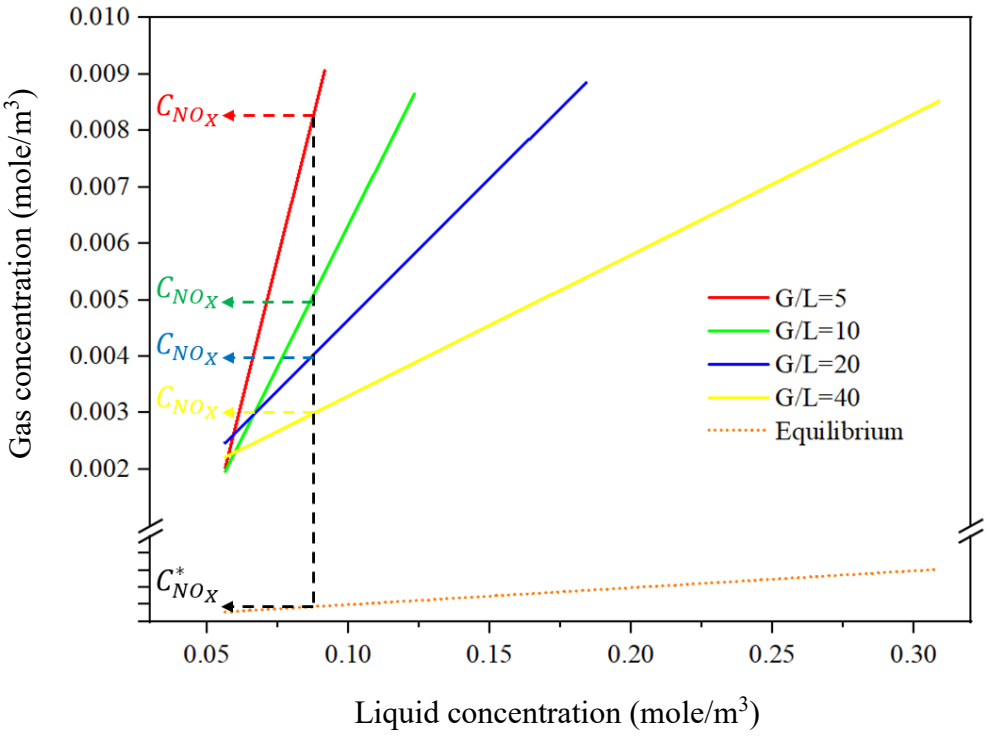

Figure 4- 9 The operating line with different gas-liquid ratio and the equilibrium line

doi:10.6342/NTU202102462

From Eq- 29, it could be known that the slope of the operating line was the reciprocal of the gas-liquid ratio (also called the liquid-gas ratio). In the case of lower gas-liquid ratios, there would be a big difference between the gas-phase concentration and the equilibrium gas-phase concentration (the gas-phase concentration in equilibrium with the current liquid-phase concentration). This concentration difference was the driving force for mass transfer (Eq- 30). In other words, a lower gas-liquid ratio has a larger driving force

$$Q_g(C_G - C_{Go}) = Q_l(C_L - C_{Li}) \quad \text{Eq- 29}$$

$$N_{NO_X} = K_G(C_{NO_X} - C^*_{NO_X}) \quad \text{Eq- 30}$$

Furthermore, the gas-liquid ratio also affected the liquid holdup and the effective mass transfer interface area [66]. The liquid holdup and effective mass transfer interface area in the experiment were calculated by using the superficial velocity of the liquid, the centrifugal force field strength and other related dimensionless parameters (Eq- 2, Eq- 4 and Eq- 5). It could be observed that the liquid holdup and the effective mass transfer area showed a downward trend as the gas-liquid ratio increased (Figure 4- 10). Namely, the decrease in gas-liquid ratio would reduce the amount of liquid that could absorb pollutants in the packed bed, and also reduce the area of gas-liquid contact, which was not conducive to the absorption of pollutants.

doi:10.6342/NTU202102462

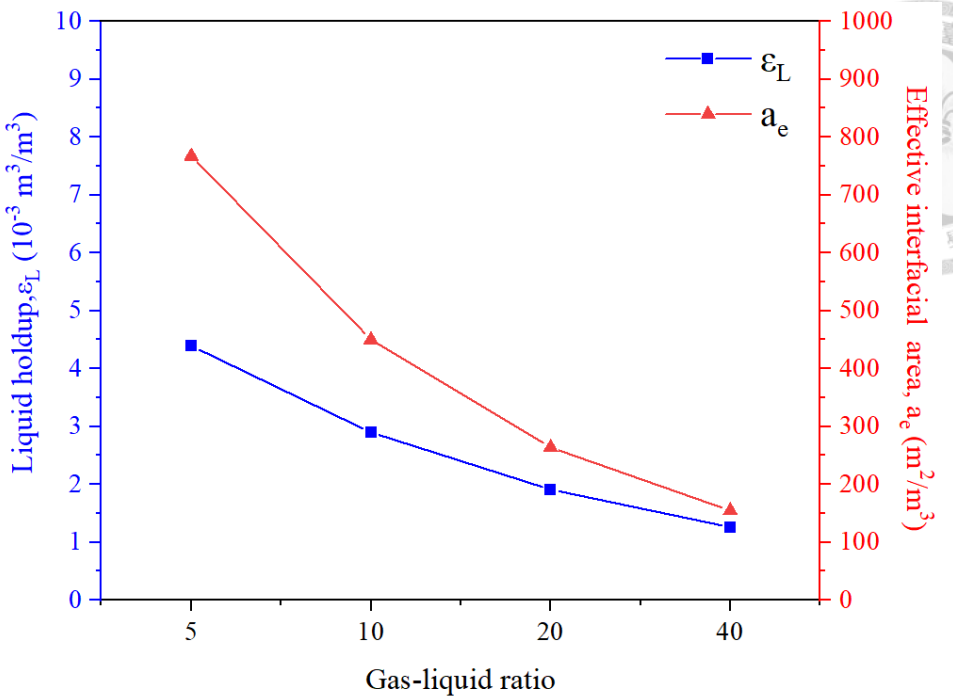

Figure 4- 10 The liquid holdup and effective mass transfer interfacial area at various level of G/L ratio

Notwithstanding many studies have pointed out that the lower gas-liquid ratio has a better absorption effect, it be found that there was a rebounds of removal efficiency with the gas-liquid ratio of 40. Therefore, the parameters were summarized that the high gas-liquid ratio was conducive to the absorption of pollutants in the experiment, including residence time and liquid film thickness. it could be intuitively understood that when the liquid flow was reduced, it would inevitably require more residence time because the liquid passes a same volume of packed bed, and a low liquid flow produced a smaller liquid film thickness under the same centrifugal force field (Figure 4- 11). Both changes contribute to the improvement of mass transfer efficiency.

doi:10.6342/NTU202102462

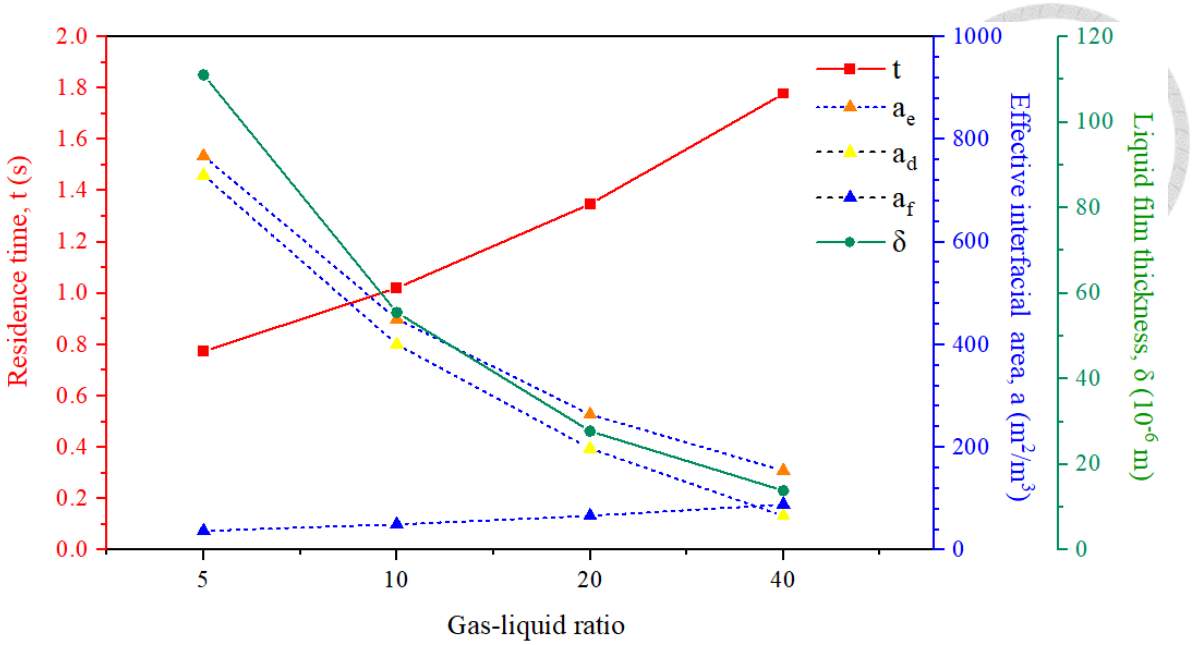

Figure 4- 11 The residence time, effective interfacial area and liquid film thickness operated at various level of G/L

It was also worth noting that a high gas-liquid ratio would cause a substantial decrease in the effective mass transfer area. In order to explore the effect of effective mass transfer interface area, residence time and liquid film thickness on the mass transfer phenomenon under high gas-liquid ratio operating conditions, the effective mass transfer interface area was divided to the liquid film area (a_f) and the effective droplet area (a_d), and the theoretical film liquid phase mass transfer coefficient (k_{Lf}) and the theoretical droplet liquid phase mass transfer coefficient (k_{Ld}) was also calculated. Here, the model proposed by Sun et al. was used to calculate the theoretical liquid phase film mass transfer coefficient and the theoretical liquid droplet mass transfer coefficient [84] (Eq- 33 and Eq- 34) (Table 4- 12).

doi:10.6342/NTU202102462

$$\frac{\partial C_{NO_X}}{\partial t} = \frac{D_L}{r^2}\frac{\partial}{\partial r}\left(r^2\frac{\partial C_{NO_X}}{\partial r}\right) - k_c C_{NO_X} \quad \text{Eq- 31}$$

$$\frac{\partial C_{NO_X}}{\partial t} = D_L\frac{\partial^2 C_{NO_X}}{\partial y^2} - k_c C_{NO_X} \quad \text{Eq- 32}$$

$$k_{Ld} = D_L\left[\frac{\sqrt{\frac{k_c}{D_L}}}{\tanh\left(\sqrt{\frac{k_c}{D_L}}\cdot\frac{d_p}{2}\right)} - \frac{2}{d_p}\right] \quad \text{Eq- 33}$$

$$k_{Lf} = \sqrt{\frac{k_c}{D_L}}\cdot \operatorname{sech}\left(\sqrt{\frac{k_c}{D_L}}\cdot\delta\right)\cdot\sinh\left(\sqrt{\frac{k_c}{D_L}}\right) \quad \text{Eq- 34}$$

Table 4- 12 The mass transfer coefficient in different gas-liquid ratio

Gas-liquid ratio	k_{Lf} (m/s)	k_{Ld} (m/s)
5	9.71×10^{-3}	5.76×10^{-12}
10	4.85×10^{-3}	5.76×10^{-12}
20	2.43×10^{-3}	5.76×10^{-12}
40	1.21×10^{-3}	5.76×10^{-12}

*k_c was the harmonic mean of k_{NO_2} [102] and k_{HNO_3}.

*$D_L = 9.71\times10^{-6}$ (m^2s^{-1})

*d_p was calculated by Eq- 3

* δ was calculated by Eq- 6

It could be observed that the liquid mass transfer coefficient was mainly provided by the liquid film, and the mass transfer coefficients of the liquid film and the droplet were different by many orders. Based on the changes in the effective interface area in Figure 4- 11, it could be found that the overall area was declining, but the variation in the droplet and the liquid film were different. It was inferred that reducing the flow rate could lower the liquid velocity, so that the liquid could more easily cover the packing and the liquid film becomes the main liquid pattern. In this way, the liquid mass transfer coefficient can be improved, so the removal efficiency was slightly increased.

doi:10.6342/NTU202102462

Although the removal efficiency was slightly improved when the gas-liquid ratio was 40, the liquid flow rate was so small that it could easily cause gas leakage and cause the experimental error in this system. Besides that, the difference in removal efficiency was not large. Therefore, subsequent experiments would continue with the gas-liquid ratio of 20.

Summarizing the gas-liquid ratio trial, the reasons for the higher removal efficiency with low gas-liquid ratio may be: (1) greater mass transfer driving force and (2) higher liquid holdup and effective mass transfer area. When operating at a high gas-liquid ratio, low liquid holdup and effective mass transfer interface area were not conducive to pollutant removal. However, because the liquid flow rate slows down, the liquid could better exist in the form of a liquid film, which improves the mass transfer coefficient of the original droplet, so the removal rate would not drop immediately.

doi:10.6342/NTU202102462

4.2.2 High-Gravity Factor

From the results of the gas-liquid ratio trial, the gas-liquid ratio of 20 was used to carry out the high-gravity factor trial. Table 4- 13 shows the parameters used in the high-gravity factor trial.

Table 4- 13 The operating conditions of High-gravity Factor Trials

Manipulated variable	Controlled variable			
High-gravity factor (β/rpm)	Gas phase agents	Liquid phase agents	Gas-liquid ratio	Concentration of NO_X
17/400	Chlorine dioxide	Tap water	20	200 ppm
38/600				
86/900				
180/1300				

The relationship between pollutant concentration changes with time and the removal of each species is shown in Figure 4- 12. After the operation time reached 2 minutes, the pollutant concentration no longer changes, and it was estimated that the system had reached a steady state. In terms of removal efficiency, the changes of NO, NO_2 and NO_X with respect to the high-gravity factor (rotational speed) all showed a trend of first rising and then falling. In addition, in terms of nitric oxide, unlike the results of the gas-liquid ratio trial and the gas-phase oxidant trial, although both were close to 100 % removal, a slight change in the removal efficiency could be observed. The rotational speed might change the liquid characteristics inside the RPB and caused the nitrous acid to regenerate nitric oxide and release it.

doi:10.6342/NTU202102462

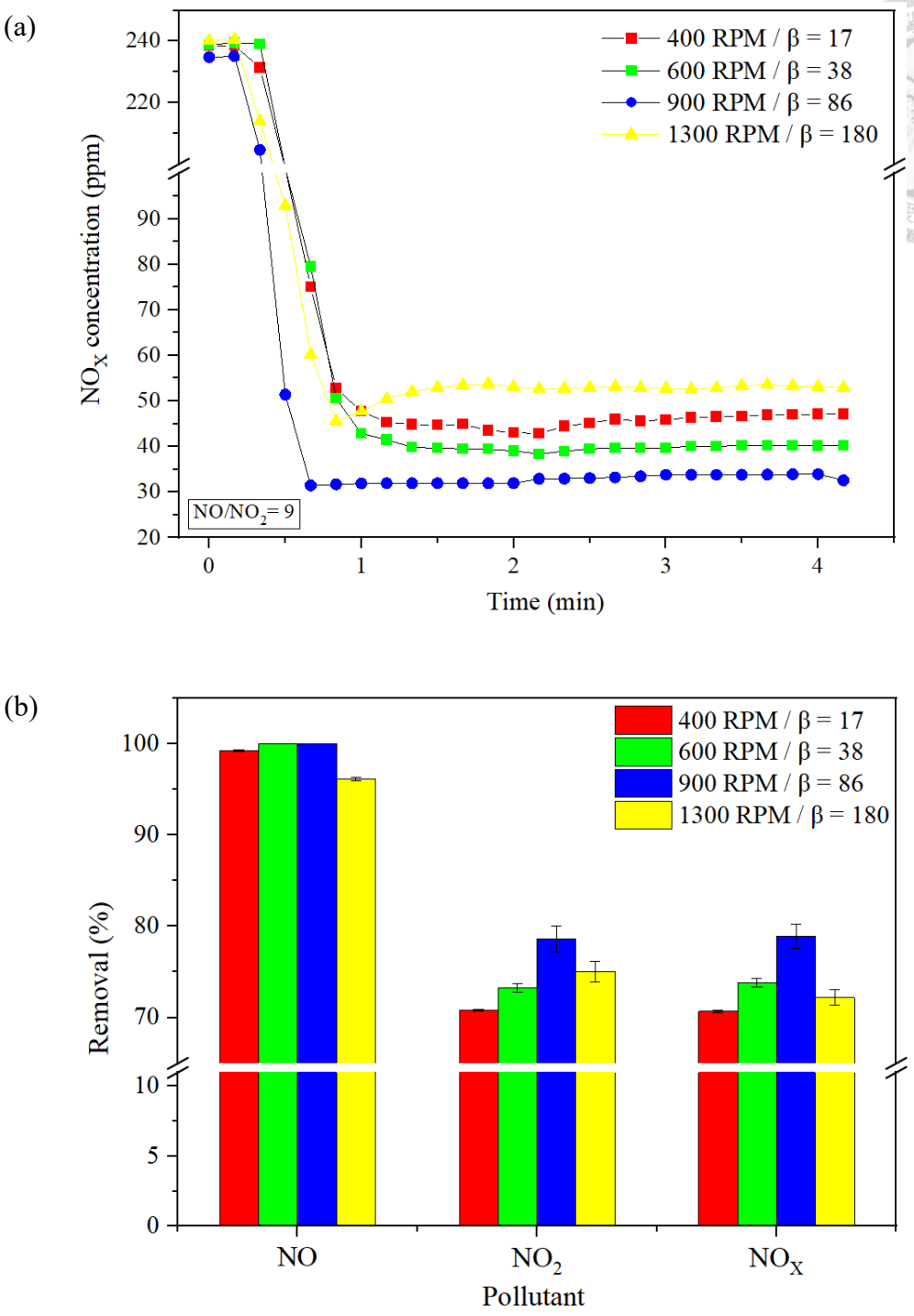

Figure 4- 12 The results in High-gravity Factor Trials (a) the relationship between operating time and concentration of nitrogen oxides (b) the removal efficiency of various nitrogen oxides

doi:10.6342/NTU202102462

On the other hand, in the removal efficiency of nitrogen dioxide, the influence of the high-gravity factor on the system could be observed clearly. Many studies have mentioned that increasing the high-gravity factor in the rotating packed bed helps to increase the mass transfer coefficient [86, 103]. The increase of the high-gravity factor could reduce the thickness of the liquid film and increase the effective mass transfer interface area. Both changes were beneficial to the removal of pollutants. Figure 4- 13 shows the liquid film thickness and effective interfacial area under different rotational speeds in this study (the calculation formula is shown in Table 2- 8). As stated in the literature, it could be perceived that the thickness of the liquid film decreases and the effective area increases.

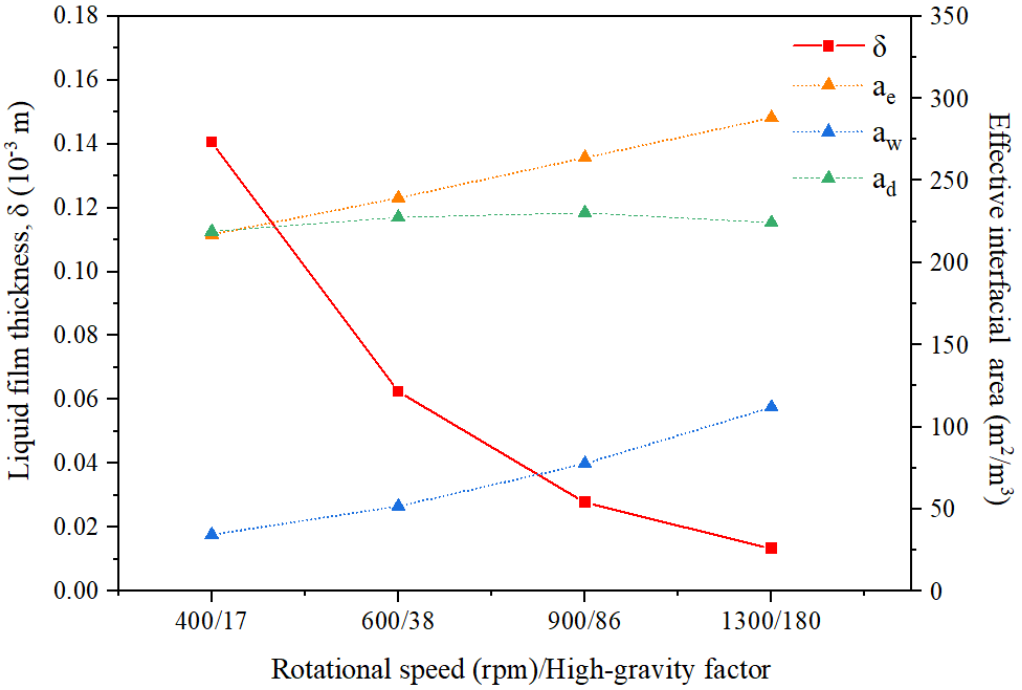

Figure 4- 13 The liquid film thickness and effective interfacial area operated under various level of high-gravity factor

doi:10.6342/NTU202102462

However, it was found that the removal efficiency would decrease after the rotating speed exceeded 900 rpm. Other studies have also found this phenomenon and attributed it to the short liquid residence time due to the high rotating speed. Moreover, it could be further observed that the liquid residence time was so short that liquid holdup would greatly reduce (Figure 4- 14). This mean that the amount of liquid that could handle contaminants in the packed bed was reduced, which would adversely affect the increase in mass transfer efficiency.

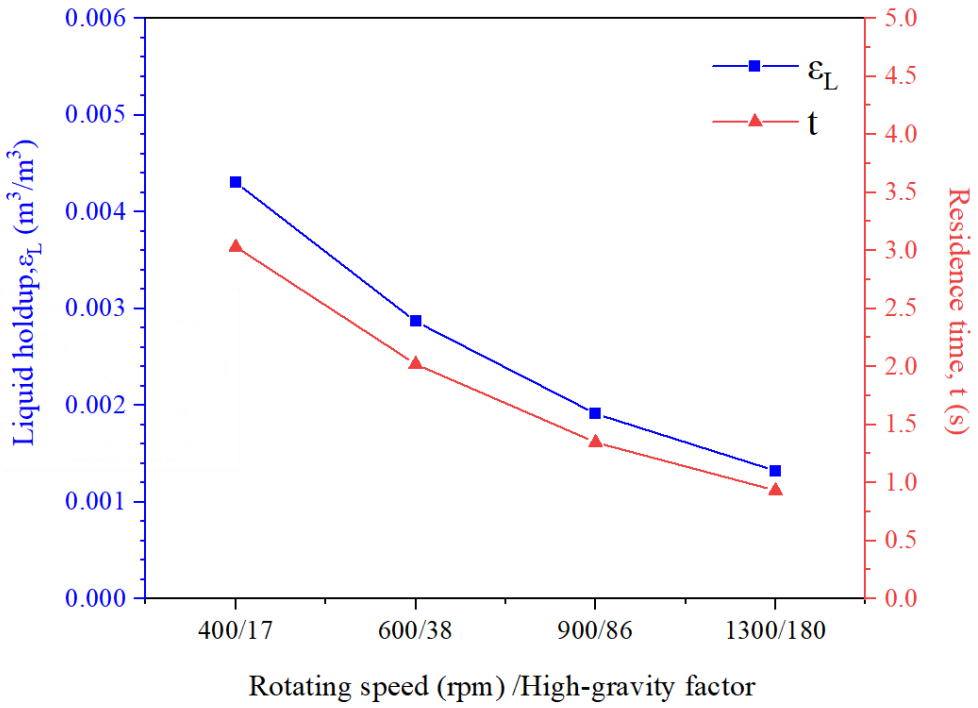

Figure 4- 14 The residence time and liquid holdup operated under various level of high-gravity factor

doi:10.6342/NTU202102462

In a nutshell, through the high-gravity factor trial, it could be concluded that (1) the augmentation of the high-gravity factor could effectually reduce the liquid film thickness and increase the effective mass transfer interface area, so it was beneficial to the absorption of pollutants; (2) the enlargement of the high-gravity factor would also make the liquid residence time shortened, and the liquid holdup decrease in the packed bed. When the speed exceeded a certain value, the latter (2) effect would be greater than the former (1), which would lessen the mass transfer efficiency.

Based on the result of the high-gravity factor trial, the best removal efficiency of 900 rpm (β=86) would be selected as the operating parameter for the subsequent " enhancement of nitrogen oxides removal efficiency" experiment.

doi:10.6342/NTU202102462

4.3 **Enhancement of NO_X Removal**

4.3.1 Combination of Gas/Liquid Agents in Process

From the direct oxidation absorption experiment, gas-liquid ratio trial and high-gravity factor trial mentioned earlier, the better operating parameters had been found out (the gas oxidant was chlorine dioxide, the gas-liquid ratio was 20, and the high-gravity factor was 86). Nevertheless, it was still unable to meet the flue gas emission standards under the best operating conditions. Therefore, regarding the results from the direct oxidation absorption experiment, the sodium hydroxide and sodium sulfite were added in the system as absorbents. Table 4- 14 shows the operating parameters of combination of gas/liquid agent trials. The relationship between pollutants and operating time in the experimental results is shown in Figure 4- 15 (a); the removal efficiency of each species is shown in Figure 4- 15 (b).

Table 4- 14 The operating conditions of Combination of Gas/Liquid Agents Trials

Manipulated variable	Controlled variable			
Liquid phase agents	Gas phase agents	High-gravity factor	Gas-liquid ratio	Concentration of NO_X
Tap water	Chlorine dioxide	86 (900 rpm)	20	200 ppm
Sodium hydroxide				
Sodium sulfite				

doi:10.6342/NTU202102462

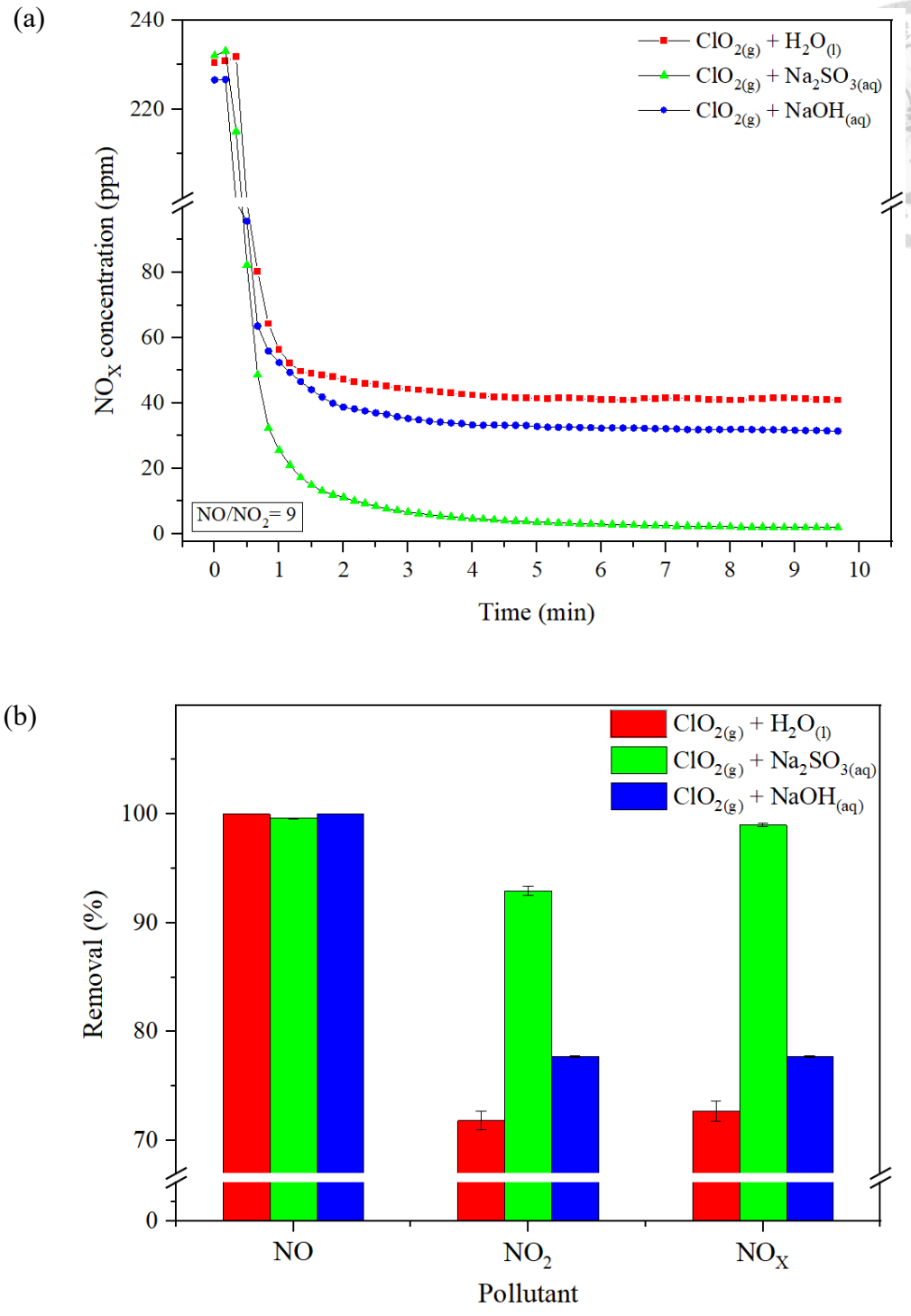

Figure 4- 15 The results in Combination of Gas/Liquid Agents Trials (a) the relationship between operating time and concentration of nitrogen oxides (b) the removal efficiency of various nitrogen oxides

doi:10.6342/NTU202102462

It could be observed that there was the best removal efficiency when sodium sulfite was used as absorbent, and the exhaust gas concentration had been lower than the legal standard. In contrast, the removal efficient was slightly improved when sodium hydroxide was used as an absorbent, but it still failed to meet the legal requirements.

Figure 4- 16 shows the enhance factor and Hatta number for different operating conditions. It could be found that there were higher E and M when chlorine dioxide was combined with sodium sulfite. Regarding this result, it was attributed to the category of product during the gas oxidation. From 4.1.2, it was deduced that the composition of the simulated exhaust gas would be transformed into pollutants dominated by nitrogen dioxide and nitric acid vapor when chlorine dioxide was used as the oxidant. The main function of sodium hydroxide was acid-base neutralization, which makes nitric acid and nitrous acid dissociate quickly (Table 2- 7). However, most of the pollutants were converted into nitric acid vapor by chlorine dioxide. The nitric acid vapor itself had the properties of high solubility and high dissociation degree. On the other hand, nitrogen dioxide needed to react with water to form nitrous acid. The reaction rate of this step was a rate controlling step [40]. Even if sodium hydroxide provided a high pH environment so that nitrous acid could dissociate quickly, the improvement effect was not obvious.

doi:10.6342/NTU202102462

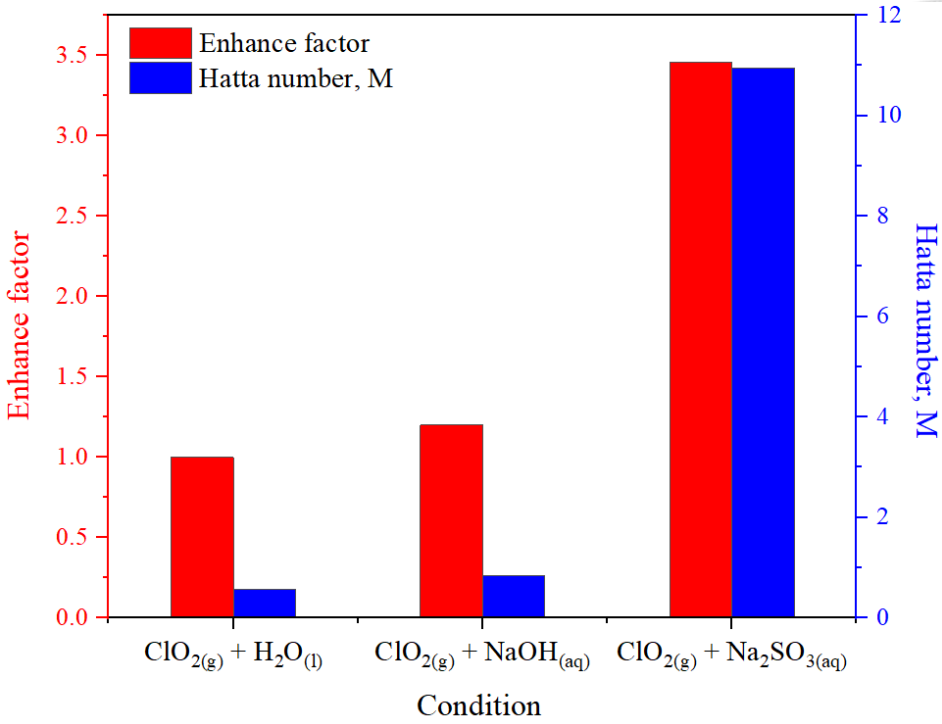

Figure 4- 16 The enhance factor and Hatta number in different operation condition

Similarly, from a chemical reaction point of view, sodium sulfite also tended to improve the absorption of nitrogen dioxide. But the difference was that sodium sulfite could directly react with nitrogen dioxide, and the process of forming nitrous acid by the reaction of nitrogen dioxide and water was skipped. In addition, sulfurous acid also provided a high pH environment and a variety of reaction pathways to react with nitrogen dioxide and nitrous acid. In a comprehensive comparison, the total reaction rate of sodium sulfite and nitrogen oxides (pseudo first-order) would be greater than the sodium hydroxide and presented the higher enhance factor and Hatta number.

doi:10.6342/NTU202102462

In addition to removal efficiency, the area of transfer unit (ATU) and height of transfer unit (HTU) were also commonly used indicators for evaluating absorption performance (Eq- 35 and Eq- 36). Figure 4- 17 shows the ATU and HTU under different operating conditions. Under the condition of using sodium sulfite, when you want to remove the same total amount of pollutants, the smaller the volume of the reactor required, it also mean that there was better absorption efficiency.

$$HTU = \frac{r_o - r_i}{NTU} \quad \text{Eq- 35}$$

$$ATU = \frac{\pi(r_o^2 - r_i^2)}{NTU} \quad \text{Eq- 36}$$

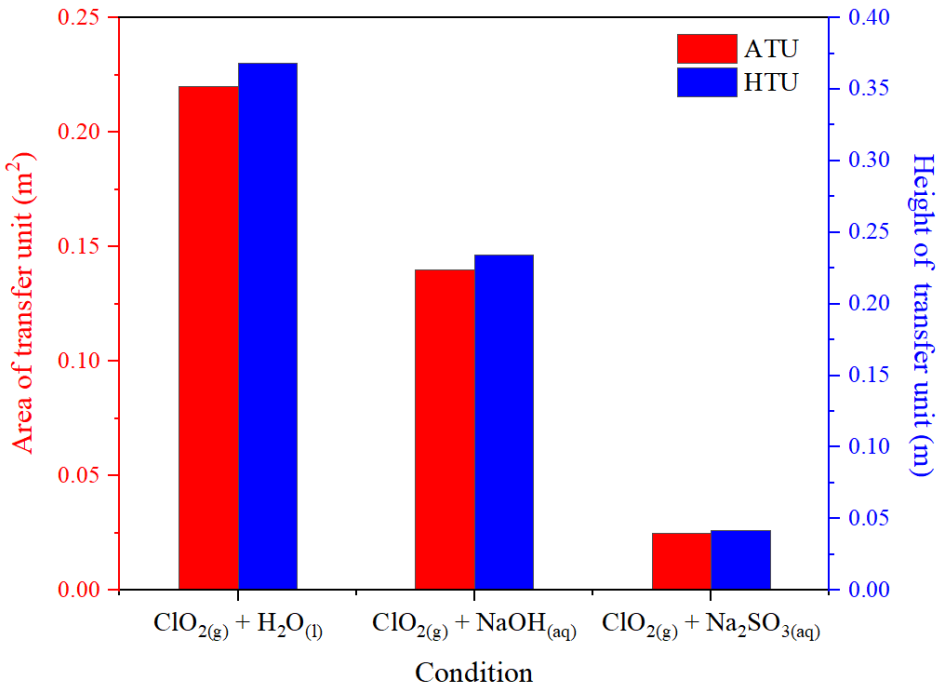

Figure 4- 17 The ATU and the HTU under different operation condition

doi:10.6342/NTU202102462

The HTU that uses absorption methods to remove nitrogen oxides in other studies [36, 40, 48, 51, 88, 100, 104-110] were compared, and it could be see that the HTU of this research was quite close to other high-efficiency absorption methods, and they were all small-volume and high-efficiency absorption procedures.

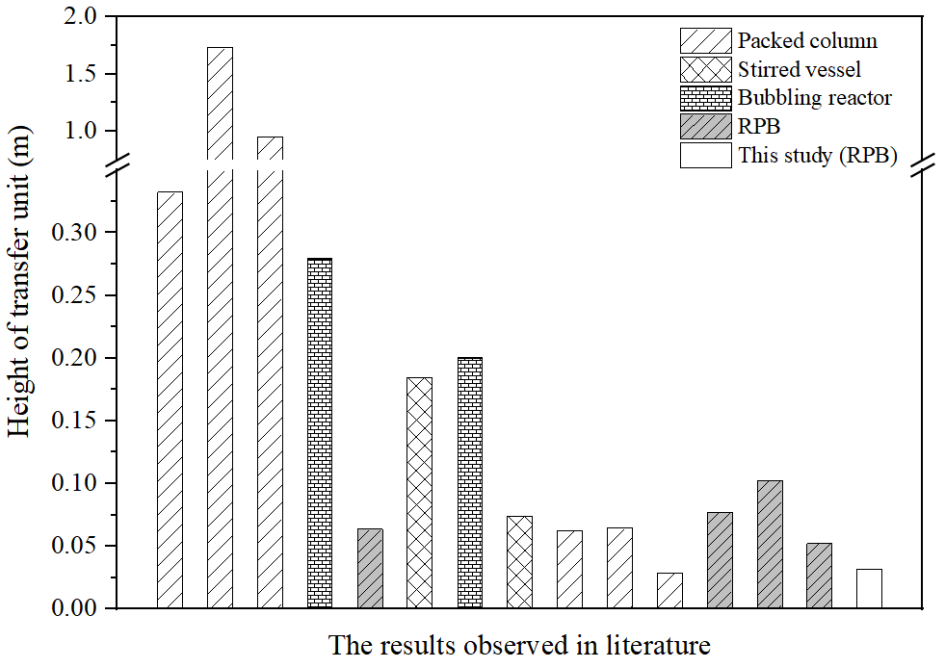

Figure 4- 18 The height of transfer unit observed in literature

Summarizing the results of the combined gas/liquid reagent test, it was concluded that gas phase chlorine dioxide combined with sodium sulfite would have a better removal efficiency. Compared with sodium hydroxide, since sodium sulfite could also provide a high pH environment and directly react with $NO_{2(aq)}$ without going through the reaction R- 47 , the improvement of the removal efficiency was greater.

doi:10.6342/NTU202102462

4.4 **Modeling NO_X Removal**

In order to better understand the ability to treat nitrogen oxides in this system, the dimensional analysis was used to establish a predictive formula for the mass transfer coefficient. Then, the mass transfer coefficient and estimate the maximum nitrogen oxide concentration that the system could handle were calculated by the prediction model. At the end of this chapter, the design process of the rotating packed bed to remove nitrogen oxides would be integrated briefly.

4.4.1 Dimensional Analysis in Mass Transfer

Buckingham's π theorem was applied for dimensional analysis. With reference to the parameters selected by Zhang et al. [111] and Zhao et al.[112], the mass transfer coefficient was a function of the gas phase diffusion coefficient (D_G), the liquid phase diffusion coefficient (D_L), the gas flow rate (u_G), the liquid flow rate (u_L), the specific surface area of the packing (a_t), etc. (Eq- 37)

$$K_G a = f(D_G, D_L, u_G, u_L, \dots, a_t) \qquad \text{Eq- 37}$$

Next, though the dimensional analysis, the five dimensionless parameters could be got. They were Sherwood number (Sh), Reynolds number of the gas phase (Re_G), Reynolds number of the liquid phase (Re_L), Schmidt number of the liquid phase (Sc_L), Grashof number of the gas phase (Gr_G) and gas-liquid molar ratio (Mr). (Eq- 38 and Table 4- 15)

doi:10.6342/NTU202102462

Table 4- 15 Dimensionless number for prediction model.

Variables	Dimensionless parameter	Presentation
Dependent π	Re_G	$d_p u_G/v_G$
	Re_L	$^*d_h u_L/v_L$
	Sc_L	v_L/D_L
	Gr_G	$\omega^2 r_{avg}(r_o - r_i)^3/v_G^2$
	Mr	$Q_g c_g/Q_l c_l$
Independent π	Sh	$K_G a/(D_G a_t^2)$

$^*d_h = 4r_h$, where $r_h = \varepsilon_L/a_e$

$$Sh = f(Re_G, Re_L, Sc_L, Gr_G, Mr) \quad \text{Eq- 38}$$

Sherwood number (Sh) was the ratio of convective mass transfer to diffusion mass transfer rate; Reynolds number (Re) was the ratio between inertial force and viscous force, which can be used to judge flow conditions; Schmidt number (Sc_L) was the ratio of momentum transfer to mass transfer effect; Grashof number (Gr_G) was a ratio between buoyancy and viscous force. In HiGee system, the centrifugal field could be analogous to the gravitational field, which could be regarded as the ratio of centrifugal force to viscous force; gas-liquid molar ratio (Mr) was the ratio of the gas molar flow rate to the liquid molar flow rate, which was related to the gas-liquid ratio of the operation.

On the other hand, consider absorption as chemical absorption, the mass transfer was not a single physical phenomenon, so an enhance factor was added to the relationship (Eq- 39).

$$Sh = f(Re_G, Re_L, Sc_L, Gr_G, Mr, E) \quad \text{Eq- 39}$$

doi:10.6342/NTU202102462

Then the actual mass transfer coefficient could be calculated through experimental data and mass balance equation. In the mass balance equation, the integral of the reciprocal of the concentration difference called the number of transfer unit (NTU).

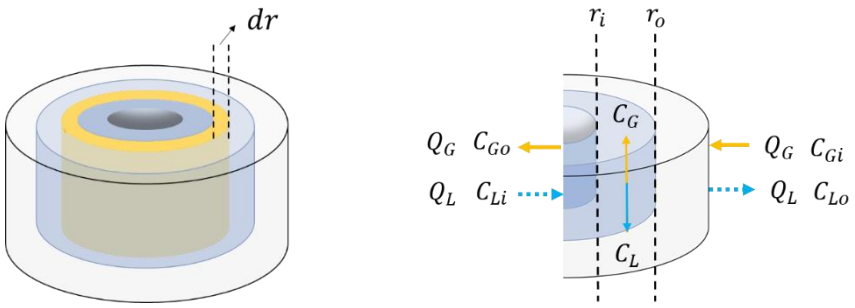

Figure 4- 19 Schematic diagram of mass balance in rotating packed bed

$$\Delta(CV\varepsilon) = Q_g C_r \Delta t - Q_g C_{r+dr} \Delta t - K_G (C - C^*) Va \Delta t \qquad \text{Eq- 40}$$

$* \quad V = -2\pi r dr Z \quad \text{and} \quad \frac{\partial C}{\partial t} = 0$

$$\rightarrow \quad \frac{\partial C}{\partial t} = \frac{Q_g}{2\pi Z\varepsilon} \frac{1}{r} \frac{\partial C}{\partial r} - \frac{K_G a}{\varepsilon} (C - C^*)$$

$$\rightarrow \quad \frac{Q_g}{2\pi Z\varepsilon} \frac{1}{r} \frac{dC}{dr} = \frac{K_G a}{\varepsilon} (C - C^*)$$

$$\rightarrow \quad \int_{r_i}^{r_o} K_G 2\pi \cdot Z \cdot a \cdot r dr = \int_{C_{Go}}^{C_{Gi}} Q_g \frac{dC_G}{(C - C^*)}$$

$$\rightarrow \quad K_G a \pi Z (r_o^2 - r_i^2) = Q_g \left(\frac{\ln\left[\left(\frac{C_{Gi} - HC_{Li}}{C_{Go} - HC_{Li}} \right) (1 - St) + St \right]}{1 - St} \right)$$

$* \quad St = \frac{HQ_g}{Q_l}$

$$* \quad NTU = \frac{\ln\left[\left(\frac{C_{Gi} - HC_{Li}}{C_{Go} - HC_{Li}} \right) (1 - St) + St \right]}{1 - St} \approx \ln\left(\frac{C_{Gi}}{C_{Go}} \right) \qquad \text{Eq- 41}$$

$$\rightarrow \quad K_G a = \frac{Q_g}{\pi Z (r_o^2 - r_i^2)} \cdot NTU \qquad \text{Eq- 42}$$

doi:10.6342/NTU202102462

Combining Eq- 39 and Eq- 42 for the regression of the mass transfer coefficient, the prediction equation of the mass transfer coefficient could be get (Eq- 43 and Table 4- 16). In the prediction formula, the Reynolds number and Schmidt number of the liquid did not appear, because the power of these phases was zero after regression. This result was ascribed to the liquid flow conditions, dynamic viscosity and liquid phase diffusion coefficient had not changed significantly in the system.

$$\frac{K_G a}{D_G a_t^2} = 1.45 \times 10^{-5} \times Re_G^{0.209} \times Gr_G^{0.0501} \times Mr^{-0.0612} \times E^{1.01} \qquad \text{Eq- 43}$$

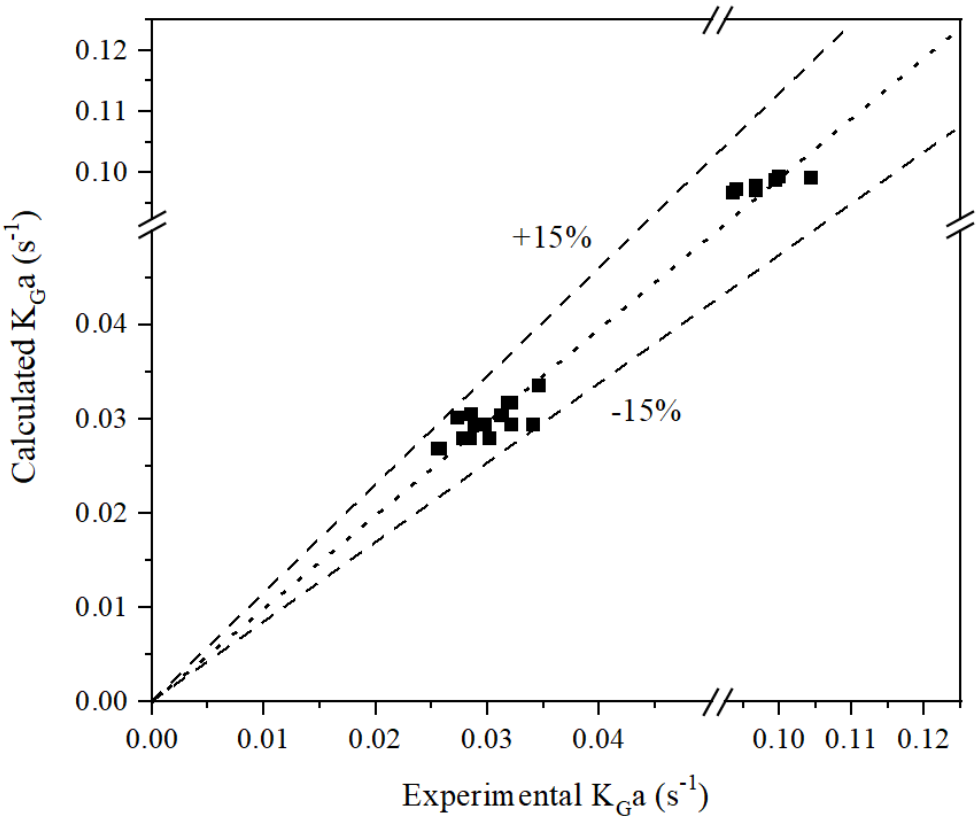

Figure 4- 20 The correlation between predicted and experimental $K_G a$ values

doi:10.6342/NTU202102462

Table 4- 16 Hypothesis testing for correlation of mass transfer coefficient

ANOVA	DF	SS	MS	F	P-value
Regression	4	8.29	2.07	1368.57	5.53E-27
Residuals	23	0.0349	0.00151	-	-
Sum	27	8.33	-	-	-

Dependent π	Range	P-value
Re_G	$3.06 \times 10^{-1} \sim 3.31 \times 10^{-1}$	0.461
Gr_G	$1.92 \times 10^{9} \sim 2.02 \times 10^{10}$	0.00559
Mr	$3.57 \times 10^{-3} \sim 2.83 \times 10^{-2}$	0.00177
E	$0.9924 \sim 3.3215$	7.99E-28

From Figure 4- 20, it could be observed that deviation between the experimental mass transfer coefficient and the predicted mass transfer coefficient was about ±15%. Therefore, the predicted mass transfer coefficient would be used in 4.4.2 to calculate the maximum pollution concentration load in the system

doi:10.6342/NTU202102462

4.4.2 Applicable Concentration Loading in this System

For the purpose of deducing the maximum pollutant load in the system from the mass transfer coefficient, it could be calculated from the mass balance equation mentioned earlier. From Eq- 40, the relationship between the concentration and the radius of the packed bed could be obtained (Eq- 44).

$$\Delta(CV\varepsilon) = Q_g C_r \Delta t - Q_g C_{r+dr} \Delta t - K_G (C - C^*) Va \Delta t \qquad \text{Eq- 40}$$

$$\rightarrow \quad \frac{Q_g}{2\pi Z\varepsilon} \frac{1}{r} \frac{dC_G}{dr} = \frac{K_G a}{\varepsilon} (C_G - C_G^*)$$

$$* \quad C_G^* = H \cdot C_L \text{ and } C_L = \frac{Q_g}{Q_l} (C_G - C_{Go}) + C_{Li}$$

$$\rightarrow \quad K_G C_G 2\pi r dr \cdot Z \cdot a = Q_g dC_G$$

$$\rightarrow \quad \int \frac{K_G \cdot 2\pi r \cdot Z \cdot a}{Q_g} dr = \int \frac{dC_G}{C_G}$$

$$\rightarrow \quad \frac{K_G a \pi Z r^2}{Q_g} = \ln(C_G) + C$$

$$\rightarrow \quad C' \cdot EXP\left[\frac{K_G a \pi Z r^2}{Q_g}\right] = C_G \qquad \text{Eq- 44}$$

After calculating the relationship between the concentration and the radius of the packing, the mass transfer coefficient in the Eq- 44 can be estimated by Eq- 45, and the constant C' could be calculated by the boundary conditions. The value of the boundary conditions was related to the exhaust gas concentration engineers designed. The current flue emission standard was 30 ppm (NO_X). For the sake of avoiding sudden load increase, it was hoped that the normal exhaust gas concentration would be controlled below 10 ppm.

doi:10.6342/NTU202102462

Here, the two exhaust gas concentrations were preset (5 ppm and 10 ppm respectively). Therefore, the boundary conditions were as Eq- 46 and Eq- 47. Then the constant C' could be obtained from Eq- 48.

$$r = r_i \rightarrow C_{G_{exhaust}} = 4.13 \times 10^{-4} \left(\frac{mole}{m^3}\right) = 10\ (ppm) \quad \text{Eq- 46}$$

$$r = r_i \rightarrow C_{G_{exhaust}} = 2.06 \times 10^{-4} \left(\frac{mole}{m^3}\right) = 5\ (ppm) \quad \text{Eq- 47}$$

$$C' \cdot EXP\left[\frac{K_G a \pi Z r_i^2}{Q_g}\right] = C_{G_{exhaust}} \quad \text{Eq- 48}$$

The relevant parameters obtained by the prediction model are shown in Table 4-17. When the exhaust gas concentration was 5 ppm and 10 ppm, the pollution source concentration was 417.96 ppm and 796.15 ppm.

Table 4- 17 The relevant parameters obtained by the prediction model

Prediction model				
Concentration (ppm)	Gas flow rate (L/min)	Liquid flow rate (L/min)	K_Ga (s^{-1})	Exhaust concentration (ppm)
398.07	5.00	0.25	0.097	5.00
796.15	5.00	0.25	0.097	10.00

However, it was difficult to completely control the gas flow rate and pollutant concentration to be the same as the prediction model in practical operation. Therefore, the parameters from the prediction model were corrected based on the actual pollutant concentration and gas flow rate, and then the predicted mass transfer coefficient was used to prognosticate the exhaust gas concentration.

doi:10.6342/NTU202102462

Figure 4- 21 shows the relationship between pollutant concentration and time for different pollutant concentrations in actual operation. Table 4- 18 shows the real exhaust gas concentration based on actual operating parameters and predicted mass transfer coefficients. The practical operating concentration were 417.96 ppm and 738.82 ppm, and the predicted exhaust gas concentration were 4.91 ppm and 10.12 ppm. After practical operation, the exhaust gas concentration were 5.04 ppm and 9.38 ppm, which were similar to the predicted results. This difference was mainly due to the fact that the mass transfer coefficients of the actual experiment were 0.0966 and 0.0993, which are slightly different from the predicted mass transfer coefficients (0.0970).

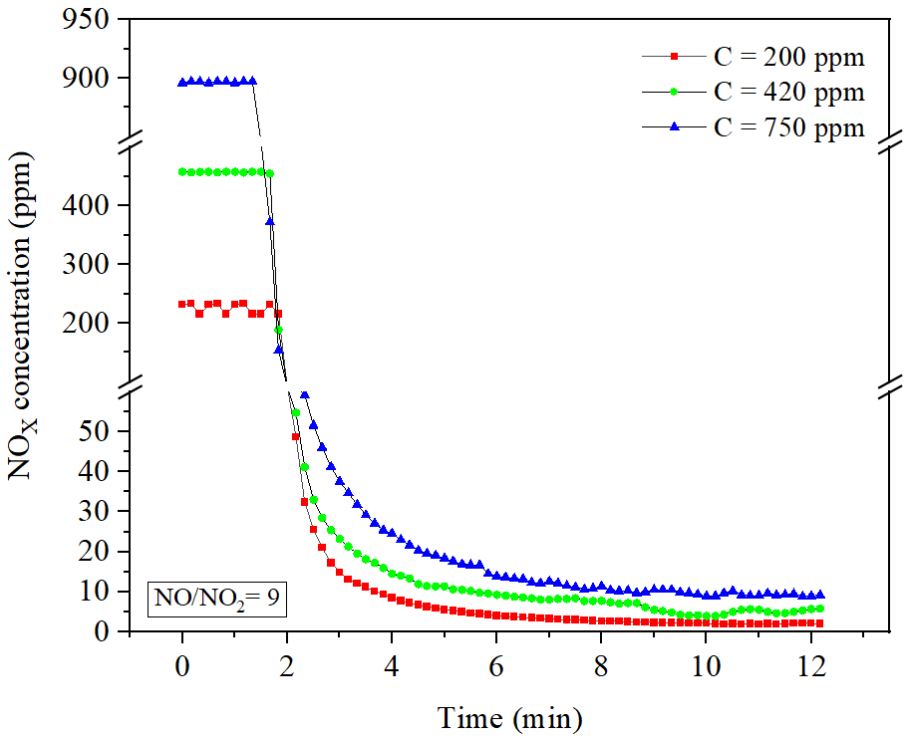

Figure 4- 21 The relationship between pollutant concentration and time for different pollutant concentrations in actual operation (Q_g= 5 LPM, G/L= 20, β= 86, and chemical agents were $ClO_{2(g)}$ and $Na_2SO_{3(aq)}$)

doi:10.6342/NTU202102462

Table 4- 18 The relevant parameters in the practical operation

Practical operation						
Concentration (ppm)	Gas flow rate (L/min)	Liquid flow rate (L/min)	K_Ga (s^{-1})		Exhaust concentration (ppm)	
417.96	4.92	0.25	Pred.	0.0970	Pred.	4.91
			Real	0.0966	Real	5.04
738.82	5.10	0.25	Pred.	0.0970	Pred.	10.12
			Real	0.0993	Real	9.38

Similarly, the data from the previous gas-liquid ratio trials and the high-gravity factor trials could be applied in the same way. The prognostic mass transfer coefficient was used to estimate the exhaust gas concentration, and it could be found that there was little difference from the actual exhaust gas concentration (Figure 4- 22), mainly due to the good mass transfer coefficient estimation model.

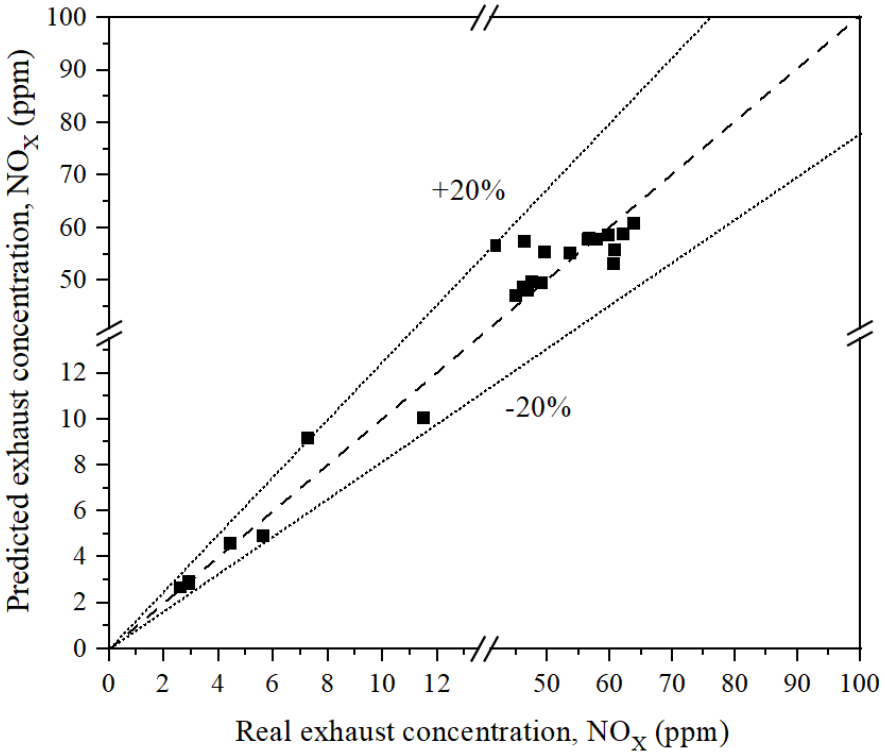

Figure 4- 22 The relationship between the prediction and the real exhaust concentration

doi:10.6342/NTU202102462

In addition to predicting the exhaust gas concentration, the relationship between the pollutant concentration and the radius of the packing could also be found out by Eq-44. This relationship could help us understand how much packing volume was needed to achieve the target emission concentration (the characteristics of the packing was the same, and the change on mass transfer coefficient by the volume could be ignored). Therefore, a specific packed bed size could be designed according to the concentration range of the pollution source.

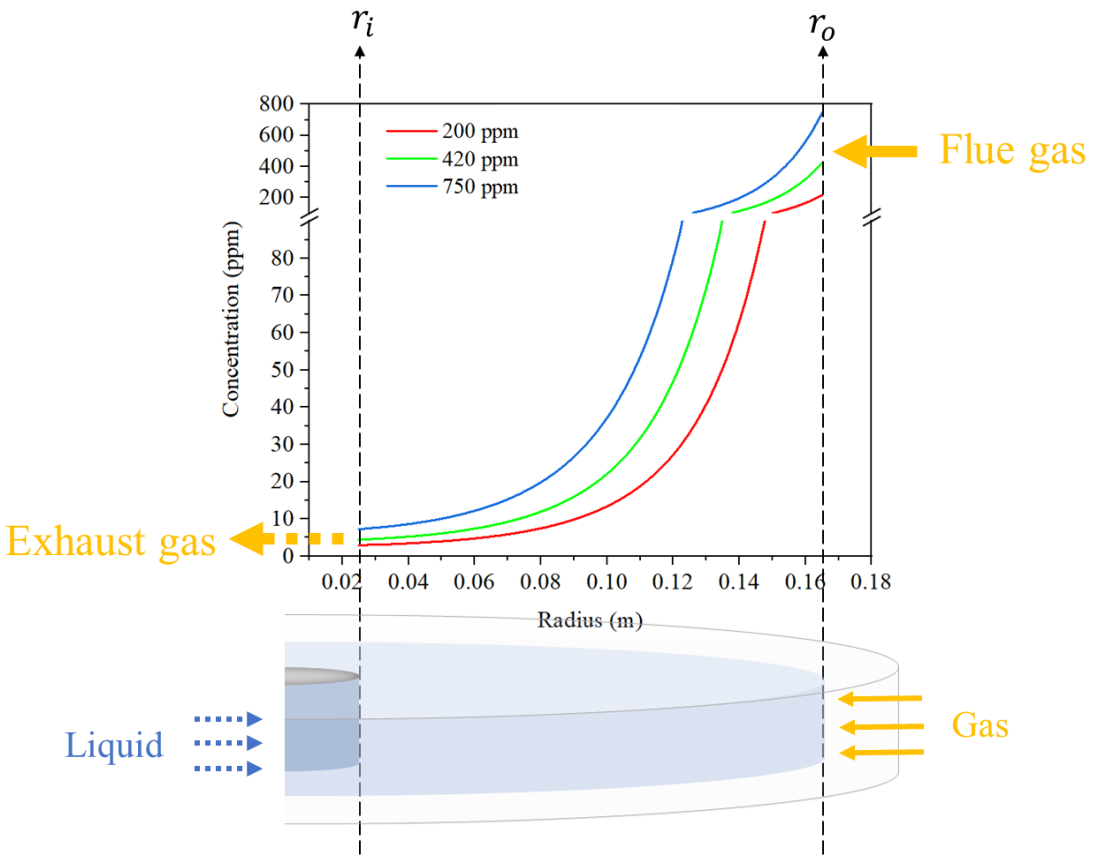

Figure 4- 23 The relationship between the pollutant concentration and the packing radius

doi:10.6342/NTU202102462

Based on the above, Eq- 43 and Eq- 44 could be used to estimate the maximum pollutant concentration that the system could handle. When the target exhaust gas concentration was 5 ppm, the pollution source concentration could reach about 420 ppm; when the target exhaust gas concentration was 10 ppm the pollution source concentration could reach about 750 ppm. Furthermore, the Eq- 44 could help design a packed bed size that meets the pollution source concentration and exhaust gas concentration requirements.

doi:10.6342/NTU202102462

4.4.3 Systematic Establishment of RPB Operation Model

It was summarized that the mass transfer model of the counter-current rotating packed bed this chapter, and systematically organized the process of treating nitrogen oxides in the rotating packed bed (Figure 4- 24). The main process included: (1) Database establishment, (2) Prediction model, (3) Target characteristics, (4) Mass transfer coefficient calculation, (5) Operation parameter determination, (6) Actual parameter execution, (7) Whether it meet the target concentration, (8) Maintain operation parameter, (9) Whether the characteristics of the pollution source was various and (10) Emission. The following briefly explained the contents of each program.

A. Database establishment

In this step, the parameter investigation and experimental design would be conduct. The parameter survey included the volume of the packed bed, the size of the inner and outer diameters, pollutant composition, etc.; the experimental design included the range of gas-liquid ratio and speed, the type of gas-phase oxidant and the type of liquid-phase absorbent.

B. Prediction model

After collecting the experimental data, determine the parameters that affect the mass transfer efficiency (refer to 4.4.1), the dimensional analysis or regression of other experimental parameters could be used.

doi:10.6342/NTU202102462

C. Target characteristics

Measure the pollutants characteristics in the system, including gas flow and initial concentration of pollutants, and determine the exhaust gas emission concentration (i.e., target concentration)

D. Mass transfer coefficient calculation

How much K_Ga was needed which was calculate by the target characteristics.

E. Operation parameter determination

Use theoretical K_Ga and prediction model to calculate the combination of operating parameters, or use operating parameters similar to theoretical K_Ga in the database.

F. Actual parameter execution

Operate the calculated parameters actually and detect the exhaust gas concentration.

G. Whether it meet the target concentration

Determine whether the exhaust gas concentration was consistent with the target concentration.

H. Maintain operation parameter

the current operating parameters are maintained when the actual exhaust gas concentration was consistent with the target exhaust gas concentration.

doi:10.6342/NTU202102462

I. Whether the characteristics of the pollution source was various

The system needs to recalculate the theoretical mass transfer coefficient when the characteristics of the pollution source changes (such as the increase in flow rate, the increase in initial concentration, tightening of regulations and standards, etc.),

J. Emission

After confirming that the exhaust gas concentration meets the regulatory standards, it would be discharged into the environment.

The above was a systematic integrated rotating packed bed removal process for nitrogen oxides. By systematically summarizing the processing flow, the program could be coded and programmed to further realize the automatic control of nitrogen oxides removal in the RPB.

doi:10.6342/NTU202102462

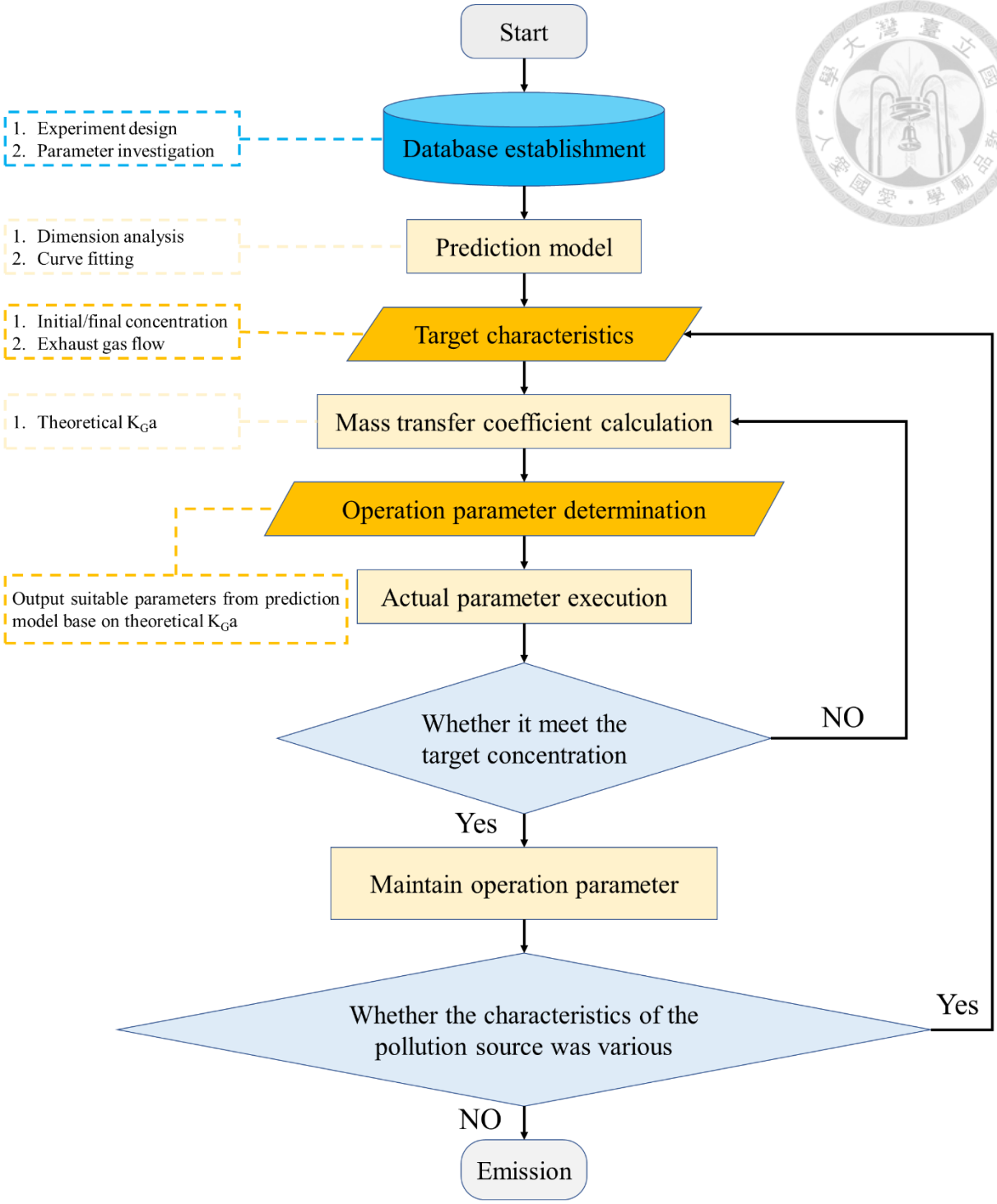

Figure 4- 24 The flow chart of RPB operation model

doi:10.6342/NTU202102462

4.5 Energy Consumption and Cost Analysis

The promotion and regulation of air pollution control technology was an important strategy for continuously reducing pollutant emissions and improving air quality. These strategies often used the four tools to achieve: (1) best available control technology (BACT), (2) reasonable available control technology (RACT), (3) reasonable available control measures (RACM), (4) least achievable emission rate (LAER). The tools mentioned above were not only supported by engineering data, but also cost-benefit analysis at the economic level and energy consumption assessment at the environmental level. Therefore, this chapter would conduct a simple energy consumption and cost-benefit analysis on the technology of "Nitrogen oxides removal via chemical oxidation absorption in rotating packed bed".

Refer to the materials and equipment mentioned in 3.2.1 Reagents and 3.2.2 Instruments and Equipment. Table 4- 19 lists the items that would be included in the energy consumption assessment and cost analysis in this study. Figure 4- 25 shows the system boundary of the energy consumption assessment and the cost analysis in this study.

doi:10.6342/NTU202102462

Table 4- 19 The items included in energy consumption and cost-benefit analysis

	Item	Energy Consumption	Cost Analysis
Reagents	[a] Gas cylinder	×	○
	[b] Gas phase oxidants	×	○
	[c] Liquid phase agents	×	○
	Standard solution	×	×
	Silicone	×	×
Equipment	Mass Flow Controller	×	×
	Flow meter	×	×
	Ozone generator	○	○
	Chlorine dioxide generator	○	○
	Precise dry-air flowmeter	×	×
	Water quality analysis	×	×
	Electronic balance	×	×
	Peristaltic Pump	○	○
	Pipeline and accessories	×	×
	PG-350 Portable gas analyzer	○	○
	Ion chromatography	×	×

[a] O_2 cylinder.

[b] Liquid phase agents are used to produce chlorine dioxide and as absorbents.

[c] Sodium hydroxide and sodium sulfite.

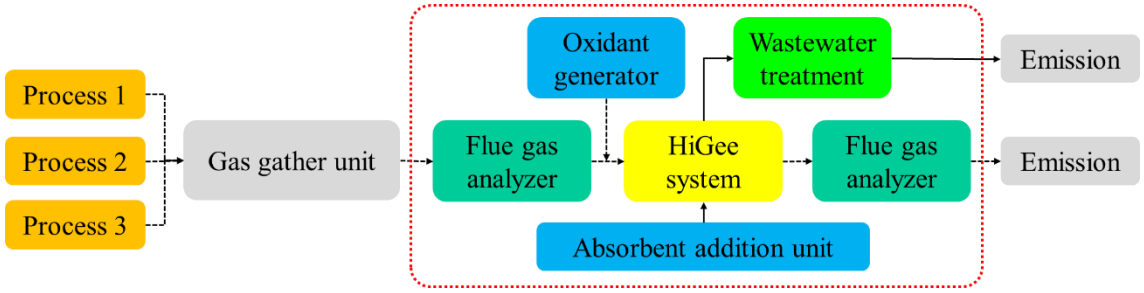

Figure 4- 25 The framework for the cost benefit analysis in this study

doi:10.6342/NTU202102462

4.5.1 Energy Consumption

At present, people hoped to adopt a more comprehensive evaluation method to analyze this new decision when adopting new processes, technologies, products etc. Energy consumption was a widely discussed field, so this section would calculate the energy consumption for various operating conditions in this study, and use the pollutants that could be captured per energy unit as an indicator of energy efficiency (g NO_X/kWh). Figure 4- 26 shows the energy consumption of rotating packed bed and liquid pump under different conditions. It could be found that the energy consumption was proportional to the operating conditions.

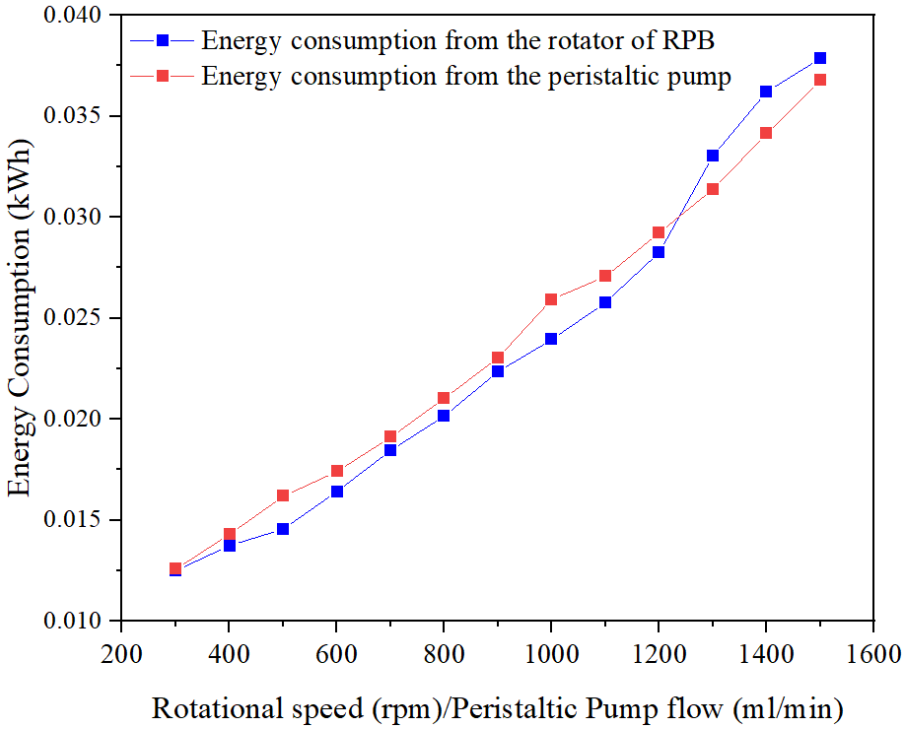

Figure 4- 26 The correlation between rotational speed, liquid flow rate and energy consumption.

doi:10.6342/NTU202102462

In addition to the rotating packed bed and the peristaltic pump, since the gas-phase oxidant was produced on-site, the electricity consumption of the ozone generator and the chlorine dioxide generator must also be calculated. Table 4- 20 shows the calculation results of energy consumption under each operating parameter in the experiment. The energy consumption changes with the increase of oxidant usage, gas-liquid ratio and high-gravity factor respectively as rise, fall and rise; while the use of liquid-phase medicament has no obvious influence on energy consumption.

It was worth noting that the NO_X capture capacity not only did not decrease, but also increases under the condition that the increasing oxidant demand and the energy consumption increased.

On the other hand, most of the operating conditions couldn't meet the nitrogen oxide emission standards, and only the operating conditions NO. 10, 12 and 13 meet the regulatory standards. The NO_X capture capacity of these operating conditions was also higher (0.189, 0.247 and 0.323 g NO_X/kWh).

doi:10.6342/NTU202102462

Table 4- 20 The relationship between the energy consumption and experimental parameters in this study

Oxidation-Absorption Trials					
NO.	Manipulated variable (Gas phase agents)	Controlled variable (L Agents+G/L+β+C_{NOx})	Energy consumption	NO_X capture capacity	Exhaust gas concentration
			Watt	g NO_X/kWh	ppm
1	-	Tap water+20+86+200	260.18	0.009	179.74
2	Chlorine dioxide		451.64	0.117	56.80
3	Ozone		436.18	0.096	74.91
Gas-Liquid Ratio Trials					
NO.	Manipulated variable (Gas-Liquid Ratio)	Controlled variable (G/L Agents+β+C_{NOx})	Energy consumption	NO_X capture capacity	Exhaust gas concentration
4	5	ClO_2/Tap water+86+200	474.26	0.114	46.94
5	10		459.18	0.109	46.52
2	20		451.64	0.117	56.80
6	40		447.87	0.104	53.61
High-Gravity Factor Trials					
NO.	Manipulated variable (High-gravity Factor)	Controlled variable (G/L Agents+G/L+C_{NOx})	Energy consumption	NO_X capture capacity	Exhaust gas concentration
7	17	ClO_2/Tap water+20+200	312.75	0.139	62.23
8	38		368.31	0.135	56.52
2	86		451.64	0.116	41.66
9	180		562.75	0.091	60.70
Combination of Gas/Liquid Agents Trials					
NO.	Manipulated variable (Gas/Liquid Agents)	Controlled variable (G/L+β+C_{NOx})	Energy consumption	NO_X capture capacity	Exhaust gas concentration
2	$ClO_{2(g)}$/Tap water$_{(l)}$	20+86+200	451.64	0.117	56.80
10	$ClO_{2(g)}$/$Na_2SO_{3(aq)}$		451.64	0.189	2.60
11	$ClO_{2(g)}$/$NaOH_{(aq)}$		451.64	0.127	44.98
Applicable Concentration Loading Trials					
NO.	Manipulated variable (Concentration)	Controlled variable (G/L Agents+G/L+β)	Energy consumption	NO_X capture capacity	Exhaust gas concentration
10	200	$ClO_{2(g)}$/$Na_2SO_{3(aq)}$+20+86	451.64	0.189	2.60
12	420		638.54	0.247	5.64
13	750		895.48	0.323	11.49

doi:10.6342/NTU202102462

Figure 4- 27 shows the relationship between energy consumption changes, exhaust gas concentration and NO_X capture capacity. In the exhaust gas concentration curve, the three lower concentrations could be found, and these points just correspond to the rising section of the NO_X capture capacity curve. Among them, it was found that the No. 10 NO_X capture capacity was improved without a change in energy consumption. The main reason was the addition of liquid-phase reagents. Therefore, the energy consumption could increase the capture capacity without significant changes.

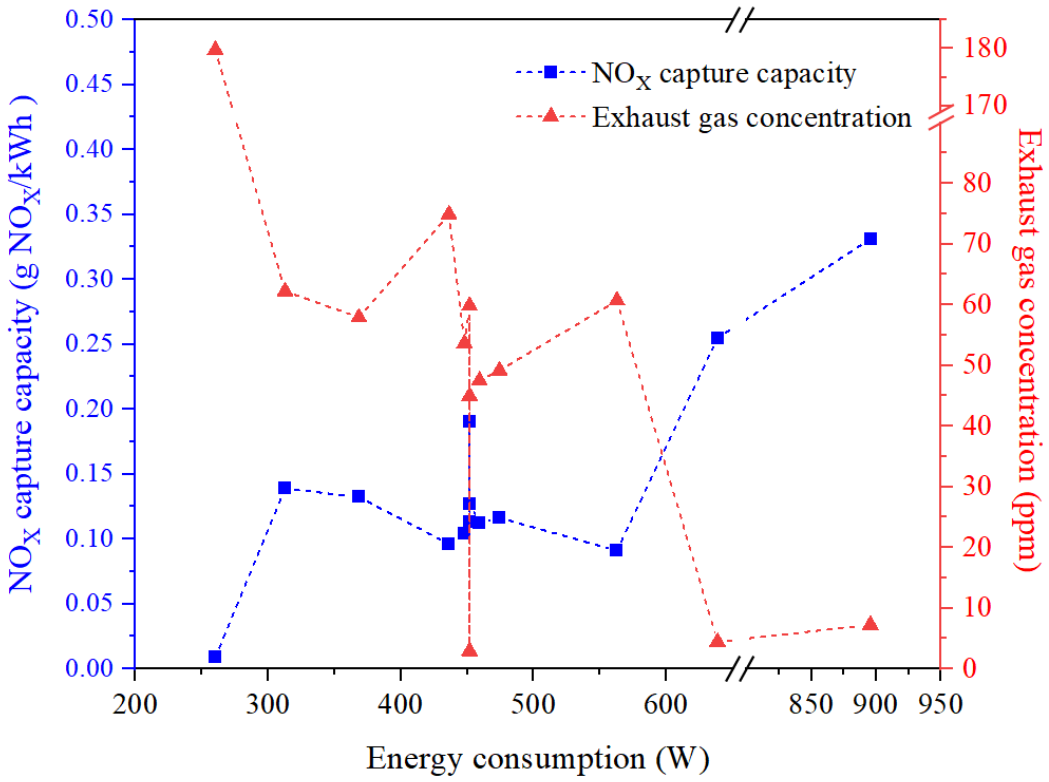

Figure 4- 27 The relationship between NO_X capture capacity, exhaust gas concentration and energy consumption in the case of rotating packed bed process

doi:10.6342/NTU202102462

The other two points were experiments NO. 12 and 13, which were also affected by the addition of liquid-phase agents. In addition, the system had also processed more nitrogen oxides, so this also corresponded to the rising section of the NO_X capture capacity curve.

Based on the data of exhaust gas concentration and energy consumption calculation, the experimental parameters that could meet the legal standards and had the better NO_X capture capacity were the best experimental parameters in this study (the highest removal efficiency). One of the main factors was the use of liquid-phase reagents. It was difficult to quantify the energy consumption during the addition of liquid-phase reagents. However, liquid-phase reagents could greatly improve the pollutant removal capacity of the system. Therefore, the next chapter would quantify the operating cost of each parameter from the perspective of cost calculation.

doi:10.6342/NTU202102462

4.5.2 Cost Analysis

In addition to energy consumption, it was also important to analyze a technology from an economic perspective. Through cost analysis, the treatment cost per unit pollutant would be used as an indicator of cost analysis (g NOx/NTD). Due to the use of pilot scale parameters for cost analysis, it was inevitable that there would be a gap between the pilot scale and the real scale (such as the amount of pollutant, the agents cost, etc.). Both the simple cost analysis in the pilot scale and the real scale were performed in this section.

Besides that, some conditions were assumed to simplify the steps of cost analysis, including: (1) the annual capital cost was converted to operation and maintenance costs at a rate of 4%; (2) the operating experimental conditions could be analogous with the operating environment of the real plant by using dimensionless parameters and the removal efficiency was equal; (3) the depreciation cycle of capital equipment was 20 years, (4) Do not calculate the fines that were imposed when the exhaust gas concentration was higher than the standard.

Table 4- 21 and Table 4- 22 list the operating conditions and calculation parameters used in the cost analysis of the pilot plant.

doi:10.6342/NTU202102462

Table 4- 21 Related data used in the cost analysis of pilot plant

Item	Value	Unit	Reference
HiGee system	500000	NTD	This study
Maintenance cost	50000	NTD/y	This study
Electricity price	2.58	NTD/kWh	Taiwan Power Company
Tap water price	12	NTD/m^3	Taiwan Water Corporation
Industrial waste treatment fee	7.56	NTD/m^3	Industrial Development Bureau
NO_x emission fee	10	NTD/kg	EPA. Taiwan (2018)
Chlorine generation cost	150	NTD/kg	HiGee Co., Ltd
Ozone generation cost	56.79	NTD/kg	Mundy et al., 2018
Sodium sulfite agent	4000	NTD/kg	Uni-ward Company in Taiwan
Sodium hydroxide agent	2000	NTD/kg	Uni-ward Company in Taiwan

Table 4- 22 Experimental parameters of pilot plant

Parameter		Value	Unit
Concentration		200/420/750	ppm
Gas flow		5	L/min
Temperature		298	K
Gas-liquid ratio (v/v)		5~40	-
High-gravity factor		17~180	g/g
Gas phase agents	O_3/NO_X	6	mole/mole
	ClO_2/NO_X	0.75	mole/mole
Liquid phase agents	Na_2SO_3/NO_X	285	mole/mole
	$NaOH/NO_X$	300	mole/mole

The cost calculation results in the pilot plant scale are shown in Table 4- 23. It was found that most of the total operating cost was about 100~200 NTD/g NOx. The highest treatment cost was NO. 1, and this group of experiments was also an experiment with poor removal efficiency. The lowest cost (39.9 NTD/g NOx) condition was NO. 13, which was an experiment where gas and liquid medicaments are added at the same time.

doi:10.6342/NTU202102462

Table 4- 23 The calculation result about pilot plant scale in cost analysis

Oxidation-Absorption Trials							
NO.	Capital	Electricity	Tap water	Water treatment	NO_x emission	Chemical agents	Total cost
	NTD/g NOx						
1	3399.69	285.59	2.7E-01	1.7E-01	2.9E-01	0.00	3686.01
2	151.47	22.09	1.2E-02	7.7E-03	6.2E-03	0.36	173.95
3	181.80	25.60	1.5E-02	9.2E-03	1.0E-02	0.77	208.21
Gas-Liquid Ratio Trials							
NO.	Capital	Electricity	Tap water	Water treatment	NO_x emission	Chemical agents	Total cost
4	145.06	22.21	4.7E-02	2.9E-02	4.9E-03	0.33	167.68
5	154.71	22.94	2.5E-02	1.6E-02	5.0E-03	0.35	178.04
2	151.47	22.09	1.2E-02	7.7E-03	6.2E-03	0.36	173.95
6	162.51	23.50	6.5E-03	4.1E-03	5.5E-03	0.36	186.39
High-Gravity Factor Trials							
NO.	Capital	Electricity	Tap water	Water treatment	NO_x emission	Chemical agents	Total cost
7	173.68	17.54	1.4E-02	8.8E-03	7.4E-03	0.39	191.63
8	160.59	19.10	1.3E-02	8.1E-03	6.1E-03	0.36	180.08
2	151.47	22.09	1.2E-02	7.7E-03	6.2E-03	0.36	173.95
9	154.95	28.15	1.2E-02	7.9E-03	6.6E-03	0.37	183.50
Combination of Gas/Liquid Agents Trials							
NO.	Capital	Electricity	Tap water	Water treatment	NO_x emission	Chemical agents	Total cost
2	151.47	22.09	1.2E-02	7.7E-03	6.2E-03	0.36	173.95
10	92.79	13.53	7.5E-03	4.7E-03	1.8E-04	17.14	123.47
11	132.78	19.36	1.1E-02	6.7E-03	4.4E-03	3.81	155.98
Applicable Concentration Loading Trials							
NO.	Capital	Electricity	Tap water	Water treatment	NO_x emission	Chemical agents	Total cost
10	92.79	13.53	7.5E-03	4.7E-03	1.8E-04	17.14	123.47
12	49.11	10.12	4.0E-03	2.5E-03	1.5E-04	9.19	68.43
13	26.96	7.79	2.2E-03	1.4E-03	1.3E-04	5.16	39.91

* means compliance with emission standards

doi:10.6342/NTU202102462

Figure 4-28, it could be found that the cost was mainly composed of capital expenditure, electricity cost and chemical agents cost in the pilot plant. The reason for the higher capital expenditures and electricity cost was that the amount of pollutants processed by the experimental scale was small. On the other hand, it was found that the increase of chemical agent cost could be found in No.10~13, the main reason was that the liquid phase agent was added in these experiments. After the addition of the liquid phase agent, although the chemical agent cost increases, the overall treatment cost decreased because of enlargement of removal efficiency.

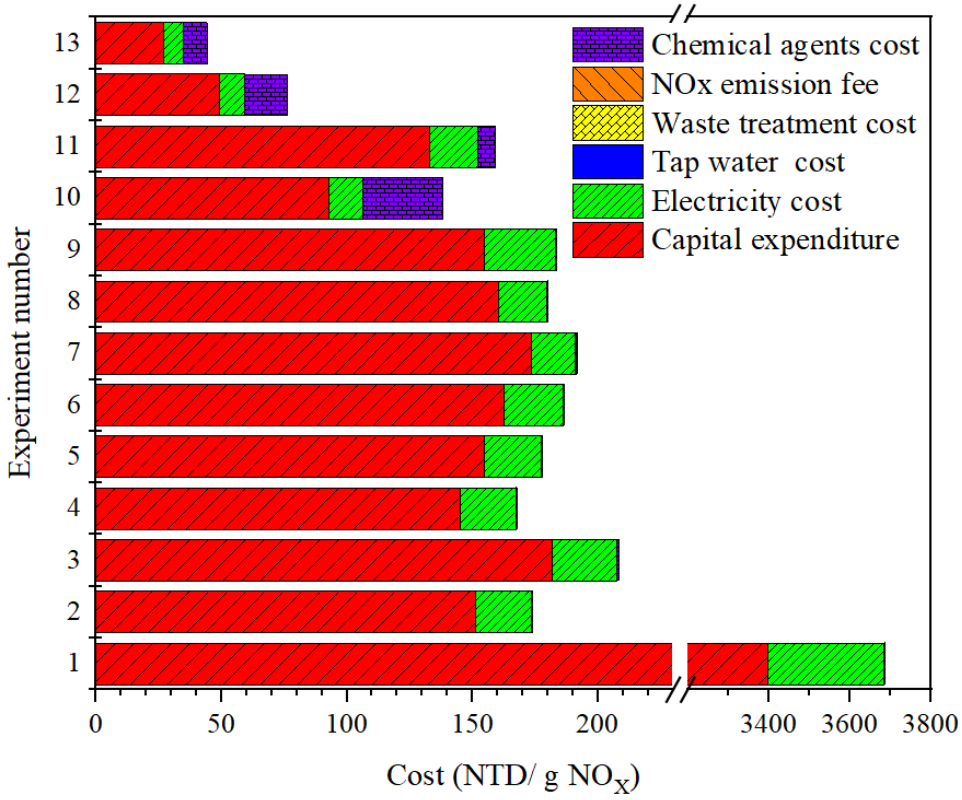

Figure 4- 28 The various costs and NO_X capture capacity in the pilot plant scale

doi:10.6342/NTU202102462

In order to avoid the large cost analysis error caused by factors such as the processing volume of the experimental scale and the cost of agents, the processing scale of the pilot plant needed to be enlarged for cost analysis. In addition to calculating the cost of the scaled-up experiment, business as usual (BAU) was also an important parameter when evaluating a control technology. The BAU used a packed tower to absorb nitrogen oxides in this study. The operating conditions were designed with reference to the results obtained by Jakob et al. [113] in the experiment, and the cost was calculated to achieve the same removal efficiency parameters as RPB. Table 4- 24 shows the calculation parameters used in the cost analysis of RPB process and BAU.

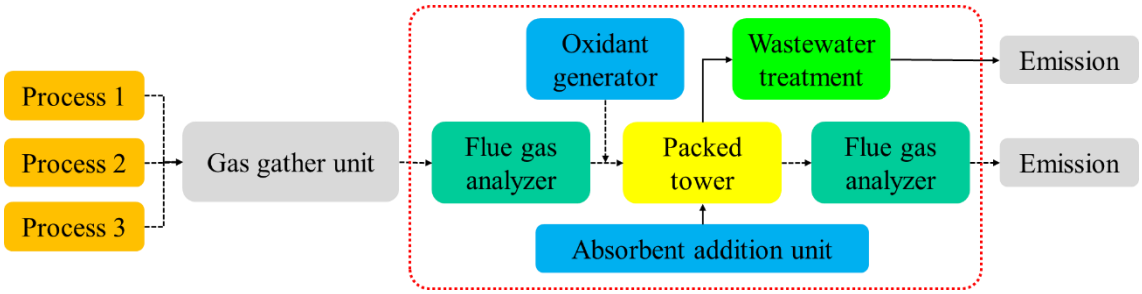

Figure 4- 29 The framework for the cost analysis of BAU in this study

Figure 4- 29 shows the system boundary of BAU in the cost analysis. It was the same as the RPB process, and both calculated the capital expenditure, tap water fee, waste water treatment fee, and chemical agent fee (including gas and liquid phase) , electricity costs, nitrogen oxide emission fees in the nitrogen oxide absorption process

doi:10.6342/NTU202102462

Table 4- 24 Related data used in the cost analysis of RPB process and BAU

RPB process			
Item	Value	Unit	Reference
HiGee system	3000000	NTD	HiGee CO.LTD
Chlorine generation system	3300000	NTD	HiGee CO.LTD
Equipment service life	20	year	Assumption
Maintain cost	250000	NTD/y	Assumption
Electricity price	2.58	NTD/kWh	Taiwan Power Company
Tap water price	12	NTD/m^3	Taiwan Water Corporation
Industrial waste treatment fee	7.56	NTD/m^3	Industrial Development Bureau
NO_x Emission Fee	10	NTD/kg	EPA. Taiwan (2018)
Chlorine generation cost	150	NTD/kg	HiGee Co., Ltd
Ozone generation cost	56.79	NTD/kg	Mundy et al., 2018
Sodium hydroxide agent	100	NTD/kg	Emperor Chemical CO.LTD
Sodium sulfite agent	160	NTD/kg	Emperor Chemical CO.LTD
BAU			
Item	Value	Unit	Reference
Scrubber	3000000	NTD	XICHENG EP LTD
Chlorine generation system	3300000	NTD	HiGee CO.LTD
Equipment service life	20	year	Assumption
Maintain cost	200000	NTD/y	Assumption
Electricity price	2.58	NTD/kWh	Taiwan Power Company
Tap water price	12	NTD/m^3	Taiwan Water Corporation
Industrial waste treatment fee	7.56	NTD/m^3	Industrial Development Bureau
NO_x Emission Fee	10	NTD/kg	EPA. Taiwan (2018)
Chlorine generation cost	150	NTD/kg	HiGee CO.LTD

Table 4- 25 shows the operating conditions of the RPB process and BAU. The operating conditions of the RPB process were based on the operating parameters used in this study, and the amount of pollutants processed was amplified. The operating conditions of BAU referred to the experimental parameters used in the literature for nitrogen oxide absorption using packed tower.

doi:10.6342/NTU202102462

Table 4- 25 Operation parameters of RPB process and BAU

Parameter		RPB process	[a] BAU
Concentration (ppm)		200/420/750	200/420/750
NO_2/NO_X		0.1	0.1
Gas flow (CMM)		50	50
Temperature (K)		298	298
Gas-liquid ratio (v/v)		5~40	66.7
High-gravity factor (g/g)		17~180	-
Overall mass transfer coefficient (1/s)		0.00059~0.099	0.051
Packing	Type	Mesh	Metal saddle
	Material	SS-316 Stainless steel	SS-316 Stainless steel
	Surface area (m^2/m^3)	2925	100
	Void fraction (v/v)	0.94	0.98
[b] Gas phase agents	ClO_2/NO_X	0.75	0.75
	O_3/NO_X	6	-
[b] Liquid phase agents	Na_2SO_3/NO_X	285	-
	$NaOH/NO_X$	300	-

[a] Refer to the experimental parameters of Jakob [113]

[b] It was presented in terms of the number of agent moles required per unit mole of pollutants ($\frac{Mole_{oxidant}}{Mole_{pollutant}}$)

Table 4- 26 and Figure 4- 30 show the cost analysis results of the RPB process and BAU. It was found that the use of RPB to absorb nitrogen oxides has a lower cost under most operating conditions. However, the operating cost is higher than BAU under the operating conditions where the exhaust gas concentration meets the regulatory standards (NO. 10, 12 and 13).

doi:10.6342/NTU202102462

Table 4- 26 The calculation result about RPB process in cost analysis

Oxidation-Absorption Trials								
NO.	Capital	Electricity	Tap water	Water treatment	NO_x emission	Chemical agents	Total cost	BAU
	NTD/g NOx							
1	1.28	0.63	5.11E-01	3.22E-01	2.88E-01	0.00	3.03	16.06
2	0.06	0.05	2.27E-02	1.43E-02	6.24E-03	0.31	0.46	0.91
3	0.07	0.06	2.73E-02	1.72E-02	1.00E-02	0.66	0.84	1.05
Gas-Liquid Ratio Trials								
NO.	Capital	Electricity	Tap water	Water treatment	NO_x emission	Chemical agents	Total cost	BAU
4	0.05	0.05	8.71E-02	5.49E-02	4.89E-03	0.29	0.54	0.88
5	0.06	0.05	4.65E-02	2.93E-02	4.99E-03	0.31	0.50	0.92
2	0.06	0.05	2.27E-02	1.43E-02	6.24E-03	0.31	0.46	0.91
6	0.06	0.05	1.22E-02	7.69E-03	5.47E-03	0.33	0.47	0.95
High-Gravity Factor Trials								
NO.	Capital	Electricity	Tap water	Water treatment	NO_x emission	Chemical agents	Total cost	BAU
7	0.07	0.04	2.61E-02	1.64E-02	7.41E-03	0.35	0.51	1.00
8	0.06	0.04	2.41E-02	1.52E-02	6.13E-03	0.33	0.47	0.94
2	0.06	0.05	2.27E-02	1.43E-02	6.24E-03	0.31	0.46	0.91
9	0.06	0.06	2.33E-02	1.47E-02	6.59E-03	0.31	0.48	0.92
Combination of Gas/Liquid Agents Trials								
NO.	Capital	Electricity	Tap water	Water treatment	NO_x emission	Chemical agents	Total cost	BAU
2	0.06	0.05	2.27E-02	1.43E-02	6.24E-03	0.31	0.46	0.91
10	0.03	0.03	1.39E-02	8.78E-03	1.79E-04	1.45	1.54	0.84
11	0.05	0.04	1.99E-02	1.26E-02	4.44E-03	0.59	0.72	0.83
Applicable Concentration Loading Trials								
NO.	Capital	Electricity	Tap water	Water treatment	NO_x emission	Chemical agents	Total cost	BAU
10	0.03	0.03	1.39E-02	8.78E-03	1.79E-04	1.45	1.54	0.84
12	0.02	0.02	7.37E-03	4.65E-03	1.50E-04	0.88	0.93	0.54
13	0.01	0.02	4.05E-03	2.55E-03	1.32E-04	0.57	0.61	0.39

* means compliance with emission standards

doi:10.6342/NTU202102462

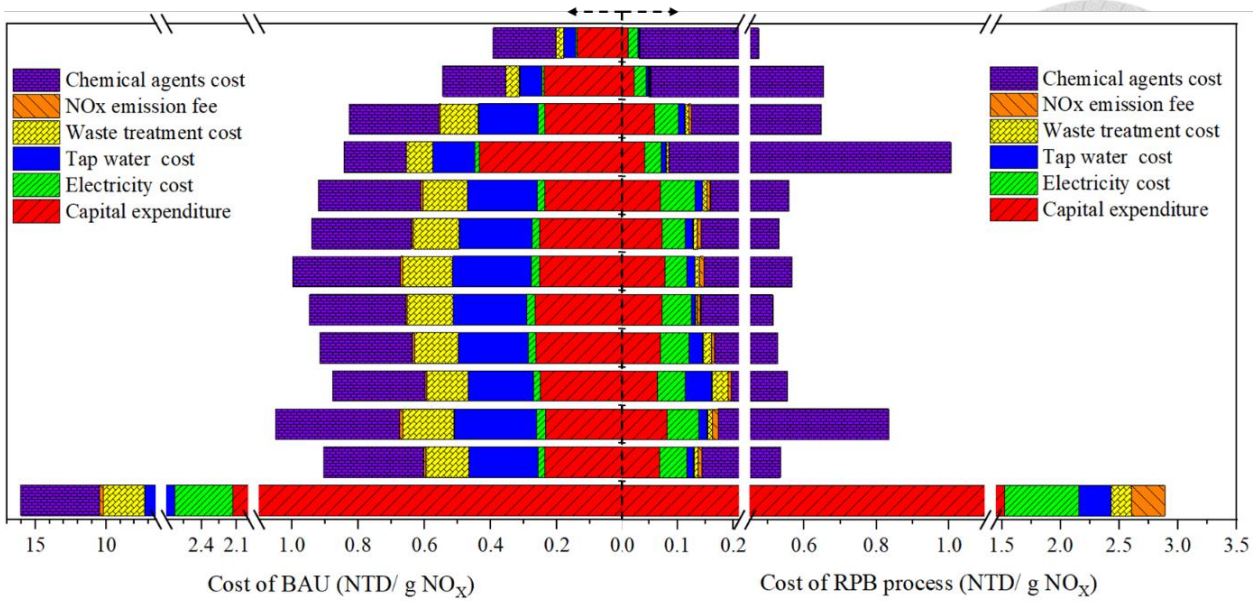

Figure 4- 30 The various costs and NO_X capture capacity in the real plant scale

The difference in these operating conditions was the use of liquid phase agents. Although the removal efficiency increases with the input of the liquid phase agent, the cost also increases relatively. Therefore, how to use agents efficiently and balance the stakes between cost and removal efficiency was a problem that needs to be solved in the future

Based on the above, the cost analysis could be concluded that: (1) the pilot scale was dominated by capital expenditure and electricity cost; (2) the cost of the actual plant (RPB process) was mainly chemical agents cost; (3) the minimum operating cost that could meet the pollutant emission standard was 0.61 NTD/g NOx.

doi:10.6342/NTU202102462

Chapter 5 Conclusions and Recommendations

5.1 Conclusions

An integrated the results about using oxidation-absorption method to remove nitrogen oxides in a rotating packed bed that could be concluded as follows:

1. Direct Oxidation Absorption

In the absorption-oxidation (reduction) experiments, sodium sulfite and sodium hydroxide exhibit a relatively higher better removal efficiency because they provided multiple reaction pathways with a faster reaction rate. In the oxidation-absorption experiments, chlorine dioxide and ozone can remove nitrogen oxides with the efficiency about 72 % and 64 %, respectively.

2. Effects of Operating Parameters on NOx Removal

The RPB operated under the low gas-liquid ratio, the driving force, liquid holdup and effective interface area would enhance the mass transfer. The RPB operated under the high gas-liquid ratio, liquid might easier exist as a film, so that the removal efficiency would not drop immediately.

The RPB operated under a higher high-gravity factor would decrease the film thickness and increase the effective area, and resulted in enhancing mass transfer; however, decrease liquid residence time and liquid holdup would not be favor in mass transfer.

doi:10.6342/NTU202102462

3. Enhancement of NOx Removal and Modeling NOx Removal.

The best removal efficiency of NOx by chlorine dioxide as a gas phase oxidizer and sodium sulfite as a liquid phase absorber could reach about 99 % under the optimum conditions, i.e., G/L of 20 and β of 86.

Through dimensionless analysis and Eq-44 ($C' \cdot EXP\left[\frac{K_G a \pi Z r^2}{Q_g}\right] = C_G$), it can be used to predict the mass transfer coefficient ($K_G a$) and the size of RPB.

4. Energy Consumption and Cost Analysis

The real plant-scale costs were dominated by chemical agents cost. The minimum operating cost that could meet the pollutant emission standard was 0.61 NTD/g NOx

doi:10.6342/NTU202102462

5.2 **Recommendations**

In order to further understand the principles and applications of nitrogen oxide removal using the oxidation-absorption method via a rotating packed bed, further research focuses on:

(1) Exploring the mechanism regarding the competitive effects among various air pollutants and nitrogen oxides during the oxidation and absorption via a RPB.

(2) Enhancing the liquid use efficiency and using reductant as absorbent (urea, Fe (II) EDTA, etc.) thereby reducing the water and chemical cost.

(3) Combining the RPB removal process with the water/steam injection method to enhance performance of the oxidation and absorption process.

(4) Using the life cycle assessment (LCA) approach in conjunction with 3E (economics, energy and environment) analysis to evaluate the performance of RPB process for NO_X removal.

doi:10.6342/NTU202102462

References

1. Jeguirim, M., M. Belhachemi, L. Limousy, and S. Bennici, Adsorption/reduction of nitrogen dioxide on activated carbons: Textural properties versus surface chemistry – A review. *Chemical Engineering Journal*, 2018. **347**: p. 493-504.

2. Suhail, M.H., A.A. Ramadan, S.B. Aziz, and O.G. Abdullah, Chemical surface treatment with toluene to enhance sensitivity of NO2 gas sensors based on CuPcTs/Alq3 thin films. *Journal of Science: Advanced Materials and Devices*, 2017. **2**(3): p. 301-308.

3. Bowman, C.T., Control of combustion-generated nitrogen oxide emissions: Technology driven by regulation. *Symposium (International) on Combustion*, 1992. **24**(1): p. 859-878.

4. Reşitoğlu, İ., *NOx Pollutants from Diesel Vehicles and Trends in the Control Technologies*. 2018.

5. Ma, S., Y. Zhao, J. Yang, S. Zhang, J. Zhang, and C. Zheng, Research progress of pollutants removal from coal-fired flue gas using non-thermal plasma. *Renewable and Sustainable Energy Reviews*, 2017. **67**: p. 791-810.

6. Gao, F., X. Tang, H. Yi, S. Zhao, C. Li, J. Li, Y. Shi, and X. Meng, A Review on Selective Catalytic Reduction of NOx by NH3 over Mn–Based Catalysts at Low Temperatures: Catalysts, Mechanisms, Kinetics and DFT Calculations. *Catalysts*, 2017. **7**(7): p. 199.

7. Gholami, F., M. Tomas, Z. Gholami, and M. Vakili, Technologies for the nitrogen oxides reduction from flue gas: A review. *Sci Total Environ*, 2020. **714**: p. 136712.

8. Zhang, W., P. Xie, Y. Li, L. Teng, and J. Zhu, Hydrodynamic characteristics and mass transfer performance of rotating packed bed for CO2 removal by chemical absorption: A review. *Journal of Natural Gas Science and Engineering*, 2020.

doi:10.6342/NTU202102462

79.

9. Su, M.-J., Y. Luo, G.-W. Chu, W. Liu, X.-H. Zheng, and J.-F. Chen, Gas-Side Mass Transfer in a Rotating Packed Bed with Structured Nickel Foam Packing. *Ind. Eng. Chem. Res.*, 2018. **57**(13): p. 4743-4747.

10. Zhao, H., L. Shao, and J.-F. Chen, High-gravity process intensification technology and application. *Chemical Engineering Journal*, 2010. **156**(3): p. 588-593.

11. EPA, U.S.E.P.A.U.S., *Integrated Science Assessment for Oxides of Nitrogen—Health Criteria (Final report, 2016)* N.C.f.E.A.-R.D.O.o.R.a. Development, Editor. 2016, U.S. Environmental Protection Agency, Office of Research and Development, National Center for Environmental Assessment- RTP Division

12. U.S, E.P.A., *Integrated science assessment for oxides of nitrogen – Health criteria (Final report, 2008)*. 2008, U.S. Environmental Protection Agency, Office of Research and Development, National Center for Environmental Assessment- RTP Division: Research Triangle Park, NC.

13. Sun, Y., E. Zwolińska, and A.G. Chmielewski, Abatement technologies for high concentrations of NOx and SO2 removal from exhaust gases: A review. *Critical Reviews in Environmental Science and Technology*, 2016. **46**(2): p. 119-142.

14. U.S, E.P.A., *Air Pollutant Emissions Trends Data*, O.o.R.a.D. U.S. Environmental Protection Agency, National Center for Environmental Assessment- RTP Division, Editor. 2019, Research Triangle Park, NC.

15. Skalska, K., J.S. Miller, and S. Ledakowicz, Trends in NOx abatement: A review. *Science of The Total Environment*, 2010. **408**(19): p. 3976-3989.

16. Kurtenbach, R., K. Becker, J. Gomes, J. Kleffmann, J. Lörzer, M. Spittler, P. Wiesen, R. Ackermann, A. Geyer, and U. Platt, Investigations of emissions and heterogeneous formation of HONO in a road traffic tunnel. *Atmospheric Environment*, 2001. **35**(20): p. 3385-3394.

doi:10.6342/NTU202102462

17. Weinhart, N. and J. Haunstetter. *Evaluation of a novel concept for combined NOx and SOx removal*. 2015.

18. Popescu, F. and I. Ionel, Anthropogenic air pollution sources. *Air quality*, 2010: p. 1-22.

19. Rao, A., R.K. Mehra, H. Duan, and F. Ma, Comparative study of the NOx prediction model of HCNG engine. *International Journal of Hydrogen Energy*, 2017. **42**(34): p. 22066-22081.

20. Hoekman, S.K. and C. Robbins, Review of the effects of biodiesel on NOx emissions. *Fuel Processing Technology*, 2012. **96**: p. 237-249.

21. Sander, R., Compilation of Henry's law constants (version 4.0) for water as solvent. *Atmospheric Chemistry and Physics*, 2015. **15**(8): p. 4399-4981.

22. Aneja, V.P., P.A. Roelle, G.C. Murray, J. Southerland, J.W. Erisman, D. Fowler, W.A. Asman, and N. Patni, Atmospheric nitrogen compounds II: emissions, transport, transformation, deposition and assessment. *Atmospheric Environment*, 2001. **35**(11): p. 1903-1911.

23. Wright, J., Environmental chemistry. 2004: Routledge.

24. Woodrow, P., Nitric oxide: some nursing implications. *Intensive and Critical Care Nursing*, 1997. **13**(2): p. 87-92.

25. Chaloulakou, A., I. Mavroidis, and I. Gavriil, Compliance with the annual NO2 air quality standard in Athens. Required NOx levels and expected health implications. *Atmospheric Environment*, 2008. **42**(3): p. 454-465.

26. Bosch, H. and F. Janssen, Formation and control of nitrogen oxides. *Catal. Today*, 1988. **2**(4): p. 369-379.

27. Seinfeld, J.H. and S.N. Pandis, Atmospheric chemistry and physics: from air pollution to climate change. 2016: John Wiley & Sons.

doi:10.6342/NTU202102462

28. Brinkmann, T., G.G. Santonja, H. Yükseler, S. Roudier, and L.D. Sancho, Best available techniques (BAT) reference document for common waste water and waste gas treatment/management systems in the chemical sector. *Publications Office of the European Union*, 2016.

29. Friebel, J. and R. Köpsel, The fate of nitrogen during pyrolysis of German low rank coals—a parameter study. *Fuel*, 1999. **78**(8): p. 923-932.

30. Javed, M.T., N. Irfan, and B. Gibbs, Control of combustion-generated nitrogen oxides by selective non-catalytic reduction. *Journal of environmental management*, 2007. **83**(3): p. 251-289.

31. Lani, B.W., T.J. Feeley III, C.E. Miller, B.A. Carney, and J.T. Murphy, DOE/NETL's NOx Emissions Control R&D Program–Bringing Advanced Technology to the Marketplace. *DOE/NETL NOx R&D Overview*, 2008.

32. Jia, Y., J. Jiang, R. Zheng, L. Guo, J. Yuan, S. Zhang, and M. Gu, Insight into the reaction mechanism over PMoA for low temperature NH3-SCR: A combined In-situ DRIFTs and DFT transition state calculations. *Journal of Hazardous Materials*, 2021. **412**: p. 125258.

33. Pronobis, M., R. Wejkowski, K. Jagodzińska, and T. Kress. *Simplified method for calculating SNCR system efficiency*. in *E3S Web of Conferences*. 2017. EDP Sciences.

34. Basfar, A.A., O.I. Fageeha, N. Kunnummal, A.G. Chmielewski, J. Licki, A. Pawelec, Z. Zimek, and J. Warych, A review on electron beam flue gas treatment (EBFGT) as a multicomponent air pollution control technology. *Nukleonika*, 2010. **55**: p. 271-277.

35. Shao, J. and K.K. Hansen, Electrochemical NO x reduction on an LSM/CGO symmetric cell modified by NO x adsorbents. *Journal of Materials Chemistry A*, 2013. **1**(24): p. 7137-7146.

36. Sun, W.-y., S.-l. Ding, S.-s. Zeng, S.-j. Su, and W.-j. Jiang, Simultaneous absorption of NOx and SO2 from flue gas with pyrolusite slurry combined with

doi:10.6342/NTU202102462

gas-phase oxidation of NO using ozone. *Journal of hazardous materials*, 2011. **192**(1): p. 124-130.

37. Lin, F., Z. Wang, Q. Ma, Y. Yang, R. Whiddon, Y. Zhu, and K. Cen, Catalytic deep oxidation of NO by ozone over MnOx loaded spherical alumina catalyst. *Applied Catalysis B: Environmental*, 2016. **198**: p. 100-111.

38. Calinescu, I., D. Martin, A. Chmielewski, and D. Ighigeanu, E-Beam SO2 and NOx removal from flue gases in the presence of fine water droplets. *Radiation Physics and Chemistry*, 2013. **85**: p. 130-138.

39. Pawelec, A., A.G. Chmielewski, J. Licki, B. Han, J. Kim, N. Kunnummal, and O.I. Fageeha, Pilot plant for electron beam treatment of flue gases from heavy fuel oil fired boiler. *Fuel Processing Technology*, 2016. **145**: p. 123-129.

40. Sun, B., M. Sheng, W. Gao, L. Zhang, M. Arowo, Y. Liang, L. Shao, G.-W. Chu, H. Zou, and J.-F. Chen, Absorption of Nitrogen Oxides into Sodium Hydroxide Solution in a Rotating Packed Bed with Preoxidation by Ozone. *Energy & Fuels*, 2017. **31**(10): p. 11019-11025.

41. Skalska, K., S. Ledakowicz, R. Louwe, and R. Szymczak, Nitrogen oxides pre-ozonation in flue gases from phosphate rock digestion. *Chemical Engineering Journal*, 2017. **318**: p. 181-188.

42. Stamate, E., W. Chen, P. Michelsen, L. Joergensen, T. Jensen, P. Kristensen, L. Tobiasen, and P. Simonsen, Pilot test and optimization of plasma based DeNO {sub x}. Final report. 2010.

43. Chang, S. and G. Lee, LBL PhoSNOX process for combined removal of SO2 and NOx from flue gas. *Environmental progress*, 1992. **11**(1): p. 66-73.

44. Percival, C.J., G.D. Smith, L.T. Molina, and M.J. Molina, Temperature and Pressure Dependence of the Rate Constant for the ClO + NO2 Reaction. *The Journal of Physical Chemistry A*, 1997. **101**(47): p. 8830-8833.

doi:10.6342/NTU202102462

45. Leu, M. and W. DeMore, Rate constant for the reaction chlorine oxide+ nitric oxide. fwdarw. atomic chlorine+ nitrogen dioxide. *The Journal of Physical Chemistry*, 1978. **82**(19): p. 2049-2052.

46. Hultén, A.H., P. Nilsson, M. Samuelsson, S. Ajdari, F. Normann, and K. Andersson, First evaluation of a multicomponent flue gas cleaning concept using chlorine dioxide gas – Experiments on chemistry and process performance. *Fuel*, 2017. **210**: p. 885-891.

47. Li, D., Z. Xiao, T.B. Aftab, and S. Xu, Flue Gas Denitration by Wet Oxidation Absorption Methods: Current Status and Development. *Environmental Engineering Science*, 2018. **35**(11): p. 1151-1164.

48. Majeed, J.G., Absorption of Nitrogen Dioxide into Sodium Carbonate Solution in Packed Column. *Inter. J. of Modern Eng. Res*, 2014. **4**(2): p. 23-35.

49. Sun, Y., X. Hong, T. Zhu, X. Guo, and D. Xie, The chemical behaviors of nitrogen dioxide absorption in sulfite solution. *Applied Sciences*, 2017. **7**(4): p. 377.

50. Susianto, M. Pétrissans, A. Pétrissans, and A. Zoulalian, Experimental study and modelling of mass transfer during simultaneous absorption of SO2 and NO2 with chemical reaction. *Chemical Engineering and Processing: Process Intensification*, 2005. **44**(10): p. 1075-1081.

51. Fang, P., C. Cen, Z. Tang, P. Zhong, D. Chen, and Z. Chen, Simultaneous removal of SO2 and NOX by wet scrubbing using urea solution. *Chemical Engineering Journal*, 2011. **168**(1): p. 52-59.

52. Guo, J., W. Jiao, G. Qi, Z. Yuan, and Y. Liu, Applications of high-gravity technologies in gas purifications: A review. *Chinese Journal of Chemical Engineering*, 2019. **27**(6): p. 1361-1373.

53. Guo, F., C. Zheng, K. Guo, Y.D. Feng, and N.C. Gardner, Hydrodynamics and mass transfer in crossflow rotating packed bed. *Chemical Engineering Science*, 1997. **52**(21-22): p. 3853-3859.

doi:10.6342/NTU202102462

54. Lin, C.-C. and H.-S. Liu, Adsorption in a centrifugal field: Basic dye adsorption by activated carbon. *Ind. Eng. Chem. Res.*, 2000. **39**(1): p. 161-167.

55. Zheng, C., K. Guo, Y. Feng, C. Yang, and N.C. Gardner, Pressure Drop of Centripetal Gas Flow through Rotating Beds. *Ind. Eng. Chem. Res.*, 2000. **39**(3): p. 829-834.

56. Liu, H.-S., C.-C. Lin, S.-C. Wu, and H.-W. Hsu, Characteristics of a Rotating Packed Bed. *Ind. Eng. Chem. Res.*, 1996. **35**(10): p. 3590-3596.

57. Sandilya, P., D.P. Rao, A. Sharma, and G. Biswas, Gas-Phase Mass Transfer in a Centrifugal Contactor. *Ind. Eng. Chem. Res.*, 2001. **40**(1): p. 384-392.

58. Rao, D.P., A. Bhowal, and P.S. Goswami, Process Intensification in Rotating Packed Beds (HIGEE): An Appraisal. *Ind. Eng. Chem. Res.*, 2004. **43**(4): p. 1150-1162.

59. Yang, W., Y. Wang, J. Chen, and W. Fei, Computational fluid dynamic simulation of fluid flow in a rotating packed bed. *Chemical Engineering Journal*, 2010. **156**(3): p. 582-587.

60. Zhao, B., W. Tao, M. Zhong, Y. Su, and G. Cui, Process, performance and modeling of CO 2 capture by chemical absorption using high gravity: A review. *Renewable and Sustainable Energy Reviews*, 2016. **65**: p. 44-56.

61. Burns, J.R. and C. Ramshaw, Process intensification: Visual study of liquid maldistribution in rotating packed beds. *Chemical Engineering Science*, 1996. **51**(8): p. 1347-1352.

62. Jianfeng, C., High Gravity Technology and Application–A New Generation of Reaction and Separation Technology. *Beijing: Chemical Industry Press*, 2003.

63. Zhang, J., K. Guo, F. Guo, J.-s. Zhu, and C. Zheng, Experimental study about flow of liquid in rotating packed bed. *Journal of Chemical Engineering of Chinese Universities*, 2000. **14**(4): p. 378-381.

doi:10.6342/NTU202102462

64. Burns, J.R., J.N. Jamil, and C. Ramshaw, Process intensification: operating characteristics of rotating packed beds — determination of liquid hold-up for a high-voidage structured packing. *Chemical Engineering Science*, 2000. **55**(13): p. 2401-2415.

65. Munjal, S., M.P. Dudukovć, and P. Ramachandran, Mass-transfer in rotating packed beds—I. Development of gas—liquid and liquid—solid mass-transfer correlations. *Chemical Engineering Science*, 1989. **44**(10): p. 2245-2256.

66. Munjal, S., M.P. Duduković, and P. Ramachandran, Mass-transfer in rotating packed beds—II. Experimental results and comparison with theory and gravity flow. *Chemical Engineering Science*, 1989. **44**(10): p. 2257-2268.

67. Guo, K., F. Guo, Y. Feng, J. Chen, C. Zheng, and N.C. Gardner, Synchronous visual and RTD study on liquid flow in rotating packed-bed contactor. *Chemical Engineering Science*, 2000. **55**(9): p. 1699-1706.

68. Onda, K., H. Takeuchi, and Y. Okumoto, MASS TRANSFER COEFFICIENTS BETWEEN GAS AND LIQUID PHASES IN PACKED COLUMNS. *Journal of Chemical Engineering of Japan*, 1968. **1**(1): p. 56-62.

69. Rajan, S., M. Kumar, M.J. Ansari, D.P. Rao, and N. Kaistha, Limiting Gas Liquid Flows and Mass Transfer in a Novel Rotating Packed Bed (HiGee). *Ind. Eng. Chem. Res.*, 2011. **50**(2): p. 986-997.

70. Luo, Y., G.-W. Chu, H.-K. Zou, F. Wang, Y. Xiang, L. Shao, and J.-F. Chen, Mass Transfer Studies in a Rotating Packed Bed with Novel Rotors: Chemisorption of CO2. *Ind. Eng. Chem. Res.*, 2012. **51**(26): p. 9164-9172.

71. Yang, Y., Y. Xiang, G. Chu, H. Zou, Y. Luo, M. Arowo, and J.-F. Chen, A noninvasive X-ray technique for determination of liquid holdup in a rotating packed bed. *Chemical Engineering Science*, 2015. **138**: p. 244-255.

72. Xie, P., X. Lu, H. Ding, X. Yang, D. Ingham, L. Ma, and M. Pourkashanian, A mesoscale 3D CFD analysis of the liquid flow in a rotating packed bed. *Chemical Engineering Science*, 2019. **199**: p. 528-545.

doi:10.6342/NTU202102462

73. Zhang, W., P. Xie, Y. Li, L. Teng, and J. Zhu, CFD analysis of the hydrodynamic characteristics in a rotating packed bed with multi-nozzles. *Chemical Engineering and Processing - Process Intensification*, 2020: p. 108107.

74. Luo, Y., G.-W. Chu, H.-K. Zou, Z.-Q. Zhao, M.P. Dudukovic, and J.-F. Chen, Gas–Liquid Effective Interfacial Area in a Rotating Packed Bed. *Ind. Eng. Chem. Res.*, 2012. **51**(50): p. 16320-16325.

75. Chen, Y.-S., Correlations of Mass Transfer Coefficients in a Rotating Packed Bed. *Ind. Eng. Chem. Res.*, 2011. **50**(3): p. 1778-1785.

76. Nernst, W., Theorie der Reaktionsgeschwindigkeit in heterogenen Systemen. *Zeitschrift für physikalische Chemie*, 1904. **47**(1): p. 52-55.

77. Brian, P., J. Hurley, and E. Hasseltine, Penetration theory for gas absorption accompanied by a second order chemical reaction. *AIChE Journal*, 1961. **7**(2): p. 226-231.

78. Asher, W.E. and J.F. Pankow, Prediction of gas/water mass transport coefficients by a surface renewal model. *Environmental science & technology*, 1991. **25**(7): p. 1294-1300.

79. Toor, H. and J. Marchello, Film-penetration model for mass and heat transfer. *AIChE Journal*, 1958. **4**(1): p. 97-101.

80. Tung, H.-H. and R.S.H. Mah, MODELING LIQUID MASS TRANSFER IN HIGEE SEPARATION PROCESS. *Chemical Engineering Communications*, 1985. **39**(1-6): p. 147-153.

81. Xinlin, D., H.U. Xiaoyong, D. Yigang, W.U. Yuanxin, and L.I. Dinghuo, A MODEL FOR THE MASS TRANSFER COEFFICIENT IN ROTATING PACKED BED. *Chemical Engineering Communications*, 2000. **178**(1): p. 249-256.

82. Saha, D., Prediction of mass transfer coefficient in rotating bed contactor (Higee)

doi:10.6342/NTU202102462

using artificial neural network. *Heat and Mass Transfer*, 2009. **45**(4): p. 451-457.

83. Liu, T., Y. Liu, D. Wang, Y. Li, and L. Shao, Artificial neural network modeling on the prediction of mass transfer coefficient for ozone absorption in RPB. *Chemical Engineering Research and Design*, 2019. **152**: p. 38-47.

84. Sun, B.-C., X.-M. Wang, J.-M. Chen, G.-W. Chu, J.-F. Chen, and L. Shao, Simultaneous absorption of CO2 and NH3 into water in a rotating packed bed. *Ind. Eng. Chem. Res.*, 2009. **48**(24): p. 11175-11180.

85. Bird, R.B., W.E. Stewart, and E.N. Lightfoot, Transport phenomena. Vol. 1. 2006: John Wiley & Sons.

86. Chen, T.-L., Y.-H. Chen, and P.-C. Chiang, Enhanced performance on simultaneous removal of NOx-SO2-CO2 using a high-gravity rotating packed bed and alkaline wastes towards green process intensification. *Chemical Engineering Journal*, 2020. **393**: p. 124678.

87. Tan, C.-S. and P.-L. Lee, Supercritical CO2 desorption of activated carbon loaded with 2, 2, 3, 3-tetrafluoro-1-propanol in a rotating packed bed. *Environmental science & technology*, 2008. **42**(6): p. 2150-2154.

88. Sun, C., N. Zhao, Z. Zhuang, H. Wang, Y. Liu, X. Weng, and Z. Wu, Mechanisms and reaction pathways for simultaneous oxidation of NOx and SO2 by ozone determined by in situ IR measurements. *Journal of Hazardous Materials*, 2014. **274**: p. 376-383.

89. DENG, X., D. TIAN, and Y. LUO, Experimental study of micron dust removal using high-gravity rotating bed. *Sulphuric Acid Industry*, 2010. **6**.

90. Pan, S.-Y., P. Wang, Q. Chen, W. Jiang, Y.-H. Chu, and P.-C. Chiang, Development of high-gravity technology for removing particulate and gaseous pollutant emissions: Principles and applications. *Journal of Cleaner Production*, 2017. **149**: p. 540-556.

doi:10.6342/NTU202102462

91. Li, J.-h. and Y. Liu, Study on NO x ozone oxidation and intensifying absorption in high gravity field. *Mod Chem Ind*, 2013. **33**(5): p. 40-44.

92. Chen, J., B. Sun, H. Zhao, C. Xu, and Y. Lo, An equipment and technology of high-gravity efficient removal of NO x. *China Patent*, 2014.

93. GAO, W.-l., Z.-q. ZENG, J.-m. CHEN, J.-f. Chen, and L. Shao, Study of wet denitration in a rotating packed bed. *Journal of Chemical Engineering of Chinese Universi-ties*, 2014. **24**(5): p. 1.

94. Liu, Y., P. Li, Y. Li, R. Kang, and J. Diao, Pilot test on treatment of high concentration nitrogen oxides by high gravity technology. *Chemical Industry and Engineering Progress*, 2007. **26**(7): p. 1058.

95. Zhang, L.-L., J.-X. Wang, Q. Sun, X.-F. Zeng, and J.-F. Chen, Removal of nitric oxide in rotating packed bed by ferrous chelate solution. *Chemical Engineering Journal*, 2012. **181**: p. 624-629.

96. Newcomer, K.E., H.P. Hatry, and J.S. Wholey, Cost-effectiveness and cost-benefit analysis. *Handbook of practical program evaluation*, 2015: p. 636.

97. Skalska, K., J.S. Miller, and S. Ledakowicz, Intensification of NOx absorption process by means of ozone injection into exhaust gas stream. *Chemical Engineering and Processing: Process Intensification*, 2012. **61**: p. 69-74.

98. Coxon, J., Reaction between chlorine dioxide and nitric oxide. *Transactions of the Faraday Society*, 1968. **64**: p. 2118-2123.

99. Joshi, J.B., V.V. Mahajani, and V.A. Juvekar, INVITED REVIEW ABSORPTION OF NOX GASES. *Chemical Engineering Communications*, 1985. **33**(1-4): p. 1-92.

100. Mok, Y.S. and H.-J. Lee, Removal of sulfur dioxide and nitrogen oxides by using ozone injection and absorption–reduction technique. *Fuel Processing Technology*, 2006. **87**(7): p. 591-597.

doi:10.6342/NTU202102462

101. Skalska, K., J. Miller, and S. Ledakowicz, Effectiveness of nitric oxide ozonation. *Chemical Papers*, 2011. **65**(2).

102. Thomas, D. and J. Vanderschuren, Modeling of NOx Absorption into Nitric Acid Solutions Containing Hydrogen Peroxide. *Ind. Eng. Chem. Res.*, 1997. **36**(8): p. 3315-3322.

103. Yang, Y., Y. Xiang, G. Chu, H. Zou, B. Sun, M. Arowo, and J.-F. Chen, CFD modeling of gas–liquid mass transfer process in a rotating packed bed. *Chemical Engineering Journal*, 2016. **294**: p. 111-121.

104. de Paiva, J.L. and G.C. Kachan, Absorption of nitrogen oxides in aqueous solutions in a structured packing pilot column. *Chemical Engineering and Processing: Process Intensification*, 2004. **43**(7): p. 941-948.

105. Wang, L., W. Zhao, and Z. Wu, Simultaneous absorption of NO and SO2 by FeIIEDTA combined with Na2SO3 solution. *Chemical Engineering Journal*, 2007. **132**(1-3): p. 227-232.

106. Deshwal, B.-R. and H.-K. Lee, Mass transfer in the absorption of SO2 and NOx using aqueous euchlorine scrubbing solution. *Journal of Environmental Sciences*, 2009. **21**(2): p. 155-161.

107. Li, Y., Y. Liu, L. Zhang, Q. Su, and G. Jin, Absorption of NOx into Nitric Acid Solution in Rotating Packed Bed. *Chinese Journal of Chemical Engineering*, 2010. **18**(2): p. 244-248.

108. Asif, M. and W.-S. Kim, Numerical Study of NOx Abatement Using Ozone Injection Integrated with Wet Absorption. *Ozone: Science & Engineering*, 2014. **36**(5): p. 472-484.

109. Jiao, W., S. Luo, Z. He, and Y. Liu, Applications of high gravity technologies for wastewater treatment: A review. *Chemical Engineering Journal*, 2017. **313**: p. 912-927.

doi:10.6342/NTU202102462

110. Sun, B., K. Dong, W. Zhao, J. Wang, G. Chu, L. Zhang, H. Zou, and J.-F. Chen, Simultaneous Absorption of NOx and SO2 into Na2SO3 Solution in a Rotating Packed Bed with Preoxidation by Ozone. *Ind. Eng. Chem. Res.*, 2019. **58**(19): p. 8332-8341.

111. Zhang, W., P. Xie, Y. Li, and J. Zhu, A machine learning model for predicting the mass transfer performance of rotating packed beds based on a least squares support vector machine approach. *Chemical Engineering and Processing - Process Intensification*, 2021. **165**: p. 108432.

112. Zhao, B., Y. Su, and W. Tao, Mass transfer performance of CO2 capture in rotating packed bed: Dimensionless modeling and intelligent prediction. *Applied Energy*, 2014. **136**: p. 132-142.

113. Johansson, J., F. Normann, N. Sarajlic, and K. Andersson, Technical-Scale Evaluation of Scrubber-Based, Co-Removal of NOx and SOx Species from Flue Gases via Gas-Phase Oxidation. *Ind. Eng. Chem. Res.*, 2019. **58**(48): p. 21904-21912.

doi:10.6342/NTU202102462

Appendix

A- 1 Flowmeter calibrated data

082-03-GL FLOWMETER CALIBRATION DATA 082/95

CUSTOMER	CUST. P.O. No	REF. CURVE NUMBER
		0796-0E-28

Max. Flow	Min. Flow	Units	Metering Fluid	Date
630	32.7	std. ml/min	ozone	01-Jul-1996

Model Number		**Metering Temperature**	70.0 °F
Tube Number	082-03-GL	**Metering Pressure**	14.70 psia
Serial Number		**Metering density**	1.989 g/ml
Float Material	glass	**Metering Viscosity**	
Float Density	2.53 g/ml	**Density at STD.Cond**	1.989 g/ml
STD. Conditions	STP: 1 atm @ 70 °	**Accuracy**	+/- 5%
Room Temperature	70.0 °F	**Barometric Pressure**	14.70 psia

SCALE READINGS AT CENTER OF FLOAT	
Scale Reading (mm)	**Flow**
150	630
140	595
130	554
120	514
110	478
100	435
90	395
80	351
70	306
60	259
50	211
40	163
30	117
20	73.5
10	32.7

doi:10.6342/NTU202102462

A- 2 Calibration checklist for flue gas detector

附表

煙道氣體分析儀校正檢查表

客戶名稱：國立台北科技大學化學工程與生物科技系
儀器廠牌：HORIBA　　檢驗日期：109.02.25
儀器型號：PG-350　　儀器編號：2Y60VD62
校正氣體濃度：
使用RANGE：

測項		Range	校正濃度	偏 差%	再現性		校正濃度	再現濃度	誤 差%
NOx		500ppm	465.2		NOx		465.2	466.3	0.236
SO2		500ppm	475.2		SO2		475.2	477.100	0.400
CO		1000ppm	934.4		CO		934.4	937.500	0.332
CO2		10%	9.08		CO2		9.08	9.100	0.220
O2		25%	24.85		O2		24.85	24.810	-0.161
					O2中濃度		12.43	12.51	0.64
		NO2濃度	反應Nox	效率		0			
NO2		49ppm	40ppm	81.70%		1			
轉換效率						2			
						3			
						4			
						5			
						6			
						7			
						8			
						9			
						10			

備註: 本分析儀的誤差值　　⟹　　: +/- 2 %F.S

晨興國際股份有限公司 TEL: 2794-8851 台北市內湖區瑞光路[illegible]

晨興國際股份有限公司
檢查人： 馮開武

doi:10.6342/NTU202102462

超技儀器有限公司

測試報告書

收件日期	2020/12/20	
校正日期	2020/12/22	
儀器單位	台大環工	
儀器名稱	五合一氣體偵測器	
廠牌型號	PG350	
儀器序號	2Y60VD62	
校正氣體	O2	
校正環境條件	環境溫度	23.0±2.0 ℃

測試結果與說明

Ⅰ.1 校正結果

	測試濃度	儀器讀值	相對器差
	%	%	%
O2	0.00	0.00	0.00
	12.50	12.52	-0.16
	25.00	25.00	0.00

機 構 名 稱：超技儀器有限公司
新北市中和區中正路716號14樓
TEL：(02)8228-0770　　FAX：(02)8228-0760
測 試 人 員：張子卿

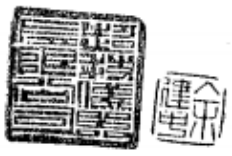

doi:10.6342/NTU202102462

A- 3 The mass balance equation and gas phase reaction considered by the equilibrium prediction model

Mass Balance				
Presentation				Number
$[NO_X]_T^* = [NO] + [NO_2] + [NO_3] + [HNO_2] + [HNO_3] + 2[N_2O_3] + 2[N_2O_4] + 2[N_2O_5]$				Eq- 26
Equilibrium Reaction				
Reaction	Definition of equilibrium constant	Value at 25°C	Unit	Number
$NO + NO_2 \rightleftharpoons N_2O_3$	$K_{35} = \frac{P_{N_2O_3}}{P_{NO}P_{NO_2}}$	5.19×10^{-1}	atm^{-1}	R- 35
$NO + NO_2 + H_2O \rightleftharpoons 2HNO_2$	$K_{36} = \frac{P_{HNO_2}^2}{P_{NO}P_{NO_2}P_{H_2O}}$	1.67×10^{-2}	m^2/kN	R- 36
$2NO_2 \rightleftharpoons N_2O_4$	$K_{37} = \frac{P_{N_2O_4}}{P_{NO_2}^2}$	6.49	atm^{-1}	R- 37
$N_2O_4 + H_2O \rightleftharpoons HNO_2 + HNO_3$	$K_{38} = \frac{P_{HNO_2}P_{HNO_3}}{P_{N_2O_4}P_{H_2O}}$	1.38×10^{-2}	-	R- 38
$2NO_2 + H_2O \rightleftharpoons HNO_2 + HNO_3$	$K_{39} = \frac{P_{HNO_2}P_{HNO_3}}{P_{NO_2}^2P_{H_2O}}$	9.36×10^{-4}	m^2/kN	R- 39
$3NO_2 + H_2O \rightleftharpoons NO + 2HNO_3$	$K_{40} = \frac{P_{NO}P_{HNO_3}^2}{P_{NO_2}^3P_{H_2O}}$	5.23×10^{-5}	m^2/kN	R- 40
$3HNO_2 \rightleftharpoons HNO_3 + 2NO + H_2O$	$K_{49} = \frac{P_{HNO_3}P_{NO}^2P_{H_2O}}{P_{HNO_2}^3}$	3.33	kN/m^2	R- 41
$NO_2 + HNO_2 \rightleftharpoons HNO_3 + NO$	$K_{50} = \frac{P_{HNO_3}P_{NO}}{P_{HNO_2}P_{NO_2}}$	5.59×10^{-2}	-	R- 42
$3NO_2 \rightleftharpoons NO + N_2O_5$	$K_{51} = \frac{P_{N_2O_5}P_{NO}}{P_{NO_2}^3}$	4.2×10^{-11}	m^2/kN	R- 43
$N_2O_3 + H_2O \rightleftharpoons 2HNO_2$	$K_{52} = \frac{P_{HNO_2}^2}{P_{N_2O_3}P_{H_2O}}$	3.18	-	R- 44
$N_2O_5 + H_2O \rightleftharpoons 2HNO_3$	$K_{53} = \frac{P_{HNO_3}^2}{P_{N_2O_5}P_{H_2O}}$	1.23×10^{6}	-	R- 45

doi:10.6342/NTU202102462